2012-12

Preparation and Characterization of Conducting Polymer Materials for Electrochromic Devices

Lavina Astratine
Technological University Dublin

Dublin Institute of Technology

Preparation and Characterization of Conducting Polymer Materials for Electrochromic Devices

Thesis presented for the award of
Doctor of Philosophy (PhD)

by

Lavinia Astratine

Under the supervision of Prof. John Cassidy, Prof. Edmond Magner and Dr. Anthony Betts

Submitted to Dublin Institute of Technology, December 2012

ABSTRACT

An attempt has been made to improve the physical-chemical properties of conducting polymers by switching from aqueous solutions towards ionic liquids as novel electrolytic media in order to fabricate novel electrochromic materials.

Formation and electrochemical characterization of Poly (2,3,5,6-Tetrafluoroaniline) (PTFA) was performed in aqueous solutions. The optical response was observed in order to establish the electrochromic properties of this material. Electrochromic activity of PTFA conducting polymer in aqueous conditions was investigated. Results indicated a slow colour change of 40 seconds, from delicate orange to a much intense orange colour.

Electrochemical copolymerization of two monomers pyrrole (Py) and 3,4-ethylenedioxythiophene (EDOT) was performed in an ionic liquid employing a novel 'micro-cell' in order to use the materials efficaciously. Characterization of the copolymers electrochemical features was performed for different Py : EDOT ratios (1:2, 1:1, 2:1) in both aqueous and ionic liquid electrolytes. A series of spectroscopic and microscopic studies were also carried out in order to prove the copolymer formation. All three copolymers presented different absorbance spectra, while the FTIR were not very clear. However, the morphology investigation highlighted the different features of copolymers which showed various distributions of globules, pores and holes.

Ionic movement between aqueous phase and ionic liquid was studied, and a model was developed to describe the interfacial processes occurring between two immiscible liquid phases. In the present work the Ferrocene ion transport across the ionic liquid / water interface was studied experimentally and in comparison to a model for a thin film of ionic liquid. Results obtained from experimental and modelling data

had similar trends of increase in the peak to peak separation with increased scan rate, but the peak to peak separation in the experimental was larger.

A new, cost-effective prototype of ‘micro-sandwich electrochromic cell’ was fabricated, based on an ‘ion jelly’ electrolyte. The ‘ion jelly’ solid state electrolyte was a successful replacement for the costly ionic liquids. This prototype of electrochromic cell showed dark-bluish and light-blue colours upon redox switch, but optimization is needed in order to reach the desirable features of a high-performance electrochromic device.

Acknowledgements

It is always difficult to express your gratitude and acknowledge to so many great people that have provided valuable advices.

I would like to thank my supervisors Prof. John Cassidy, Prof. Edmond Magner and Dr. Anthony Betts for their excellent guidance, great suggestions, never-ending patience, support and encouragement throughout the whole PhD course. I will always be grateful to them for the opportunity to take up a postgraduate position in Ireland. Most of all, without their help, this thesis would never come to completion.

I would like to address many thanks to the UL/DIT Joint Common Interest Group scheme for funding and supporting this project.

I wish to thank members of E. Magner Research Group: Sarah, Darragh, Simon, Neelima, Ula, and Micheal for their friendship and all good moments that we shared together during my PhD.

Above all, I am very grateful to my parents for their long-distance support. Finally, I would like to thank my fiancée for listening to me every time when I felt down. Without his optimism, support and patience I could have never achieved this much!

Declaration

The work presented here, unless otherwise stated, is the original work of the author and was carried out at the University of Limerick, on behalf of Dublin Institute of Technology as part of DIT/UL CIG. No part of this thesis has been previously submitted to this or any other university.

Lavinia Astratine

December, 2012

TABLE OF CONTENTS

List of Abbreviations

BMIM PF_6	1-butyl-3-methylimidazolium hexafluorophosphate
EMIM TFSI	1-ethyl-3-methylimidazolium bis(trifluoromethansulfon)imide
BMIM BF_4	1-butyl-3-methylimidazolium tetrafluoroborate
CE	coloration efficiency
CPs	conducting polymers
CV	cyclic voltammetry
D	diffusion coefficient
DMSO	dimethyl sulfoxide
ΔE_p	difference between oxidation/ reduction peak potentials
E_g	the band-gap
EC	electrochromic material
ECD	electrochromic device
EDOT	3,4-ethylenedioxythiophene
Fc	ferricenium
FTO	fluorine doped SnO_2
HOMO	the highest occupied molecular orbital
$HClO_4$	perchloric acid
ITIES	immiscible electrolyte solutions
ITO	indium tin oxide glass
i_{pb}/i_{pf}	the corrected peak current ratio
j_p	peak current
LUMO	the lowest unoccupied molecular orbital
MPyr TFSO	3-methyl-1-propylpyrridinium bis(trifluoromethylsulfonyl)imide
$NaBF_4$	sodium tetrafluoroborate
PANI	polyaniline
PEDOT	poly(3,4-ethylenedioxythiophene)
PET	polyethyleneterephthalate
PPy	polypyrrole
PTh	polythiophene
PPy-co-PEDOT	copolymer of Py and EDOT
PTFA	poly(2,3,5,6-tetrafluoroaniline)
PVC	poly(vinyl chloride)
PSS	polystyrenesulphonate
Q	charge
RTILs	room temperature ionic liquids
SEM	Scanning Electron Microscopy
THF	tetrahydrofuran
TMOs	transition metal oxides
WO_3	tungsten trioxide
XPS	X-ray photoelectron spectroscopy
ν	scan rate
$\nu^{1/2}$	square root of scan rate
$\sqrt{(at)}$	dimensionless current

Chapter 1. Introduction

1.1 Polymers versus Conducting Polymers

Over the course of the past decade, much effort has been made to develop cleaner and more environmentally friendly technologies. The industrial progress achieved by society comes with many drawbacks: global pollution, the depletion of the ozone layer, the green house effect, most of which the general public are aware. The book edited by J. Clark and D. MacQuarrie [1] presents the fundamental aspects and the need for 'green chemistry and technology' which would constitute a benefit to human health and environment. They proposed '12 Principles of Green Chemistry' [2] to guide researchers in the development of new materials and processes.

The major area of interest in this research work is the formation of conducting polymers (CPs) [3] [4], in conjunction with room temperature ionic liquids (RTILs) [5] [6], to produce electrochromic thin films [7] [8]. Such films, which reversibly change colour in response to changes in electrical potential, could be used in electronic display devices [9] and in light and energy-control applications [10] (e.g. smart windows which control light transmittance). Most current electrochromic materials suffer from manufacture and performance limitations (including stability issues) and they are generally made with relatively expensive and/or toxic compounds (making disposal difficult). Production of improved electrochromic devices [11] with low-cost manufacturing, using solution-processing of film-forming polymers in a more environmentally-friendly 'Green Chemistry' approach is a desirable goal and the present study addresses some of these issues.

What is a polymer? The first thing that people think of are plastics (e.g. poly(ethylene terephthalate): PET or poly(vinyl chloride): PVC). The list continues

with rubbers (e.g. polyisoprene - natural rubber), different fibres (natural and synthetic fibres) and fabrics (velvet, satin). Polymers consist of extremely large, chain-like molecules that are, in turn, made up of numerous smaller, repeating units called monomers and they are part of our everyday life.

A polymer's ability to conduct electricity was once considered absurd, as polymers were mostly employed as insulators. Conducting polymers are defined as organic polymers which are able to conduct electricity when charging/discharging of the material happens upon application of certain potentials. The field of conducting polymers is of great interest for the research community and is currently the focus of much attention (Figure 1.1). The work within the area of CPs has developed significantly and these compounds have become prospective materials for many technological applications because they can be easily synthesised either chemically [12] or electrochemically [13]. The most interesting aspect of conjugated polymers from an electrochemical perspective is their ability to behave as electronic conductors. Electronically conducting polymers are extensively conjugated molecules and it is believed that they possess a spatially delocalised band-like electronic structure (Figure 1.2). The tendency of materials to conduct electricity is generally expressed in terms of surface resistivity, reflecting the resistance due to the transfer of electrical charges.

Actually, in 1976, Alan J. Heeger, Alan MacDiarmid and Hideki Shirakawa, together with their research groups, discovered CPs and the ability to dope/undope these polymers over the full range from insulator to metal state. They subsequently [14], demonstrated that the molecular arrangement in conducting polymers (CPs) must contain alternating single and double bonds in order to allow the formation of delocalized electronic states.

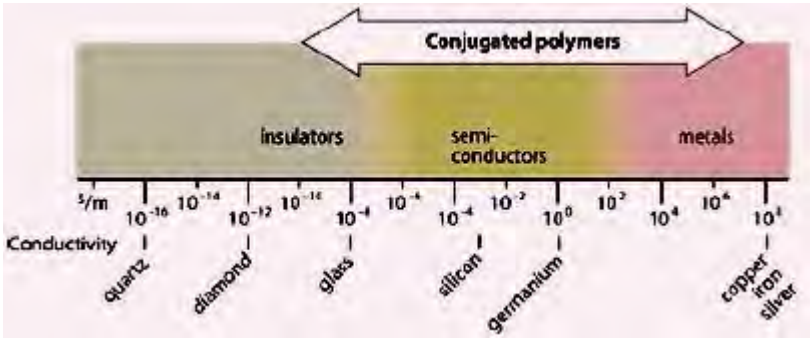

Figure 1.1 Diagram showing range of conductivity for various materials including conducting polymers [15].

It is generally agreed that the doping process is an effective method to produce electroactive polymers [15]. Doping allows electrons to flow due to the introduction of extra bands and as doping occurs, the electrons in the conjugated system, which are loosely bound, are able to 'jump around' the polymer chain [16].

The polymer is called a 'conjugated polymer' because of the alternating single and double bonds in the polymer chain. Thanks to the special conjugation in their chains, it enables some of the π-electrons to be de-localized and shared throughout the polymer. The de-localized electrons may move around the whole system and become the charge carriers to make the polymer conductive. This polymer can be transformed into a conducting form when electrons are removed from the backbone resulting in cations or added to the backbone resulting in anions. Anions and cations behave as charge carriers, jumping from one site to another under the influence of an electrical field, thus increasing conductivity [17]. During the doping process, the polymer changes its redox state (oxidized/ reduced form) and this is of primary interest for the present work.

1.2. Conduction Mechanism of Conducting Polymers

The conductivity of CPs can be adjusted to vary over a very wide range, starting from insulating and moving towards a more conductive form (metallic form) by varying the concentration of the dopant. Although the conduction mechanism of CPs cannot be always fully understood, it was noticed that their behaviour is similar to a semiconductor where electrons under thermal excitation jump from the valence band (VB) to the conduction band (CB) giving rise to conductivity. This is true for a narrow band-gap, but if the band-gap is very wide, then the electrons under thermal excitation at room temperature don't have enough energy to travel across the gap. So, in addition to band theory, it is essential to also study the properties of charge carriers. Most of the known CPs are p-type doped and this involves formation of an abundance of mobile or "carrier" holes in the material, while in n-type doping the carriers are electrons. The model for the conduction mechanism of CPs can be explained using band theory [18].

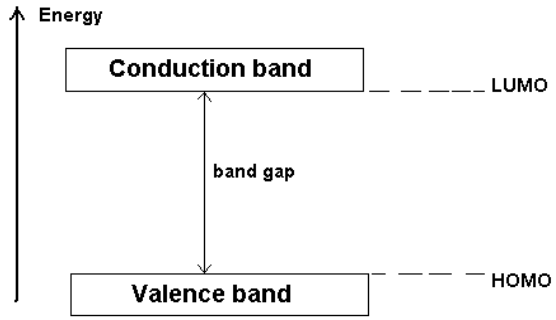

Figure 1.2 Band structure in an electronically conducting polymer

In Figure 1.2, HOMO means the highest occupied molecular orbital and LUMO is the lowest unoccupied molecular orbital which are sometimes referred to as frontier orbitals. The energy difference between the HOMO and LUMO is termed

the band-gap (E_g). The intrinsic optical properties of these materials is given by the energy gap between the highest occupied π electron band (valence band, VB) and the lowest unoccupied band (conduction band, CB) [19]. A reduction of the band gap makes the material more conductive and attempts are being made to obtain a polymer with very low band gap, close to that of metals. When the band gap of the polymer is greater than 2.0 eV, it can be adjusted through various methods [18].

One of the approaches towards formation of small band gap conjugated polymers is the copolymerization approach [20], by altering the properties of a polymer in a desired direction. This method allows formation of a new polymeric material with some properties expected from the individual monomer types, based upon their physical and chemical interactions.

Common examples of conducting polymers (Figure 1.3) include polypyrrole (PPy) [21] [22], polythiophene (PTh) [23] [24] and polyaniline (PANI) [25] [26].

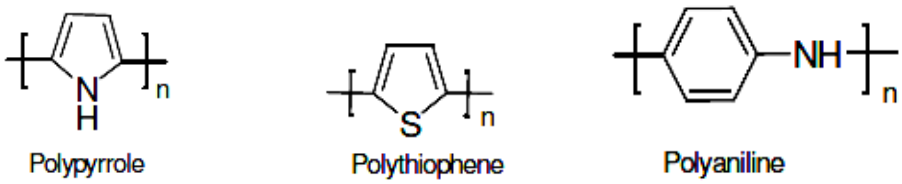

Figure 1.3 Structures of some common conducting polymers

The charge carriers, either positive p-type or negative n-type are the products of oxidizing or reducing the polymer respectively. p-type or n-type doping can be presented in analogy to the mechanism of generation of charge carriers in doped inorganic semiconductors [18]. A number of general observations can be made regarding the behaviour of the polymers studied.

Oxidation of the polymer initially generates a radical cation with both spin and charge, referred to as a polaron [18]. This process causes the presence of localised electronic states in the gap due to a local upward shift ΔE of the HOMO and a downward shift in the energy of the LUMO. When an electron is removed from the polymer chain, the ionization energy is lowered by ΔE, and if ΔE is larger then E_{dis} (distortion energy necessary to distort the lattice around the charge), this charge localization process is favourable relative to the band process [18]. The cation and radical form a bound species, since any increase in the distance between them would necessitate the creation of additional higher energy quinoid units (Figure 1.4).

Aromatic Quinoid

Figure 1.4 Two possible structures for polyisothianaphthene: aromatic and quinoid units [3]

At low doping levels, the charge is accommodated in polaron states, while upon going to higher doping levels, a polaron to bipolaron (doubly charged defects) transition is observed (Figure 1.5). As polarons migrate up and down the polymer chain, they could run into each other and give rise to a bipolaron. Two adjacent polarons combine to form a lower energy bipolaron, which is a spin-free, doubly-charged, partially-localised structure [17].

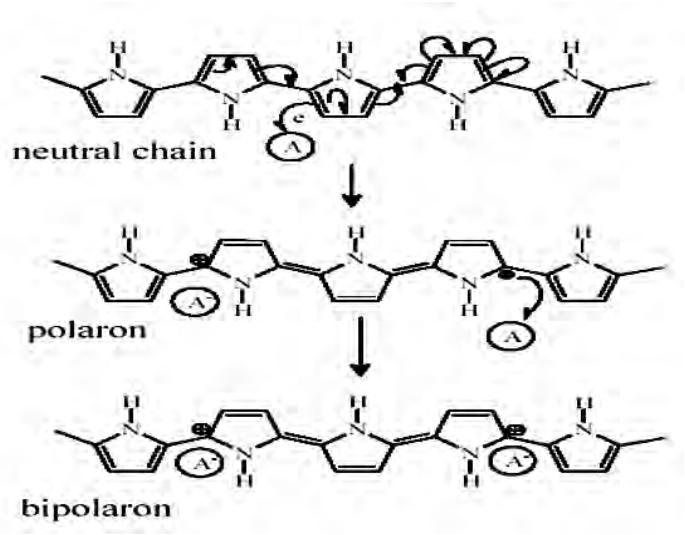

Figure 1.5 Conduction mechanism for the oxidative polymerization of polypyrrole

The polypyrrole (PPy) system is a model system and has been studied intensively. The evolution of the PPy electronic band structure upon doping is shown in Figure 1.6. It can be seen that the overlap of polaron states leads to the formation of two 0.4 eV wide bipolaron bands [18]. Polypyrrole is formed in the oxidized state, PPy^{+1}, and it can be reduced to the neutral, insulating form, PPy^{0}. The anion frequently utilised for the electrochemical formation of polypyrrole films is the perchlorate (ClO_4^-) anion because this counter ion produces films with a high degree of uniformity and reproducibility [27]. This is due to the relatively small radius of the ClO_4^- ion that makes it quite mobile within the film matrix [28]. Upon electropolymerization process, the polypyrrrole film goes from its reduced state, which is an insulating hydrophobic polymer, to a conductive oxidized state which contains a high cationic charge density.

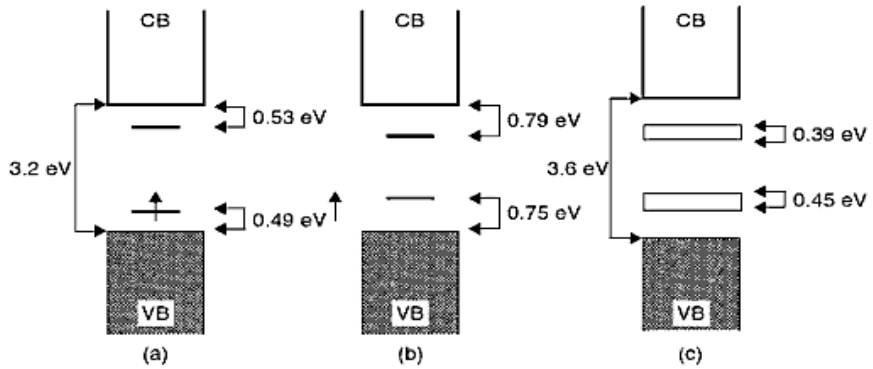

Figure 1.6 (a) low doping level, polaron formation; (b) moderate doping level, bipolaron formation; (c) high (33 mol %) doping level, formation of bipolarons bands for polypyrrole [29]

All conducting polymers are potentially electrochromic in thin-film form [30] [31], redox switching giving rise to new optical absorption bands associated with electron transfer. In their oxidised states, conducting polymers are 'doped' with counter anions (p-doping) and possess a delocalised π-electron band structure. The HOMO-LUMO energy gap provides a first estimation of the electronic excitation energy which in turn can be measured by UV/Vis spectroscopy and provides the colours in the materials.

1.3 Electrochromic Materials and Electrochromic Devices

Electrochromism is the phenomenon displayed by some materials in which colour can reversibly change when a certain electrical potential is applied. It occurs when a material is oxidized or reduced as result of changes in the band-gap of the material induced by the potential change. A large number of electrochromic materials are available from almost all branches of synthetic chemistry. Organic electrochromic materials represent a major class of materials used for electrochromic devices and they are divided into three categories.

1.3.1 Type I – Electrochromes

A type-I material is soluble in both reduced and oxidized states, and remains in solution at all times during electrochromic usage. Examples include methyl viologen (1,1’-di-methyl-4,4’-bipyridilium), which changes its colour from colourless to intense blue during a reductive electrode reaction [17] .

1.3.2 Type II – Electrochromes

Type II electrochromes are soluble in one redox state, but form a solid film on the surface of an electrode during electron transfer. These types of materials are exemplified by aqueous viologen systems such as heptyl or benzyl viologens [19] [32], or methoxyfluorene compounds in acetonitrile solutions. The viologens are characterized by three redox states as presented in Figure 1.7, of which the dicationic state is ascribed to be the most stable. The solid form of 1,1'-di-n-heptyl-

4,4'-bipyridilium (heptyl viologen) showed an intense yellow colour in its dicationic state, but in solution it appears as a pale yellow/or colourless material.

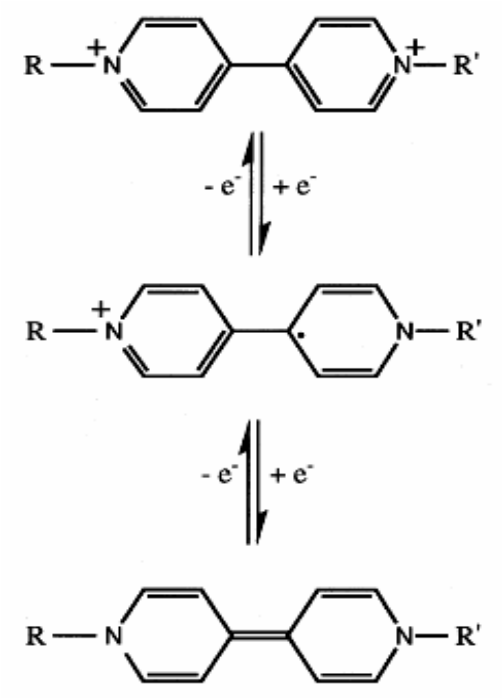

Figure 1.7 Scheme representing the three common viologen redox states [19].

1.3.3 Type III – Electrochromes

Type III electrochromic materials, such as conducting polymers, remain solid at all times [19, 33]. These electrochromic materials are in general studied at a single working electrode using a three electrode cell, under potentiostatic or galvanostatic control. For materials characterization techniques such as cyclic voltammetry, coulometry, chronoamperometry with in situ spectroscopic measurements are often employed [34]. Electrochemical Impedance Spectroscopy can also be employed for characterization of conducting polymers [35] [36].

In order to obtain a good electrochromic material (EC), there are certain required properties such as fast switching time/speed (few seconds) [37], high

stability (long life time) [38], good contrast and reversibility of colour change. The electrochromic properties result from the oxidation/ reduction of the polymer backbone, and arise from the formation of bipolaron bands. This often has large effects on the electronic absorption spectra, producing high contrast colour changes. For example, the reduced yellow form of polypyrrole film displays a maximum absorption wavelength at 400 nm, while the fully oxidized blue/black form has a broad absorbance with a maximum around 800 nm [39].

The colours that CPs might present in the different redox states are shown in Table 1.1. In the simplest approach, substitution of the parent heterocycle is used to control the band gap through induced steric or electronic effects.

Table 1.1 Examples of conducting polymers

Electroactive polymer	**Colour in oxidized form**	**Colour in reduced form**
polypyrrole	dark grey	yellow
polythiophene	blue	red
poly(3-methylthiophene)	blue	red / purple
poly(3,4-ethylenedioxythiophene)	almost transparent blue	dark blue
polyaniline	Emeraldine: blue/ green Pernigraniline: blue/violet	Leucoemeraldine: white/clear and colorless

The speed of the colour changes depends on the rate at which the dopant ions can migrate in and out of the polymer matrix.

1.3.4 Inorganic Electrochromic Materials

Another category of materials, besides conducting polymers, which exhibit electrochromic properties are the transition metal oxides (TMOs). There are many inorganic oxide compounds containing transition metals like iridium [40], ruthenium [41], tungsten [42], manganese [43], cobalt [44] and others used for designing electrochromic devices [45]. Relevant description of the properties and applications of various TMOs as electrochromic materials can be found in books by Granqvist [46] and Monk et al [7], as these materials have at least one redox state (colorless ⇔ colored).

Tungsten trioxide (WO_3) is of particular interest for electrochromic devices [47] because of its ability to show electrochromic properties in both the visible and near-infrared regions when an appropriate potential is applied. Regarding the WO_3 film formation, increased attention is paid in optimising the deposition conditions, since the techniques involved in the deposition process are more sophisticated [48]. Also nickel oxide films [49] are of interest for use in electrochromic devices and a recent literature review [49] refers to nickel oxide films used for thin film batteries, super-capacitors, electrocatalysis, etc. The electrochromic materials like tungsten oxide and nickel oxide were intensively used in the work with inorganic electrochromic materials as they have superior electrochromic properties than other inorganic oxides.

The work done by E. Avendano et al. [50] presents interesting data about the optical absorption in both tungsten oxide and nickel oxide films, illustrating mainly the higher coloration efficiency thanks to their nanocrystalline structure. The optical absorption properties of electrochromic films are related to the injected charge per unit area of the active electrode.

The coloration efficiency ( ) is an important parameter for electrochromic devices and is defined as the ratio of the change (between bleached and coloured state) in absorbance to the charge injected per unit area of the display electrode [46]. The coloration efficiency is related to the device performance and it depends upon chemistry, microstructure and film thickness used for the electrochromic device.

As stated earlier, a conducting polymer film can be easily formed by chemical [51] or electrochemical polymerization [52], while inorganic materials require more complicated methods such as vacuum evaporation [53] [54], spray pyrolysis [55] [56], sputtering [57] [58], and cryo-vacuum [59] deposition. In terms of processibility of the materials, the inorganic oxide materials are described as materials with poor processibility and for this reason also the number of colours that an inorganic material can yield is more limited than in the case of conducting polymers. The number of colours that conducting polymers can display is various and is correlated with the doping percentage, monomer type, the working potential and electrolyte's nature [32].

Tungsten oxide (WO_3) thin films [60] have been extensively used in applications like electrochromic mirrors especially because of their ability to change in a reversible manner from clear to deep blue for up to 10^6 cycles. However, conducting polymers are attractive for the capability of displaying various colours when changing between oxidized and reduced forms, but the lifetime of these systems is limited to 10^4-10^6 cycles. The lifetime of an electrochromic device is an important parameter from both a research and commercial point of view and nowadays efforts are continuously being made to reduce device costs, to improve the lifetime of the systems and to prevent degradation [45]. In conclusion, conducting polymers are preferred for applications in electrochromic devices

because of large number of colours they are able to exhibit during chemical or electrochemical redox processes. In the same time, conducting polymers showed very high contrast (e.g. 43 % optical contrast retained by poly(1,2-bis(2-(3,4-ethylenedioxy)thienyl)vinylene) [61] compared to inorganic oxide materials [45].

Electrochromic devices [41] [62] have attracted increasing attention in recent years because of the valuable energy saving functions that the technology can provide. For example electrochromic "smart" glazing systems offer the possibility of optimizing the balance of daylight input into large buildings, consistent with minimizing air conditioning load, by active control of the glazing reflectivity. These devices require high photonic contrast materials that can switch between redox states of different coloration at the lowest possible energy cost [63]. An electrochromic device (ECD) has at its center an electrolyte or ion conductor, which is in contact with films that provide optical modulation, ion storage, and (transparent) electrical conduction. Use of appropriate electrolyte systems is important in terms of long time stability of electrochromic devices [63].

Electrochromic contrast is probably the most important factor in evaluating an electrochromic material. It is often reported as a percent transmittance change (Δ%T) at a specified wavelength where the electrochromic material has its highest optical contrast. For some applications, it is more useful to report a contrast over a specified range rather than a single wavelength. In order to obtain an overall electrochromic contrast, measuring the relative luminance change provides more realistic contrast values since it offers a perspective on the transmissivity of a material as it relates to the human eye perception of transmittance over the entire visible spectrum [64].

Switching speed is often reported as the time required for the colouring/bleaching process of an EC material to occur. It is important especially for

applications such as dynamic displays and switchable mirrors [30]. The switching speed of electrochromic materials is dependent on several factors such as ionic conductivity of the electrolyte, accessibility of the ions to the electroactive sites (ion diffusion in thin films), magnitude of the applied potential, film thickness, and the morphology of the thin film. In the field of EC materials, one of the great strengths of conjugated polymers is the ability to tailor the EC properties *via* modification of the polymer structure. Through band gap control, one can vary the accessible colour states in both the doped and neutral forms of the polymer. Numerous synthetic strategies exist for tuning the band gap of conjugated polymers [65]. An ECD must undergo stable redox processes for its electrochromic properties to be reproducible upon repeated switching. Typical degradation processes which can appear include irreversible redox behaviour because of high potentials, water and oxygen redox interferences with the EC components, degradation of electrode materials or evaporation of the electrolyte, and resistive heating on repeated switching.

Electrochromic cells go from opaque to transmissive at selected regions of the electromagnetic spectrum. Electrochromic cells require that the cathodic and anodic reactions balance nearly exactly (cyclic voltammetry is a good comparison tool).

The electrochromic window is similar in operation to a battery with some additional requirements: at least one of the electrodes must be transparent to the given region of the electromagnetic spectrum; the cathode material (which colours upon being oxidized) must be electrochemically reversible, the ion-conducting electrolyte must not only provide physical separation between cathode and anode, a source of cations and anions to balance redox reactions, but must also be transparent to the given region of the spectrum and the anode material (which colors upon being reduced) must also be electrochemically reversible [66].

1.4 Quantification of Colour

A very desirable goal regarding the electrochromic reactions is the colour quantification. The most common method used is based on the integration of experimental power distributions derived from visible region spectra over the CIE (Commission Internationale de l'Éclairage) 1931 colour-matching functions [67]. The colorimetric data provide a numerical specification at unit wavelength steps from which can be calculated tristimulus values for any spectral power distribution (Figure 1.8). The CIE 1931 defined a standard system for colorimetry, based on 2° colour matching and the basic data were averaged chromaticity coefficients of Wright (1929) and Guild (1931). So the two equivalent statements colour-matching behaviour of the CIE 1931 were established in the (R,G,B) and (X,Y,Z) system units [68].

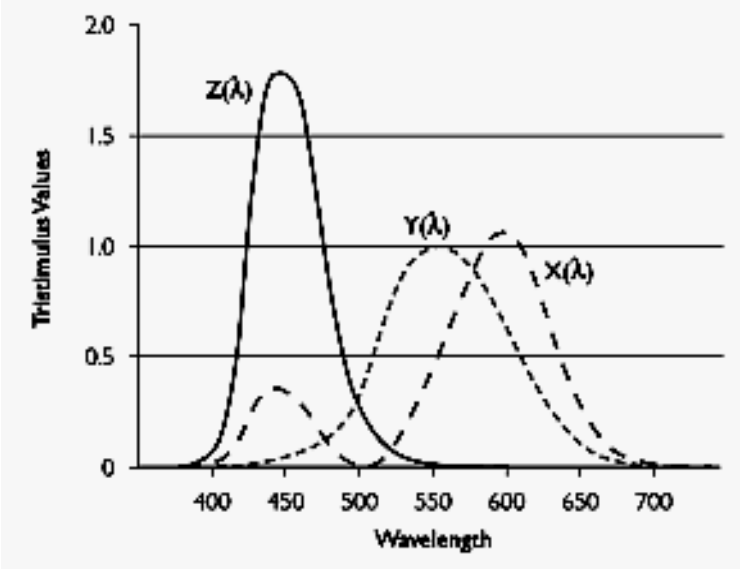

Figure 1.8 CIE 1931 color matching functions. Spectral tristimulus values of constant radiance stimuli for different wavelengths. The three functions of wavelength define the color-matching properties of the CIE 1931 standard colorimeter observer. [68]

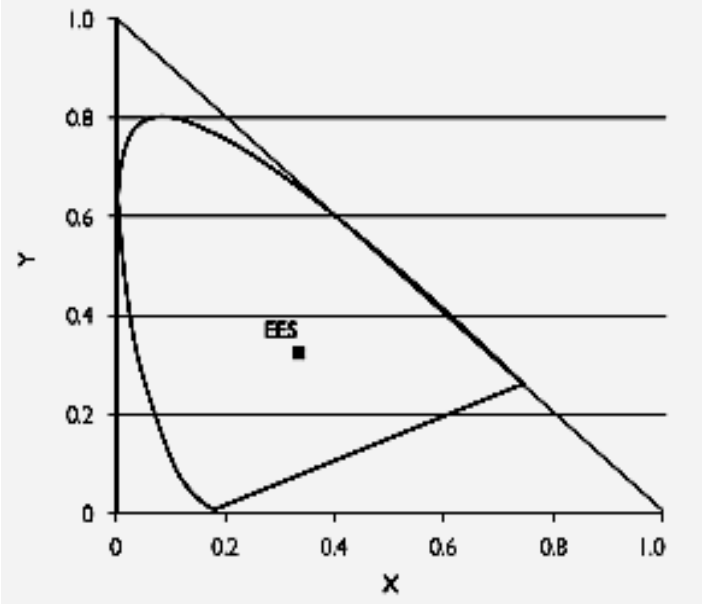

.

Figure 1.9 CIE 1931 chromaticity diagram. CIE 1931 (x,y)-chromaticity diagram. [68]

While electrochromic materials like polypyrrole, poly(3,4-ethylenedioxythiophene) and polyaniline give the desired optical contrast initially, their performance often decays when the device is cycled for prolonged periods of time [69]. The high operating potentials used to achieve optimum optical contrast from the CPs may eventually lead to damage of the electrochromic films and the electrolyte and ultimately degrades the device performance [70]. Therefore there is a need to lower the potential used in cycling these devices to achieve practical lifetimes suitable for commercial exploitation.

1.5 Ionic Liquids and Conducting Polymers

For this reason ionic liquids (ILs) were considered the best replacement of common water/ organic solvent, in order to increase the electrochromic device performance. There are several advantages to take into consideration when replacing the traditional solvents with ILs; these include wide potential window and low volatility. A very simple definition attributed to this new class of solvents is that of low-temperature molten salts which are liquids at room temperature and composed of ions only. This new class of solvents known as Ionic Liquids (ILs) had become extremely popular for their possible applications to various research areas because of their advantageous physical and chemical properties [71] [72].

These 'molten salts' are not perfect as they can present sometimes disadvantages such as high viscosity and solubility issues. However, replacement of traditional solvents with IL has brought improvement of different electroactive polymers systems and also the number of research studies involving ionic liquids had always increased since 1990 (Figure 1.10).

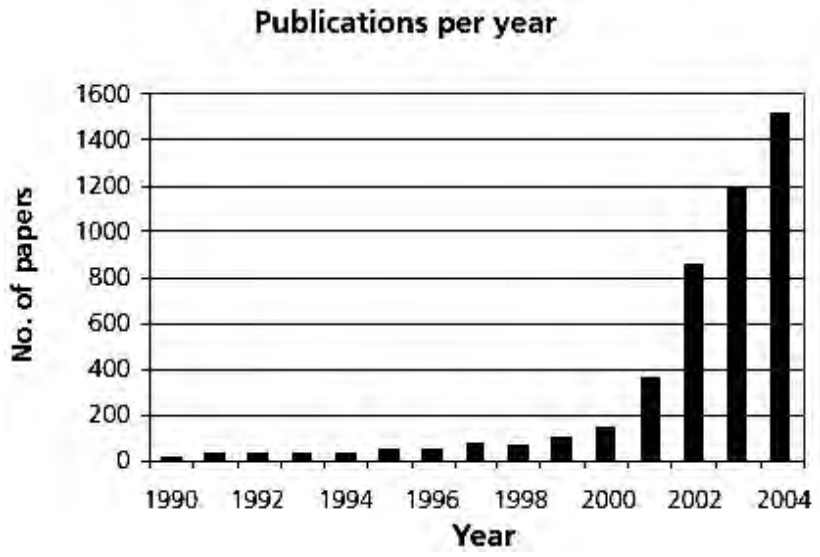

Figure 1.10 Scheme showing the continuous increase of publications number on ionic liquids; source Sci-Finder. http://www.sigmaaldrich.com, accessed in December 2012.

G.G. Wallace, J.R Reynolds and R.J. Mortimer have performed various studies employing conducting polymers such as poly(3,4-ethylenedioxythiophene), polypyrrole, polyaniline in order to create and improve electrochromic devices. G.G. Wallace indicates in his work an important property of the electrolyte, regarding the optical transparency of the electrolyte when it comes to a practical application. An optically transparent electrolyte will always be the best choice since it will provide high transmission over the visible range. The electrolytes used by G.G. Wallace ensured a 90 % transmission and proved the use of ionic liquid as a non-volatile plasticizer instead of common organic platicizers in a gel-polymer electrolyte system with conducting polymer [73].

Other work resulted in the increase of polyaniline stability and reversible behaviour when ionic liquids such as 1-butyl-3-methylimidazolium hexafluorophosphate (BMIM PF_6) and 1-ethyl-3-methylimidazolium bis(trifluoromethansulfon)imide (EMIM TFSI) were employed. Results showed during successive potential cycling a stable and reversible response up to 150 cycles, compared to films formed in aqueous-acidic solution which seemed to lose their electroactivity after only 15-16 cycles [26].

Efforts have been made to find the best candidates for both conjugated polymers and ionic liquids, in order to make a viable electrochromic device for industrial applicability. Usually thin films are prepared during electrochemical polymerization, a process which involves either radical-cation/ radical-cation coupling or an attack of a radical-cation on neutral monomer. The film growth can be controlled through the charge passed, while the polymer is forming. Actually for electrochromic devices thin films are made supported by an electrode surface, which can be electrochemically cycled between oxidized (conducting state) and neutral

(insulating state). Thicker films are formed in their oxidized state and can be peeled from the electrode surface to serve as free-standing, electrically conducting films. In this case the thicker films represent polymeric cations and their overall charge balance is achieved by the incorporation of counter-anions which arise from the electrolyte of the solution [4].

1.6 Ionic Liquids as Electrolytes for Conducting Polymers Electrodeposition

Ionic liquids represent superior media for electrodeposition of metals [74] [75] and semiconductors [76], possessing wide electrochemical windows, spanning up to 6 V in some cases.

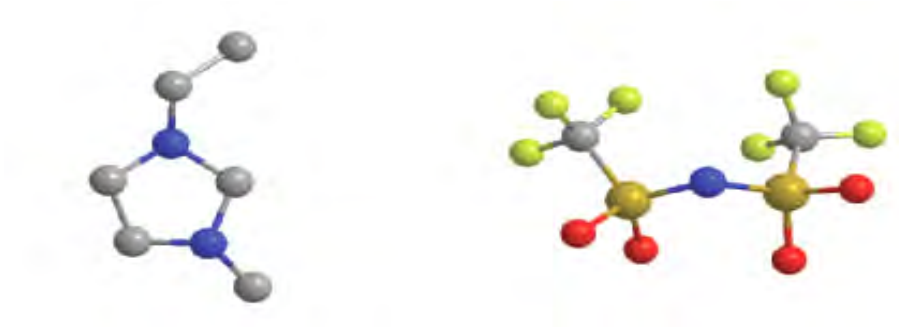

a large CATION **a delocalised ANION**

Figure 1.11 Cartoon of two components of an ionic liquid

As presented in Figure 1.11 ILs comprise a large bulky cation (imidazolium, pyridinium, pyridazinium, pyrimidinium, pyrazinium) and a delocalised anion (e.g. bis(trifluoromethylsulfonyl)imide). They are characterized by low melting points being liquid at room temperature or even below, and are free of any molecular solvent. Their physical and chemical properties are the same as high temperature ionic liquids, but the practical aspects involving maintenance or handling is different enough to allow a distinction. ILs are also known as room temperature ionic liquids (RTILs) and are usually quaternary ammonium salts like tetraalkylammonium [77] or based on cyclic amines, both aromatic (pyridinium, imidazolium) and saturated (piperidinium, pyrrolidinium). The first RTILs comprised chloroaluminate anion which was improved later by having 1-ethyl-3-methylimidazolium (EMIM) cation and tetrafluoroborate (BF_4) anion, which are resistant to moisture traces. During the last decade the number of publications

involving ionic liquids work has exponentially increased from approximately 50 papers in 1997 to 4000 papers in 2011 [78] [79]. Some examples of both anions and cations for RTILs can be seen in Figure 1.12.

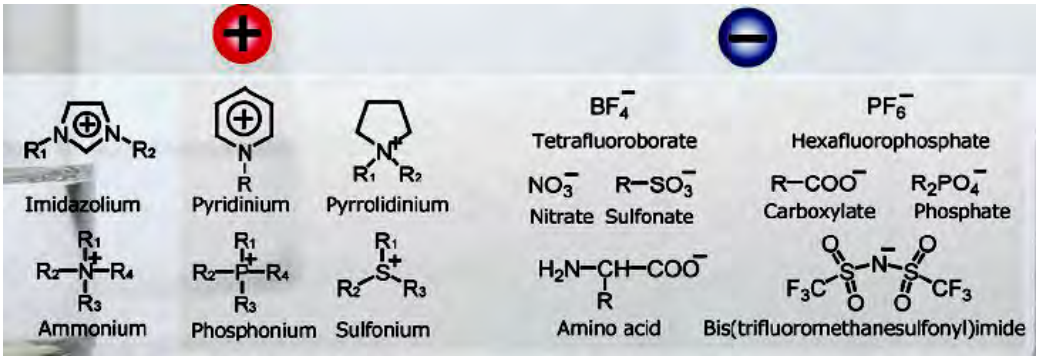

Figure 1.12 Examples of cations (+) and anions (–) for ILs [80]

Ionic liquids are no longer laboratory curiosities, as they have become important factors in the materials science field and this is reflected through the multitude of reviews available [81] [82]. There remain aspects of the behaviour of ionic liquids which still need to be investigated, since they have been named 'the green solvents' due to their attractive properties. ILs are characterized by a series of desirable properties which can ease the experimental conditions; these include thermal and chemical stability, low melting point, high ionic conductivity, negligible volatility, moderate viscosity and solubility (affinity) with many compounds [59]. RTILs are suggested as alternative to traditional organic solvents which are volatile and limited for their practical usage. A basic characteristic of these solvents used for producing conducting polymers is increased potential windows and relatively high conductivities. ILs have these attractive features that can accomplish this need and allow the electrochemical study to be undertaken without addition of supporting electrolyte. Several studies are based on CPs/ILs

systems as ILs have improved the redox behaviour of these materials which were used in applications such as actuators [83], supercapacitors [84] [85], electrochromic devices [86] and solar cells [87]. Another aspect for which ILs are employed extensively for conducting polymers film formation is their good ionic conductivities. They are more viscous than common solvents, denser than water, thermally stable up to 450° C and allow significantly larger electrochemical windows.

1.6.1 Ionic Liquids Conductivity

However, IL conductivities are much lower than those of conventional aqueous electrolytes which can reach up to 540 or 730 mS cm^{-1} (Table 1.2). In general, ILs conductivity values are typically in the range from 0.1 to 18 mS cm^{-1}.

The imidazolium based ionic liquids containing the 1-ethyl-3-methylimidazolium cation reach quite high conductivity values (σ) around 10 mS cm^{-1}, while those based on 1-butyl-3methylimidazolium only display a conductivity of around 3 mS cm^{-1}. On closer examination, it can be easily noticed that imidazolium based ionic liquids have better conductivity than the rest of ionic liquids which are based on tetraalkylammonium, pyrrolidinium, piperidinium and pyridinium cations, ranging from 0.1 to 5 mS cm^{-1} [78].

Electrolyte	Solvent	[mS/cm]
H_2SO_4 (30 wt. %)	**H_2O**	**730**
KOH (29.4 wt. %)	**H_2O**	**540**
NH_4Cl (25 wt. %)	**H_2O**	**400**
$[Et_4N]^+ [BF_4]^-$ (1 mol/dm^3)	**AN**	**60**
LiN $(CF_3SO_2)_2$ (1 mol/dm^3)	**EC + DME (1:1)**	**13.3**
LiN $(CF_3SO_2)_2$ (1 mol/dm^3)	**EC + DMC (1:1)**	**6.5**
$LiCF_3SO_3$ (1 mol/dm^3)	**EC + DME (1:1)**	**8.3**
$LiPF_6$ (1 mol/dm^3)	**EC + DME (1:1)**	**16.6**
$[Et_4N]^+ [BF_4]^-$ (0.65 mol/dm^3)	**PC**	**10.6**
$[EtMeIm]^+[BF4]^-$ (2 mol/dm^3)	**AN**	**47**
$[EtMeIm]^+[BF4]^-$ (2 mol/dm^3)	**PC**	**16**

AN = acetonitrile; EC = ethylene carbonate; DME = l,2-dimethoxyethane; PC = propylene carbonate; DMC = dimethyl carbonate

Table 1.2 Examples of conductivity values for different classical electrolytes [78].

1.6.2 Ionic Liquids Viscosity

Another important aspect of the ionic liquids properties is their increased viscosity (η) which is inversely proportional to their conductivity and this represents one of the main barriers to the applications of ILs. In comparison to conventional water/organic solvents, ILs viscosity values are up to two or three times greater, which produces a reduction in the rate of many organic reactions and a decrease in the diffusion rate of redox species. The imidazolium based ionic liquids having the hexafluorophosphate (PF_6) anion are highly viscous having the value of 450 mPa s for 1-butyl-3-methylimidazolium hexafluorophosphate (BMIM PF_6) [88]. It is quite difficult to choose a low viscosity IL, but imidazolium ILs have the tendency to show a decrease in viscosity following the order of anion species [89]:

$$Cl^- > [PF_6]^- > [BF_4]^- > [NTf_2]^-$$

A short table presenting the viscosity values of several RTILs in comparison to water/organic solvents can be seen in Table 1.3 [77]. In general, ionic liquids are more viscous than molecular solvents with viscosities ranging between 10 mPa s up to nearly 700 mPa s at room temperature. However, highly viscous ionic liquids are not appealing candidates for applications in chemical processes, as high viscosity leads to low conductivity in ionic liquids.

Liquid		Viscosity /cP
$[EMIM]^+$	**$[BF_4]^-$**	**43**
	$[PF_6]^-$	**15 (80 °C)**
	$[(CF_3SO_2)_2N]^-$	**28**
	$[(CF_3CF_2SO_2)_2N]^-$	**61**
	$[CF_3CO_2]^-$	**35**
	$[CF_3SO_3]^-$	**45 (30 °C)**
$[BMIM]^+$	**$[BF_4]^-$**	**291**
	$[PF_6]^-$	**450**
	$[(CF_3SO_2)_2N]^-$	**69**
	$[(CF_3CF_2SO_2)_2N]^-$	**77**
	$[CF_3CO_2]^-$	**70**
	$[CF_3SO_3]^-$	**93**
$[HMIM]^+$	**$[BF_4]^-$**	**314 (20 °C)**
	$[PF_6]^-$	**585**
	$[(CF_3SO_2)_2N]^-$	**68**
$[OMIM]^+$	**$[BF_4]^-$**	**439**
	$[PF_6]^-$	**682**
	$[(CF_3SO_2)_2N]^-$	**93**
	$[(CF_3CF_2SO_2)_2N]^-$	**492**
Water		**0.89**
Methanol		**0.54**
Acetic Acid		**1.13**
Acetone		**0.30**
Acetonitrile		**0.34**
N,N- dimethylformamide		**0.80**
Ethylene Glycol		**16.1**
Propylene Glycol		**40.4**
Glycerol		**934**

$[HMIM]^+$: 1-hexyl-3-methylimidazolium; $[OMIM]^+$: 1-octyl-3-methylimidazolium

Table 1.3 Viscosity of several liquids at room temperature (25 °C ± 1) [77]

An elaborate study was done by Bonhote et al in order to determine the multitude of parameters for ILs such as density, melting point, viscosity, conductivity, refractive index, electrochemical window, thermal stability, and miscibility with water and organic solvents [88] [90]. Their analysis was limited to imidazolium cations together with six different anions of which bis(trifluoromethanesulfonyl)amides displayed exceptional properties. This suggests a good choice as a solvent for synthetic and electrochemical applications.

However, when it comes to using CPs in conjunction with ILs that function at room temperature, the electrochemical window is an important key parameter when ionic liquids are used for electrodeposition. The electrochemical

window is defined as the electrochemical potential range over which the electrolyte can not be reduced or oxidized at an electrode [18].

CPs are generally formed during potentiostatic (application of constant potential over a period of time) or potentiodynamic (successive oxidation/reduction over a potential interval) methods. While the polymer film is grown in galvanostatic mode, the potential applied should be closely monitored to ensure that overoxidation of polymer does not arise. Even if the potentiodynamic method (like cyclic voltammetry) is the most time-consuming method, it is considered beneficial for electrochemical studies because the redox states of the polymer film can be monitored during film growth [91].

The oxidation potential of the various monomers is different in ILs than in traditional solvents, and this is reflecting in the increased electrochemical windows of ILs which allow them to be employed as superior electrolytes for electrodeposition. While the electrochemical window of aqueous electrolytes is limited to +1.2 V, the ILs electrochemical window is significantly larger, sometimes up to 6 V [65].

When an ionic liquid is employed as the solvent/electrolyte for the electropolymerization of CPs, the anion and the cation of the ionic liquid are involved during the oxidation/ reduction processes and of course the nature of each one should be considered. RTILs are ideal replacements for the more toxic and volatile solvents (e.g. acetonitrile) and thus prevent the problems of solvent evaporation which occur in the long-term use of volatile solvents. The large range of ion combinations, along with good thermal stability makes the ionic liquids, desirable and also extremely favourable for device applications. While regarding ionic liquids as supporting electrolytes, their conductivity and electrochemical

stability allows them to be utilised as solvents for the electrochemical synthesis of conducting polymers [91].

A systematic study of the physical properties of aqueous solutions of room temperature ionic liquids based on imidazolium is presented by W. Liu et al. [92]. Because the available air and water stable RTILs are employed to progressively replace organic solvents in a variety of chemical processes, some measurements were done to see the effect of association between ionic liquid and water. The study involves the effects on physical properties of aqueous solutions of room-temperature ionic liquids such as density, refractive index, viscosity, conductivity and surface tension over the whole concentration range to establish basic data for the polymer/ionic liquid/water system. It was noticed by W. Liu et al. that for different concentrations of ILs there were changes of physical properties of the solutions. A series of ILs were employed namely BMIM Cl, BMIM Br, EMIM Br and BMIM BF_4 which resulted in striking differences when compared to aqueous solutions. The results indicated that the density of ionic liquids decreases and the refractive index increases with increasing the length of alkyl chain, which is a cause of the "bulkyness" of the volume of cation.

W. Liu et al. concluded that the trend of surface tension change of BMIM BF_4 is different compared to the other three ionic liquids in the study because it actually acts like a cationic surfactant. Also for the conductivity of ionic liquids and water mixtures, similar properties with the classical properties of concentrated saline solutions with a maximum conductivity were reported (e.g. maximum conductivity of 47.1 mS cm^{-1} for BMIM BF_4 [93]). The curve of equivalent conductivity was different because the ionic liquid aqueous solution goes through two different regions: the water-rich region and the salt-rich region, so the equivalent conductivity is decreasing in the whole concentration range. According to W. Liu et al. the ionic

liquids physical properties suffered changes for different ionic liquid/ aqueous solution concentrations. It is important to know and to understand these effects for the future applications of the RTILs in the field of conducting polymers [92].

For example, J.M. Pringle et al. [94] described the work done on pyrrole in conjunction with various ionic liquids, suggesting that in some cases, when the film is oxidized and reduced in an ionic liquid, the intercalation/ loss of a cation occurs rather than anion intercalation/explusion. Because ionic liquids have wide electrochemical windows, during growth of polypyrrole the potentials used were higher than in conventional electrolytes. However results achieved depended on the nature of ionic liquid used.

In experiments conducted in 1-butyl-3methylimidazolium hexafluorophosphate (BMIM PF_6) or N,N-butylmethylpyrrolidinium bis(trifluoromethansulfonyl) amide (N,N-butylmethylpyrrolidinium TFSA), the polypyrrole films yield a small electrochemical response. Still, improvement of the electrochemical response was more obvious in ionic liquids when compared to the polypyrrole film grown in lithium perchlorate/acetonitrile solution as can be seen in Figure 1.13.

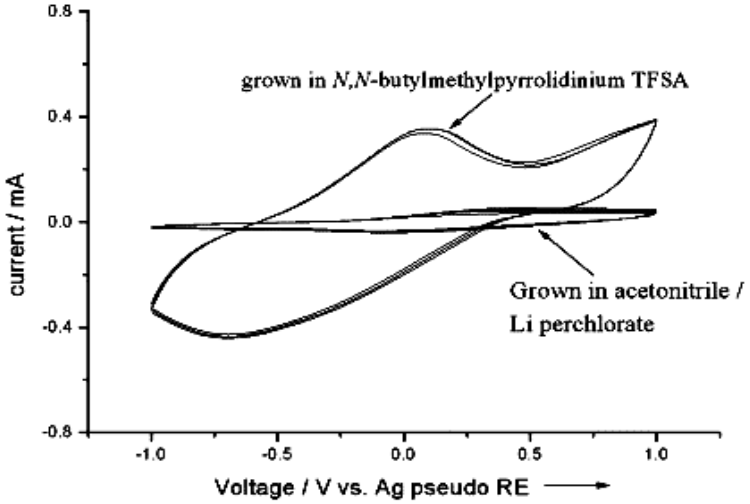

Figure 1.13 Comparison of the cycling polypyrrole films in an acetonitrile/$LiClO_4$ solution. Scan rate: 100 mV/s. [94]

Also the thickness of the films was strongly dependent on the nature of the ionic liquid used. For films grown in, 1-ethyl-3-methylimidazolium TFSA, a more significant increase in the oxidation/ reduction current was seen during the growth and films exhibited a good electrochemical response when cycled in the ionic liquid, even if they are thicker. Another important aspect is the morphology of the polypyrrole films, which typically is a nodular surface morphology. To have good electronic properties a smooth and dense film would normally have a good conductivity because it can better facilitate charge transport through the film [94].

An improvement in the quality of polypyrrole film was achieved by K. Sekiguchi et al. [95] using the water and air stable ionic liquid 1-ethyl-3-methylimidazolium trifluoromethanesulfonate (EMIM CF_3SO_3). The imidazolium ionic liquids, having stable counter anions such as BF_4^-, PF_6^- and $CF_3SO_3^-$, were considered as good candidates for the polymerization process as they do not require special conditions to run the experiments. The room temperature ionic liquid EMIM CF_3SO_3, used as a medium for electropolymerization process, had improved

polymerization rate, electrochemical capacity and electroconductivity. This can be explained by the fact that the charge neutrality during film formation is maintained by anion and cation exchange with the ionic liquid [95].

Another conducting polymer, polythiophene has been of great interest for researchers because of its stability and good electrochemical properties and known also for its electrochromic properties. Compared to polypyrrole, both polythiophene and polythiophene derivatives have the great advantage of being stable to oxygen and moisture both in their undoped and in their doped states, and it can be considered a more superior material.

Electropolymerization of three derivatives of thiophene, 3-methylthiophene (MeT), 3-hexylthiophene (HexT) and 3-octylthiophene (OcT) was performed in ILs [96]. Spectroelectrochemical measurements of the electrochromic films obtained, poly(3-methylthiophene), poly(3-hexylthiophene) and poly(3-octylthiophene) were also performed. The thiophene derivatives, 3-hexylthiophene and 3-octylthiophene, were used in conjunction with 1-butyl-3-methylimidazolium hexafluorophosphate (BMIM PF_6), achieving quite high quality electrochromic polymers. Using ionic liquids both as solvent and electrolyte there is the advantage of carrying out the experiments at room temperature because BMIM PF_6 is stable to air and just a slight nitrogen overpressure was kept during the experiment. The total volume solutions of 5 ml which contained the ionic liquid BMIM PF_6 with monomer (0.1 M MeT, 0.1 M HexT or 0.1 M OcT) were used to obtain during successive electrodeposition poly(3-methylthiophene), poly(3-hexylthiophene) and poly(3-octylthiophene) respectively (Figure 1.15).

During the polymerization process a gradual increase in the current density on each potential sweep was seen, indicating the polymer film deposition at the electrode surface. Similar film thicknesses were obtained by simply adjusting the

number of potential scans (20 runs) in the potential window of -0.4 V to 1.7 V at 50 mV/s scan rate. As a result it is believed that polymer film of three-substituted thiophenes having long alkyl chain looks more uniform and this can be seen in the differences between oxidation/ reduction peak potentials (ΔE_p) which are smaller with increasing the length of alkyl chain as can be seen in Figure 1.14. ΔE_p values observed have decreased from 0.8 V for poly (3-methylthiophene), to 0.3 V for poly (3-hexylthiophene) and down to aproximatively 0.15 V for poly (3-octylthiophene).

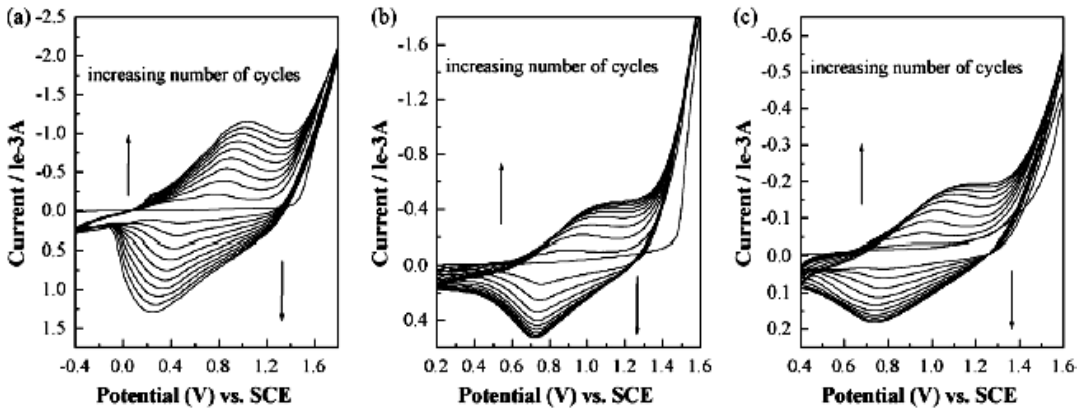

Figure 1.14 Cyclic voltammograms during electropolymerization of (a) 0.1 M MeT (20 runs), (b) 0.1 HexT (20 runs), (c) 0.1 M OcT (20 runs) on platinum sheet working electrode in pure [BMIM] [PF_6] ionic liquid. Scan rate: 50 mV/s. [96]

Also the voltammetry of the resulting films PMeT, PHexT and POcT was performed in pure ionic liquid BMIM PF_6 varying the scan rates between 10 to 400 mV/s. There is a linear relationship between peak currents upon oxidation/ reduction and square root of scan rate, which demonstrates that the processes are mainly diffusion controlled.

The 3-subtituted thiophene films exhibited very nice electrochromic behaviour. Different colours were obtained for the different redox states; the reduced form was bright red, orange red and orange yellow and bright blue, blue and black blue in the oxidized state for PMeT, PHexT and POcT.

Another advantage is that it provides some insight into the polymer colour according to the location of the absorption maxima and intensity of the peak on the main π-π* transitions. It was found that λ_{max} values for π-π* transitions in the completely reduced state for PMeT, PHexT and POcT are located at shorter wavelengths like 500, 460 and 440 nm. For display applications it is important that the polymer can change rapidly between oxidized and reduced states and can exhibit a striking colour change. In the paper by Y. Pang the square-wave method known as chronoabsorptometry was used to test the switching time and contrast of these polymers [96].

The results indicated improved electrochromic properties of poly (3-subtituted thiophenes) formed in the presence of an ionic liquid and they can serve as materials for designing electrochromic devices.

Another monomer available commercially since 1990 is 3,4-ethylenedioxythiophene (EDOT) which displays many interesting properties; high environmental stability, high conductivity and excellent transparency in its doped state. An interesting feature of EDOT is its progressive emergence as one building block for the synthesis of different classes of molecular π-conjugated systems. Overall poly(3,4-ethylenedioxythiophene) (PEDOT) is mentioned many times as a polymer exhibiting outstanding electrochemical stability while cycling, superior air and thermal stability and good electrical properties.

The paper by Shahada Ahmad, M. Deepa and S. Singh [97] reported the deposition of PEDOT in ionic liquid medium, in this case 1-ethyl-3.-methylimidazolium bis(perfluoroethylsulfonyl)imide (EMIM PFSI). During polymerization in the ionic liquid, both the cation (imidazolium) and the anion ($PFSI^-$) of the RTIL are swallowed by the polymer matrix and formed an integral part of the polymer. This difference regarding polymer doping illustrates that the

ionic liquid is both the growth medium and the dopant used to make the polymer film. The film was formed under potentiostatic conditions by applying a constant potential of +0.8 V for 5 minutes using a Ag/AgCl as pseudo-reference electrode. PEDOT was also successfully deposited (at constant potential of +0.8 V for 5 minutes) on SnO_2/F coated glass from an extremely hydrophobic ionic liquid without any additional dopant [97].

Since ionic liquids are known as charge-rich media mainly characterized by electrostatic forces, they become interesting for electrodeposition processes and film formation, especially because of the significant effect on the thermodynamics and kinetics processes. They represent a 'green' alternative to many traditional electrolytes. Ionic liquids have been used since their early development for many electrochemical processes and with a great range of materials [98].

Even though ionic liquids are characterised by various attractive physicochemical properties, they also present some drawbacks. The first condition for a successful electrochemical deposition of a conducting polymer is to find the appropriate ionic liquid. The choice of ionic liquid involves a series of other considerations such as stability, size and nature of ionic liquid ions, the monomer solubility and the viscosity parameter, which can influence the electropolymerization process.

When electrochemical deposition of conducting polymers is performed from ionic liquids, the high viscosity at room temperature (e.g. 1-Hexyl-3-Methylimidazolium Chloride) of some ionic liquids may inhibit formation of electroactive polymers at the electrode surface. A very high viscosity produces a significant decrease in the conductivity and slows down the rate of ion diffusion within the ionic liquid. Due to increased ion size (3-5 Å) of ionic liquids when

compared to aqueous electrolytes (1-2 Å), conductivity at the electrode/ionic liquid interface could be altered.

The water content in the atmosphere is a factor that should be taken into consideration, as water can affect the physical properties of many ionic liquids. In order to prevent moisture contamination, the ionic liquids should always be stored in a dry place. Another issue of ionic liquids refers to their purity, as air moisture has a negative impact on the properties of ionic liquids.

Another limitation is the high cost of ionic liquids. For the present work the relatively high cost of ionic liquids represented an inconvenience and this led to designing a different experimental set-up, namely 'microcell' which is described in Chapter 3.

1.7 Project Aim

The general aim of this project is to use conducting polymers (CPs), in conjunction with Room Temperature Ionic Liquids (RTILs), to produce electrochromic films. Such films, which change colour in response to electrical potential changes, could be used in electronic display devices and in light and energy-control applications (e.g. smart windows which control light transmittance). Most electrochromic materials suffer from manufacture and performance limitations (including stability issues). In addition they are generally made with relatively expensive and/or toxic compounds (making disposal difficult). Production of improved electrochromic devices, using a more environmentally-friendly "Green Chemistry" approach is a desirable goal. This project addresses many of these issues.

This project will produce valuable information concerning the electrochemical formation, optical and electrochemical performance and physical properties of both CPs and RTILs and the combined CP/RTILs system(s).

These main points were investigated and the findings will be discussed in the following chapters:

A. To investigate the electrochemical formation and characterization of poly (2,3,5,6-tetrafluroaniline) as electrochromic material in aqueous medium (Chapter 2).

B. To perform electrochemical copolymerization of 3,4-ethylenedioxythiophene and pyrrole monomers in RTILs and conduct further electrochemical studies of the new material (Chapter 3). Comparison will be made with published investigations concerning the role of various species, such as dopants in aqueous solutions versus RTILs.

C. To develop a method for employment of small quantities of ionic liquid for CPs formation and characterization (Chapter 3).

D. To use spectral monitoring to provide information on chromatic contrast, other optical properties and also some information of their response to electrical potential perturbations. Also comparison with the spectral characteristics of similar materials in conventional solvent/ electrolytes which will provide information concerning the role of the RTILs.

E. To perform the morphological characterisation of the polymeric materials using scanning electron microscopy (SEM).

F. To investigate the ion transport at the interface of a thin layer of IL and aqueous solutions/ buffer pH 7.0 using a model redox sytem (Chapter 4).

G. To develope a prototype device for an electrochromic cell using a new CP/ILs system.

1.8 References

[1] J.H. Clark, D.J. Macquarrie, Handbook of green chemistry and technology, Blackwell Science, Oxford; Malden, MA, 2002.
[2] P.T. Anastas, J.C. Warner, Green Chemistry: Theory and Practice, Oxford University Press, USA, 2000.
[3] T.A. Skotheim, R.L. Elsenbaumer, J.R. Reynolds, Handbook of conducting polymers, Marcel Dekker, 1998.
[4] R.J. Waltman, J. Bargon, Can J Chem, 64 (1986) 76-95.
[5] H. Ohno, Electrochemical Aspects of Ionic Liquids, Wiley, 2005.
[6] P. Danielsson, J. Bobacka, A. Ivaska, J Solid State Electr, 8 (2004) 809-817.
[7] P. Monk, R. Mortimer, D. Rosseinsky, Electrochromism and Electrochromic Devices, Cambridge University Press, 2007.
[8] X. Tu, X. Fu, Q. Jiang, Displays, 31 (2010) 150-154.
[9] J. Kawahara, P.A. Ersman, I. Engquist, M. Berggren, Org Electron, 13 (2012) 469-474.
[10] A. Ritter, Smart Materials in Architecture, Interior Architecture and Design, Birkhäuser, 2007.
[11] S.A. Sapp, G.A. Sotzing, J.L. Reddinger, J.R. Reynolds, Adv Mater, 8 (1996) 808-&.
[12] J. Duchet, R. Legras, S. Demoustier-Champagne, Synthetic Met, 98 (1998) 113-122.
[13] L.M. Martins dos Santos, J.C. Lacroix, K.I. Chane-Ching, A. Adenier, L.M. Abrantes, P.C. Lacaze, J Electroanal Chem, 587 (2006) 67-78.
[14] A.J. Heeger, Rev Mod Phys, 73 (2001) 681-700.
[15] A.G. MacDiarmid, Angewandte Chemie International Edition, 40 (2001) 2581-2590.
[16] G. Inzelt, Conducting Polymers: A New Era in Electrochemistry, Springer, 2008.
[17] J.L. Bredas, R.R. Chance, R. Silbey, Phys Rev B, 26 (1982) 5843-5854.
[18] J.L. Bredas, G.B. Street, Accounts Chem Res, 18 (1985) 309-315.
[19] R.J. Mortimer, Electrochim Acta, 44 (1999) 2971-2981.
[20] R. Holze, Electrochim Acta, 56 (2011) 10479-10492.
[21] B. Garcia, D. Bélanger, Synthetic Met, 98 (1998) 135-141.
[22] M. Deepa, S. Ahmad, Eur Polym J, 44 (2008) 3288-3299.
[23] M. Deepa, A. Awadhia, S. Bhandari, S.L. Agrawal, Electrochim Acta, 53 (2008) 7266-7275.
[24] J.M. Pringle, M. Forsyth, D.R. MacFarlane, K. Wagner, S.B. Hall, D.L. Officer, Polymer, 46 (2005) 2047-2058.
[25] H. Tang, A. Kitani, M. Shiotani, Electrochim Acta, 41 (1996) 1561-1567.
[26] P.C. Innis, J. Mazurkiewicz, T. Nguyen, G.G. Wallace, D. MacFarlane, Curr Appl Phys, 4 (2004) 389-393.
[27] M.D. Levi, C. Lopez, E. Vieil, M.A. Vorotyntsev, Electrochim Acta, 42 (1997) 757-769.
[28] J. Chengyou, Y. Fenglin, Sensors and Actuators B: Chemical, 114 (2006) 737-739.
[29] M. Freund, B. Deore, Self-doped conducting polymers, John Wiley & Sons, 2007.
[30] J.-H. Kang, Y.-J. Oh, S.-M. Paek, S.-J. Hwang, J.-H. Choy, Solar Energy Materials and Solar Cells, 93 (2009) 2040-2044.

[31] P. Camurlu, C. Gültekin, Solar Energy Materials and Solar Cells, 107 (2012) 142-147.
[32] R.J. Mortimer, A.L. Dyer, J.R. Reynolds, Displays, 27 (2006) 2-18.
[33] R.J.M. P.M.S. Monk, D.R. Rosseinsky, Electrochromism: Fundamentals and Applications, Cambridge University Press, New York, 1995.
[34] R.J. Mortimer, Chem Soc Rev, 26 (1997) 147-156.
[35] J. Bobacka, A. Lewenstam, A. Ivaska, J Electroanal Chem, 489 (2000) 17-27.
[36] W.C. Chen, T.C. Wen, C.C. Hu, A. Gopalan, Electrochim Acta, 47 (2002) 1305-1315.
[37] C.-W. Hu, K.-M. Lee, K.-C. Chen, L.-C. Chang, K.-Y. Shen, S.-C. Lai, T.-H. Kuo, C.-Y. Hsu, L.-M. Huang, R. Vittal, K.-C. Ho, Solar Energy Materials and Solar Cells, 99 (2012) 135-140.
[38] L. Ma, Y. Li, X. Yu, Q. Yang, C.-H. Noh, Solar Energy Materials and Solar Cells, 92 (2008) 1253-1259.
[39] K. Crowley, J. Cassidy, J Electroanal Chem, 547 (2003) 75-82.
[40] A. Azens, C.G. Granqvist, Appl Phys Lett, 81 (2002) 928-929.
[41] S.-H. Lee, P. Liu, H.M. Cheong, C.E. Tracy, S.K. Deb, Solid State Ionics, 165 (2003) 217-221.
[42] P.R. Patil, S.H. Pawar, P.S. Patil, Solid State Ionics, 136–137 (2000) 505-511.
[43] A. Azens, J. Isidorsson, R. Karmhag, C.G. Granqvist, Thin Solid Films, 422 (2002) 1-3.
[44] H.-S. Shim, V.R. Shinde, H.J. Kim, Y.-E. Sung, W.B. Kim, Thin Solid Films, 516 (2008) 8573-8578.
[45] P.R. Somani, S. Radhakrishnan, Mater Chem Phys, 77 (2003) 117-133.
[46] C.G. Granqvist, Handbook of Inorganic Electrochromic Materials, Elsevier Science, 1995.
[47] J. Zhang, X.L. Wang, X.H. Xia, C.D. Gu, Z.J. Zhao, J.P. Tu, Electrochim Acta, 55 (2010) 6953-6958.
[48] K. Sauvet, L. Sauques, A. Rougier, J Phys Chem Solids, 71 (2010) 696-699.
[49] S.A. Mahmoud, S.A. Aly, M. Abdel-Rahman, K. Abdel-Hady, Physica B: Condensed Matter, 293 (2000) 125-131.
[50] E. Avendano, L. Berggren, G.A. Niklasson, C.G. Granqvist, A. Azens, Thin Solid Films, 496 (2006) 30-36.
[51] M. Ferenets, A. Harlin, Thin Solid Films, 515 (2007) 5324-5328.
[52] S.B. Saidman, O.V. Quinzani, Electrochim Acta, 50 (2004) 127-134.
[53] T. Tesfamichael, N. Motta, T. Bostrom, J.M. Bell, Applied Surface Science, 253 (2007) 4853-4859.
[54] J. Velevska, M. Ristova, Solar Energy Materials and Solar Cells, 73 (2002) 131-139.
[55] S.A. Mahmoud, A.A. Akl, H. Kamal, K. Abdel-Hady, Physica B: Condensed Matter, 311 (2002) 366-375.
[56] H. Kamal, E.K. Elmaghraby, S.A. Ali, K. Abdel-Hady, Thin Solid Films, 483 (2005) 330-339.
[57] S.J. Yoo, J.W. Lim, Y.-E. Sung, Solar Energy Materials and Solar Cells, 90 (2006) 477-484.
[58] E. Avendaño, A. Azens, J. Isidorsson, R. Karmhag, G.A. Niklasson, C.G. Granqvist, Solid State Ionics, 165 (2003) 169-173.
[59] E. Masetti, F. Varsano, F. Decker, A. Krasilnikova, Electrochim Acta, 46 (2001) 2085-2090.
[60] R. Sivakumar, A. Moses Ezhil Raj, B. Subramanian, M. Jayachandran, D.C. Trivedi, C. Sanjeeviraja, Materials Research Bulletin, 39 (2004) 1479-1489.
[61] G.A. Sotzing, J.R. Reynolds, P.J. Steel, Chem Mater, 8 (1996) 882-889.

[62] V. Jain, R. Sahoo, J.R. Jinschek, R. Montazami, H.M. Yochum, F.L. Beyer, A. Kumar, J.R. Heflin, Chemical Communications, (2008) 3663-3665.
[63] O. Winther-Jensen, S. Desai, R.L. Shepherd, P.C. Innis, B. Winther-Jensen, M. Forsyth, G.G. Wallace, D.R. MacFarlane, Electrochem Commun, 12 (2010) 1505-1508.
[64] B.C. Thompson, P. Schottland, G. Sonmez, J.R. Reynolds, Synthetic Met, 119 (2001) 333-334.
[65] R.L. Elsenbaumer, K.Y. Jen, G.G. Miller, L.W. Shacklette, Synthetic Met, 18 (1987) 277-282.
[66] J.D. Stenger-Smith, Progress in Polymer Science, 23 (1998) 57-79.
[67] R. J. Mortimer, T.S. Varley, Displays, xxx (2010).
[68] S.K. Shevell, The science of color, Second Edition ed., Optical Society of America, 2003.
[69] D.M. Welsh, A. Kumar, E.W. Meijer, J.R. Reynolds, Adv Mater, 11 (1999) 1379-1382.
[70] I. Schwendeman, R. Hickman, K. Zong, D.M. Welsh, J.R. Reynolds, J. Hwang, D.B. Tanner, Abstr Pap Am Chem S, 223 (2002) D66-D66.
[71] C. Chiappe, D. Pieraccini, Journal of Physical Organic Chemistry, 18 (2005) 275-297.
[72] B. Bittner, R.J. Wrobel, E. Milchert, The Journal of Chemical Thermodynamics, 55 (2012) 159-165.
[73] S. Desai, R.L. Shepherd, P.C. Innis, P.Murphy, C. Hall, R. Fabretto, G.G. Wallace, Electrochim Acta, (2010).
[74] A.P. Abbott, K.J. McKenzie, Phys Chem Chem Phys, 8 (2006) 4265-4279.
[75] P. Yu, J. Yan, J. Zhang, L. Mao, Electrochem Commun, 9 (2007) 1139-1144.
[76] F. Endres, ChemPhysChem, 3 (2002) 144-154.
[77] F. Endres, D. MacFarlane, A. Abbott, Electrodeposition from Ionic Liquids, Wiley, 2008.
[78] M. Galinski, A. Lewandowski, I. Stepniak, Electrochim Acta, 51 (2006) 5567-5580.
[79] F. Endres, Phys Chem Chem Phys, 14 (2012) 5008-5009.
[80] Y. Kohno, H. Ohno, Chemical Communications, 48 (2012) 7119-7130.
[81] K.R. Seddon, Nat Mater, 2 (2003) 363-365.
[82] M. Petkovic, K.R. Seddon, L.P.N. Rebelo, C. Silva Pereira, Chem Soc Rev, 40 (2011) 1383-1403.
[83] J. Ding, D.Z. Zhou, G. Spinks, G. Wallace, S. Forsyth, M. Forsyth, D.R. MacFarlane, Chem Mater, 15 (2003) 2392-2398.
[84] A. Balducci, U. Bardi, S. Caporali, M. Mastragostino, F. Soavi, Electrochem Commun, 6 (2004) 566-570.
[85] J.D. Stenger-Smith, C.K. Webber, N. Anderson, A.P. Chafin, K.K. Zong, J.R. Reynolds, J Electrochem Soc, 149 (2002) A973-A977.
[86] W. Lu, A.G. Fadeev, B.H. Qi, E. Smela, B.R. Mattes, J. Ding, G.M. Spinks, J. Mazurkiewicz, D.Z. Zhou, G.G. Wallace, D.R. MacFarlane, S.A. Forsyth, M. Forsyth, Science, 297 (2002) 983-987.
[87] C.H. Yang, Q.J. Sun, J. Qiao, Y.F. Li, J Phys Chem B, 107 (2003) 12981-12988.
[88] K.N. Marsh, J.A. Boxall, R. Lichtenthaler, Fluid Phase Equilibr, 219 (2004) 93-98.
[89] S.V. Dzyuba, R.A. Bartsch, Chemphyschem, 3 (2002) 161-+.
[90] P. Bonhote, A.P. Dias, N. Papageorgiou, K. Kalyanasundaram, M. Gratzel, Inorg Chem, 35 (1996) 1168-1178.

[91] F. Endres, Andrew P. Abbott, D.R. Macfarlane, Electrodeposition from ionic liquids, Wiley-VCH Verlag GmbH & Co. KGaA, 2008.
[92] L.C. Weiwei Liu, Yumei Zhang, Huaping Wang, Mingfang Yu, Journal of Molecular Liquids, 140 (2008) 68-72.
[93] W. Liu, T. Zhao, Y. Zhang, H. Wang, M. Yu, J Solution Chem, 35 (2006) 1337-1346.
[94] J.M. Pringle, J. Efthimiadis, P.C. Howlett, J. Efthimiadis, D.R. MacFarlane, A.B. Chaplin, S.B. Hall, D.L. Officer, G.G. Wallace, M. Forsyth, Polymer, 45 (2004) 1447-1453.
[95] K. Sekiguchi, M. Atobe, T. Fuchigami, Electrochem Commun, 4 (2002) 881-885.
[96] Y.H. Pang, X.Y. Li, H.L. Ding, G.Y. Shi, L.T. Jin, Electrochim Acta, 52 (2007) 6172-6177.
[97] S. Ahmad, M. Deepa, S. Singh, Langmuir, 23 (2007) 11430-11433.
[98] D.R. MacFarlane, J.M. Pringle, P.C. Howlett, M. Forsyth, Phys Chem Chem Phys, 12 (2010) 1659-1669.

Chapter 2. Electrochemical and Electrochromic Properties of Poly-(2,3,5,6-Tetrafluoroaniline) Thin Films in Aqueous Solution

2.1 Introduction

As described in chapter 1, electronically conductive polymers are an extremely interesting class of materials that have gained popularity in the last decade. This is seen in the variety of industrial applications available, which include sensors [1] and batteries [2].

Polypyrrole (PPy), polythiophene (PTh) and polyaniline (PANI) [3] [4] are formed during anodic oxidation and are amongst the most extensively studied electroactive polymers [5]. Polyaniline (PANI) and its derivatives are of particular interest due to their stability [6], but also because of the low cost and ease of preparation. Polyaniline belongs to the family of conducting polymers resulting from the oxidation of aniline monomers during the electropolymerization process.

Polyaniline (PANI) can be found in a variety of forms that differ in chemical and physical properties. This polymer is particularly interesting because of the three oxidation states which can occur: leucoemeraldine -white/clear and colourless, emeraldine - green or blue, pernigraniline -blue/violet. These oxidation states are represented in Figure 2.1.

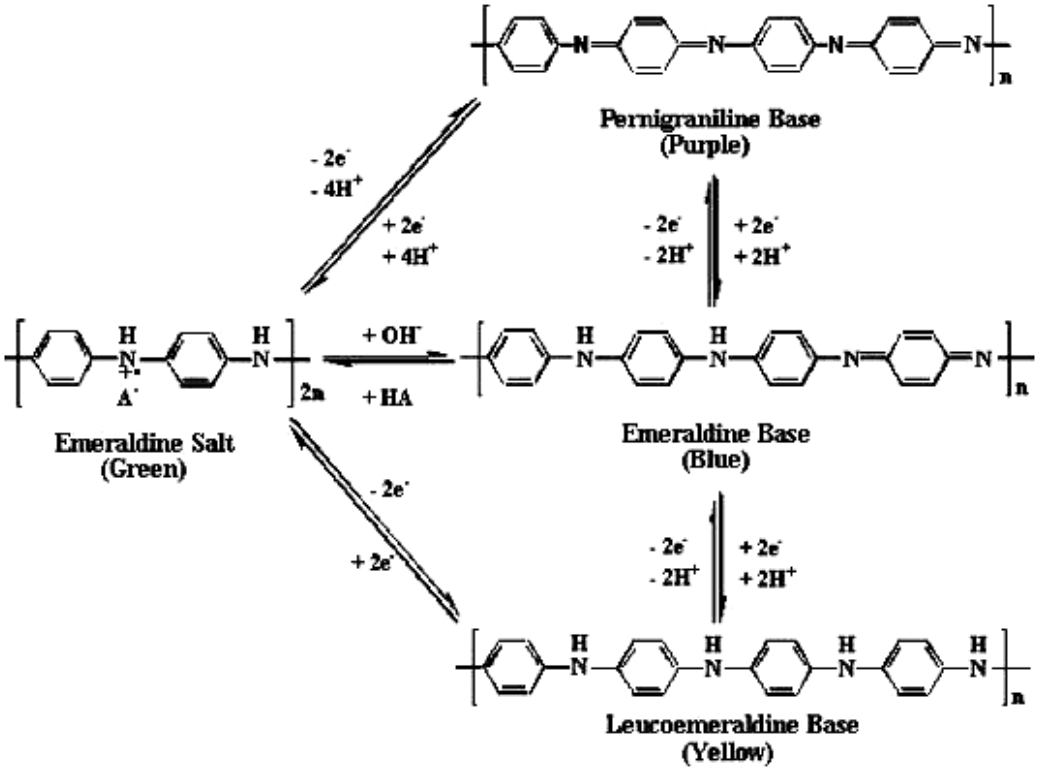

Figure 2.1 Various possible oxidation states of polyaniline [7]

The leucoemeraldine form represents the fully reduced form, emeraldine is half-oxidized and pernigraniline is the fully oxidized state of polyaniline. The electrical conductivity of polyaniline based materials can be closely controlled over a wide range. For neat polyaniline, conductivity levels as high as 100 S cm^{-1} can be achieved. The full range of conductivity levels from less than 10^{-10} to 10^{-1} S cm^{-1} (melt processing) to 10 S cm^{-1} [8] (solution processing), can be achieved for polymer blends containing polyaniline.

Polyaniline films have been formed during electrochemical deposition using potentiostatic, potentiodynamic and galvanostatic methods [9]. However, only the potentiodynamic method known as cyclic voltammetry (CV) [10] was most useful in understanding the electrochemical behaviour of polyaniline. Cycling voltammetry offered the possibility of switching between the polymer oxidation states: leucoemeraldine (neutral), emeraldine (polaron) and pernigraniline (bipolaron).

According to the different oxidation forms, the electrical conductivity of polyaniline based materials may be closely controlled over a wide potential range. The most common, protonated emeraldine, can display a high conductivity of almost 100 S cm^{-1}, similar to that of a semiconductor [9].

Polymerization of aniline monomers containing fluorine has been performed both chemically and electrochemically; however the properties of these polymers have not been fully characterised. Monofluoro-substituted anilines [11] have been synthesised from acidic solutions using a chemical oxidation process and characterised by a range of spectroscopic methods. Upon chemical synthesis of poly(2-fluoroaniline) and poly(3-fluoroaniline), the absorption spectra showed similar features to that of the 2-fluoroaniline monomer. Dehalogenation occurred during polymerization of the 4-fluoroaniline monomer, with fluorine being displaced to yield a more favourable head-to-tail polymer, with the resultant UV-Vis spectrum being identical to that of polyaniline [11]. However, solubilities of polyfluoroanilines in organic solvents were improved in comparison to polyaniline [11].

Poly(tetrafluroaniline) has been previously used as a substrate for a bacterial fuel cell [9], but was not examined as an electrochromic material. In this work electrochemical polymerization of 2,3,5,6-tetrafluoroaniline was carried out in aqueous-acidic solutions by applying constant potentials for different time periods. Poly(2,3,5,6-tetrafluoroaniline) modified platinum electrodes showed improved stability compared to poly(2-fluoroaniline) when they were exposed to microbially aggressive conditions such as sewage or sewage sludge for long time periods [9]. Poly(2,3,5,6-tetrafluoroaniline) proved to be the most resistive material towards microbial degradation and prevented poisoning of platinum by metabolic by-products [9].

The electrochemical behaviour of different mono-fluoroanilines (2-fluoroaniline, 3-fluoroaniline and 4-fluoroaniline) electrodeposited on a platinum

electrode were examined in both aqueous acidic and organic media using $NaClO_4$ as supporting electrolyte [12]. During electrochemical oxidation, poly (2-, 3- and 4-) fluoroanilines were successfully deposited on the surface of the electrode, but the transition from the emeraldine to the pernigraniline form was not observed, due to presence of the fluorine electron withdrawing group [12].

A significant number of reports have described the development of transparent conducting polymers and in particular the use of chemically synthesized poly(3,4-ethylenedioxythiophene) (PEDOT) with polystyrenesulphonate (PSS) as counter ion to form conductive films. For example, dispersions of films of PEDOT: PSS in DMSO with single walled carbon nanotubes have been sprayed on polyethyleneterephthalate (PET) [13]. The resultant films had a resistance of 118 Ω/sq and 90 % transmittance over the wavelength range 400 - 800 nm. When the in-situ polymerization of EDOT with 2,3-dichloro-5,6-dicyanobenzoquinone (DDQ) (molar ratio of 1: 1.33) was performed, films with 80 % transmittance over the range 300 – 700 nm were obtained [14]. Similar films have been formed with a sulfonated derivative of polythiophene [15]. Even though these films were able to switch between coloured and colourless (transparent) redox states, no electrochromic studies have been described for these transparent polymers. However a polypyrrole/ polythiophene co-polymer had a broad absorbance between 400 nm and 800 nm while reduced [16]. Upon oxidation a strong absorbance band at 600 nm occurred. A co-polymer of aniline/ thiophene displayed a relatively constant change in absorbance over the visible range with various applied potentials, but a slight absorbance maximum at 800 nm appeared [17]. When constant potentials from 0 V to 1.9 V were applied until the oxidized state was reached, the UV-Vis absorbance of aniline/ thiophene copolymer successively increased.

No electrochromic studies of PTFA material have been described to date. In this study the formation of PTFA thin films on a conducting ITO substrate by

successive potential cycling in acidic solutions was achieved and characterised by electrochemical and spectroscopic techniques. The electrochemical study of PTFA electrodes was examined in solutions containing monomer, and also in aqueous-acidic conditions with and without the addition of tetrahydrofuran (THF). The effects of different electrolytes on the properties of the polymer are described. Beside spectroelectrochemistry, the chronoamperometry technique was utilized in order to investigate the PTFA electrochromic behaviour. From the chronoamperometric studies it was seen that PTFA required around 40 s to switch between its redox states. In addition, SEM analysis of the PTFA polymer was used to characterize the film morphology. XPS was employed to characterise the oxidised and reduced states of the material.

2.2 Experimental

The 2,3,5,6-tetrafluoroaniline and tetrahydrofuran were purchased from Sigma-Aldrich and perchloric acid (60%) from BDH Laboratory Supplies, UK. In order to avoid degradation, 2,3,5,6-tetrafluoroaniline was stored under dry conditions away from moisture. Cyclic voltammetry (CV) was employed to grow PTFA films onto conducting indium tin oxide glass (ITO). A three electrode cell was used with an ITO glass slide (Solaronix, Switzerland), platinum coil (0.5 mm, Alfa-Aesar, UK) and Ag/AgCl (3M KCl) (CH Instruments Inc, UK) as working, counter and reference electrodes, respectively. All potentials were reported versus Ag/AgCl (3M KCl).

The dimensions of the ITO electrodes were 0.5 cm x 2.5 cm and the electrodes connections were made with conductive silver-epoxy adhesive. The ITO sheet resistance was 18 ohms per square (ohm/sq). The electrodes were carefully cleaned by successive ultrasonication in deionized water, followed by acetone and then deionized water to ensure removal of all traces of acetone and finally dried in air prior to use. Deionized water with a resistivity of 18 MΩ cm (Elgastat Maxima) was used for all studies. Solutions (10 ml volume) containing 50 mM monomer (2,3,5,6-tetrafluoroaniline) and 2 M $HClO_4$ were prepared in deionized water. Monomer solutions were deoxygenated with nitrogen for 5 minutes before starting the CV experiments. All solutions were freshly prepared for each experiment and all measurements were performed at room temperature. The electrodes were connected to a three-electrode CHI 620 model potentiostat. UV-Vis absorption spectra were recorded on a Shimadzu 1800 UV-Vis spectrophotometer.

Chronoamperometry was used to determine the value of the coloration efficiency when the potential was successively switched between 0 V to 1.2 V. SEM images of PTFA films were obtained using a Hitachi SU-70 scanning electron

microscope. X-ray photoelectron spectroscopy (XPS) analysis was obtained on a AXIS 165 X-ray photoelectron spectrometer**.**

2.3 Results and Discussion

2.3.1 Cyclic Voltammetry of PTFA on ITO Substrate

PTFA films were deposited onto ITO electrodes during successive potential cycling in aqueous media with the addition of perchloric acid ($HClO_4$) as dopant. The best electrochemical window to grow PTFA on an ITO substrate was in the potential range -0.2 V to +1.4 V at a constant scan rate of 40 mVs^{-1}. The current density increased with the number of potential scans, which indicated formation of a PTFA layer on the ITO electrode (Figure 2.2). The peak currents increased slightly at ca. 0.9 V on successive scans. On the anodic potential scan, monomer oxidation seemed to have started at a potential of ca. 1.2 V. The films formed (Figure 2.2) were thin films since thicker films possess an increased resistance which can compromise the conductivity of the polymers.

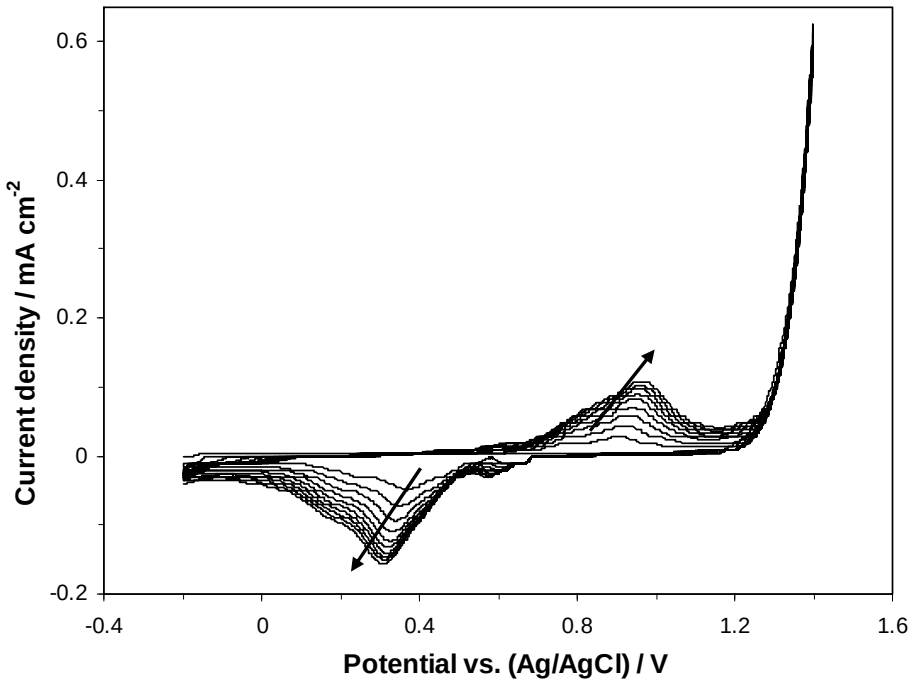

Figure 2.2 Cyclic voltammograms of PTFA film deposited on ITO glass from an aqueous solution containing 50 mM TFA and 2 M $HClO_4$. Scan rate of 40 mVs^{-1}. Number of cycles: 15.

As the number of cycles increased, the potential corresponding to oxidation of the polymer increased to more positive values and the potential for reduction to more negative values. The large separation of anodic and cathodic peaks resulted in an asymmetric CV (Figure 2.2). Also on the reduction step, close to the main reduction peak at 0.3 V, an additional peak appeared at 0.6 V as film thickness was increased. The appearance of the small peak at ca. 0.6 V was dependent on the upper potential limit. When a higher potential of 1.6 V was used, the reduction peak potential at 0.3 V also shifted to 0.4 V.

Electropolymerisation of 2,3,5,6-tetrafluoroaniline on ITO is proposed to occur via the same mechanism (Figure 2.3) described for the polymerisation of aniline. As evident from the first anodic scan, it is the electron-withdrawing effect of fluorine which most likely gives rise to the increase in potential required for monomer oxidation. On continuous sweeping, the peak potential separation increased indicating that the polymer oxidation/ reduction process is more difficult and this was due to the increased hydrophobicity of the film. Previous work involved PTFA electrodeposition as thin films on fluorine doped SnO_2 (FTO). However, the PTFA films on fluorine doped SnO_2 showed very poor electrochemical response and all studies were thus performed with ITO electrodes.

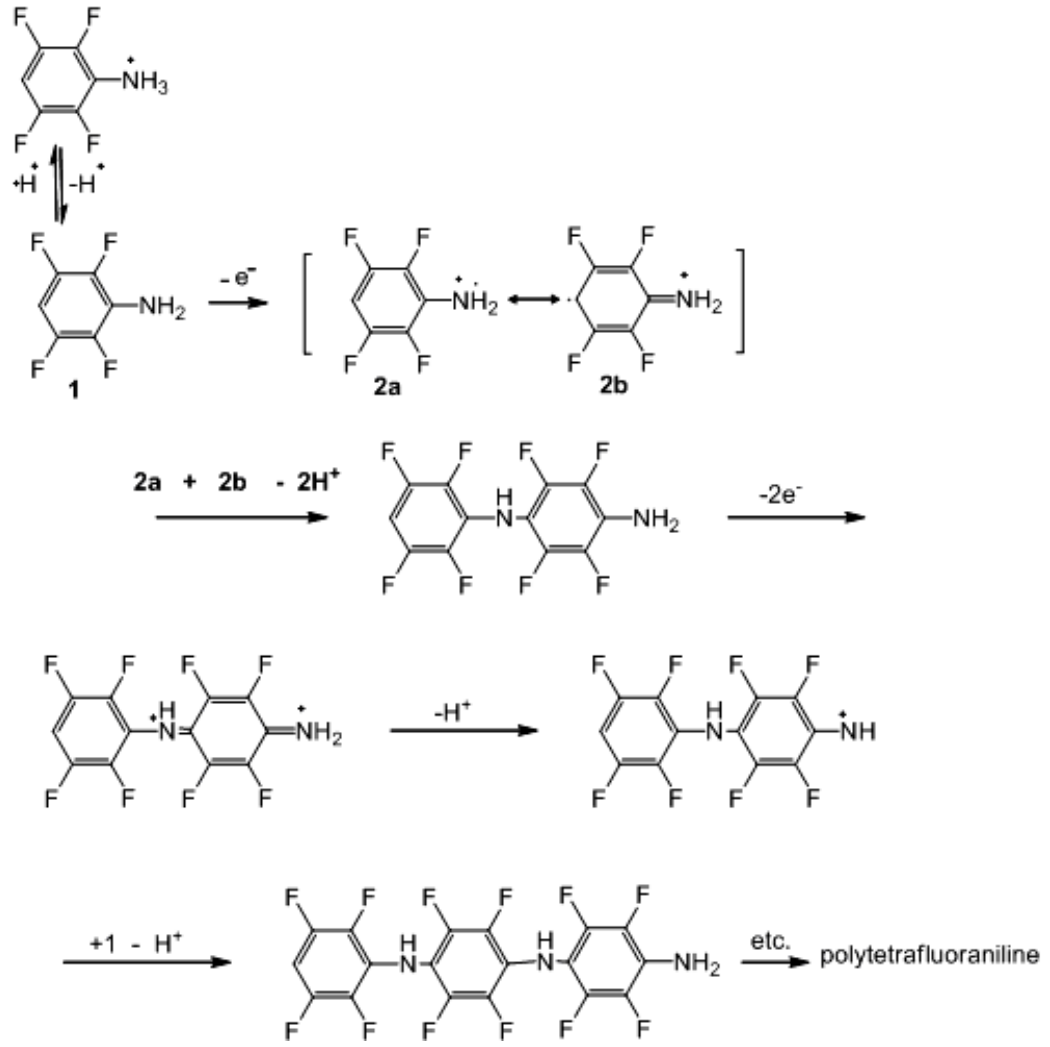

Figure 2.3 Proposed mechanism for polymerisation of 2,3,5,6-tetrafluoroaniline

2.3.2 Electrochemical Characterization of the PTFA/ITO Films

PTFA polymer characterization was performed in different solutions: with background electrolyte alone, with the addition of monomer, or with the addition of tetrahydrofuran. The nature of the supporting electrolyte used during electrochemical cycling of PTFA indicated that it has a considerable influence on the properties of the polymer [18]. Voltammetric characterization of the PTFA films deposited on ITO glass

was performed in the same solution used for film formation, over the potential range -0.2 V and 1.0 V to avoid further monomer oxidation. The polymer was characterised in the presence of the monomer as the voltammetric response deteriorated in solutions containing only background electrolyte. The resultant cyclic voltammograms (Figure 2.4) exhibited a similar response to that obtained during polymer deposition (Figure 2.2). On the cathodic sweep, both anodic (j_{pa}) and cathodic (j_{pc}) peak currents were well defined, while upon oxidation the peak potentials shifted towards more positive values with increasing scan rate. The ratio of j_{pa} to j_{pc} should be close to one for an ideal thin layer system, but the rate of the oxidation process was slow and j_{pa} could not be determined (Figure 2.4).

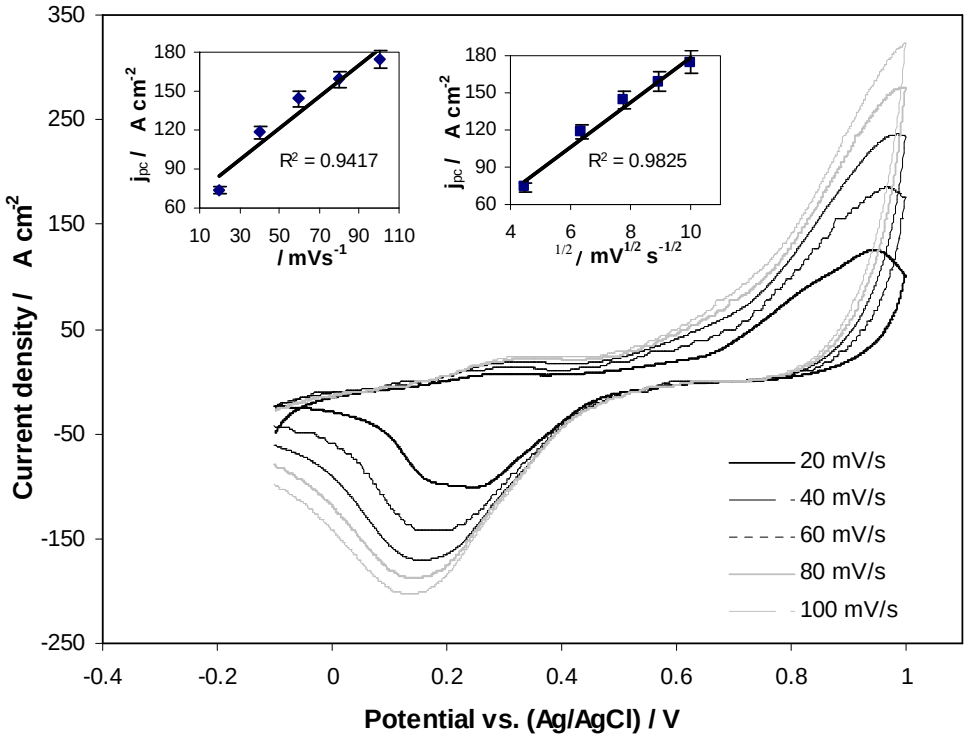

Figure 2.4 Cyclic voltammograms of PTFA film as a function of scan rate in a solution containing 50 mM TFA and 2 M $HClO_4$. Inset graph shows plot of cathodic peak current vs. scan rate ( ) and square root of scan rate ( ).

Cyclic voltammograms of films in the presence of monomer displayed an increase in the oxidation peak potential with increasing scan rate and also a slight shift in the peak potentials with increased scan rate. The inset in Figure 2.4 shows that the polymer does not display thin layer behaviour, instead displaying behaviour corresponding to bulk diffusion. The linear plot of j_p versus square root of scan rate ($^{1/2}$) can be ascribed to slow ion movement arising from the hydrophobic nature of the film [19].

On transferring the electrode to monomer-free solution containing 2 M $HClO_4$ a dramatic change in response was observed (Figure 2.5). The anodic peak currents were significantly reduced and the peaks broadened, possibly indicating that ion incorporation during the polymer oxidation/ reduction process was not rapid. It is obvious that the absence of the monomer caused a decrease in the peak currents which are three times lower in 2 M $HClO_4$ compared to those in the monomer solution. The electrochemical response of PTFA in background electrolyte alone is in contrast with other conducting polymers such as polypyrrole and polythiophene which have large capacitive currents [20] [21]. In general, for conducting polymers the conductivity correlates with the capacitance of the film [22]. In aqueous 2 M $HClO_4$ the decrease in current densities is due to a loss in conductivity of the film.

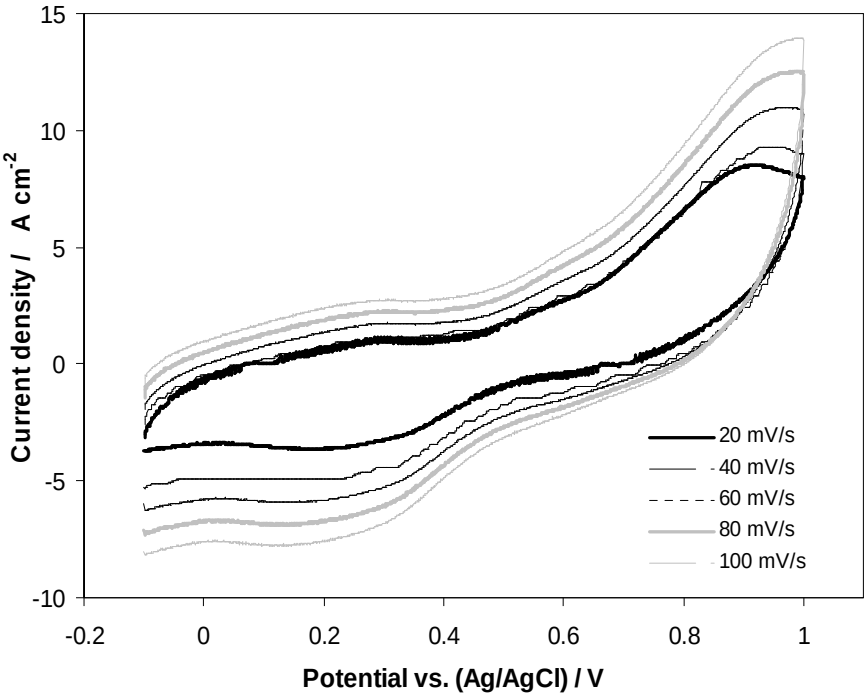

Figure 2.5 Cyclic voltammograms of PTFA film deposited on ITO as a function of scan rate in 2 M $HClO_4$ aqueous solution.

It was interesting to note that after the PTFA film was removed from the electrolyte solution and placed back in the monomer solution, the polymer recovered its electroactivity (Figure 2.6). This test indicated that PTFA preserved its conducting polymer features only when it was kept in its growth medium. There was an obvious similarity of the shape of the PTFA film scanned for the first time in monomer solution (Figure 2.4). The peak currents of PTFA films were drastically decreased in the monomer-free solution, which had diminished the film's electroactivity (Figure 2.5).

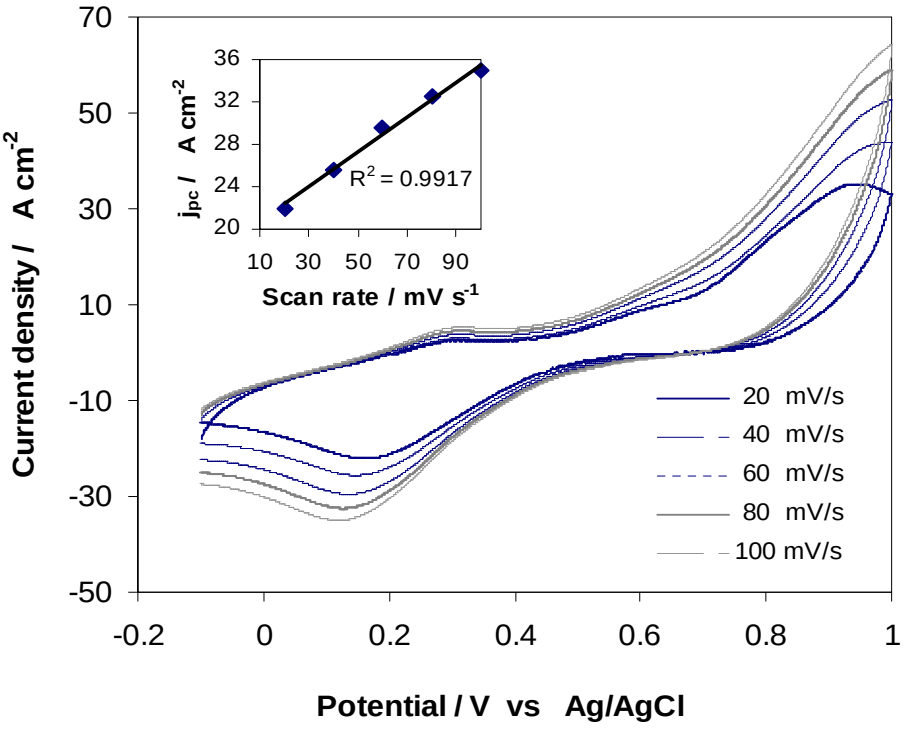

Figure 2.6 CVs of PTFA film removed from 2 M $HClO_4$ electrolyte solution placed back in 50 mM TFA/ 2 M $HClO_4$ monomer solution. Inset graph shows plot of cathodic peak current vs. scan rate ( ).

PTFA films also could be formed on FTO glass in the potential range of -0.2 V to 1.6 V versus Ag/AgCl (3 M KCl). Films formed on FTO were more resistive due to the increased oxidation potential of the monomer recorded at 1.6 V (Figure 2.7.a). During successive potential cycling in background electrolyte (2 M $HClO_4$), the PTFA/ FTO films showed a decrease of electrochemical response and the peak currents couldn't be measured (Figure 2.7.b). When FTO substrate was replaced by ITO substrate it was possible to deposit PTFA thin films with decreased resistivity at lower oxidation potentials like in Figure 2.4.

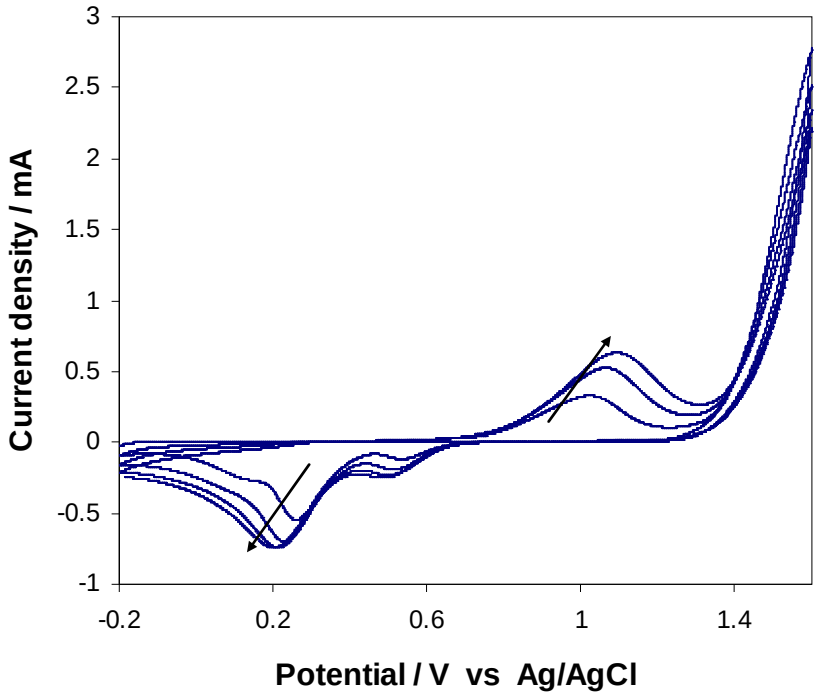

Figure 2.7.a Cyclic voltammograms of PTFA film deposited on FTO glass from an aqueous solution containing 50 mM TFA and 2 M $HClO_4$. Scan rate of 40 mVs^{-1}. Number of cycles: 4.

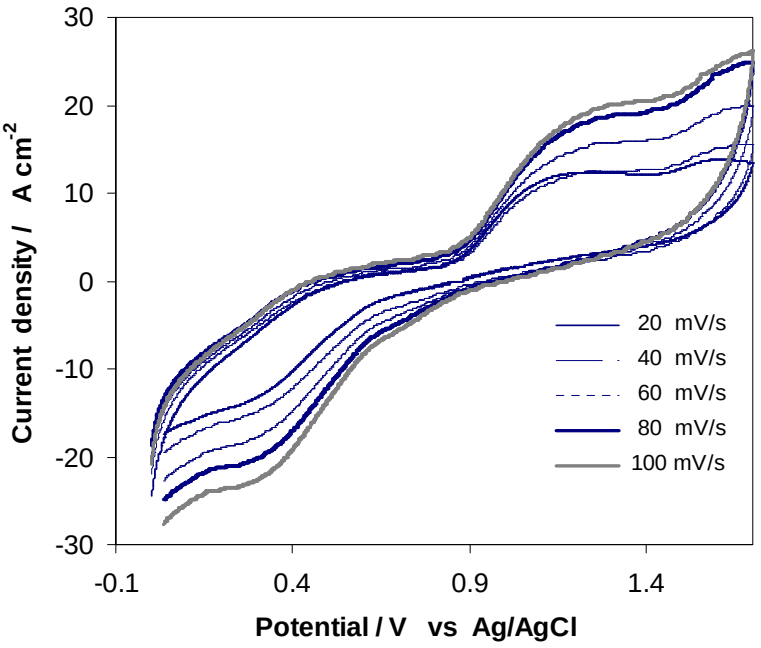

Figure 2.7.b Cyclic voltammograms of PTFA film deposited on FTO as a function of scan rate in 2 M $HClO_4$ aqueous solution.

The addition of tetrahydrofuran to the aqueous 2 M $HClO_4$ solution changed the electrochemical behaviour of the polymer (Figure 2.8). Tetrahydrofuran (THF) is a polar aprotic solvent characterised by a low dielectric constant of 7.5 [23]. In the presence of THF there was an obvious increase in the peak currents. This could be possible because the hydrophobic polymeric layer was more opened pore and allowed counter ions to move in and out more readily during the redox cycle.

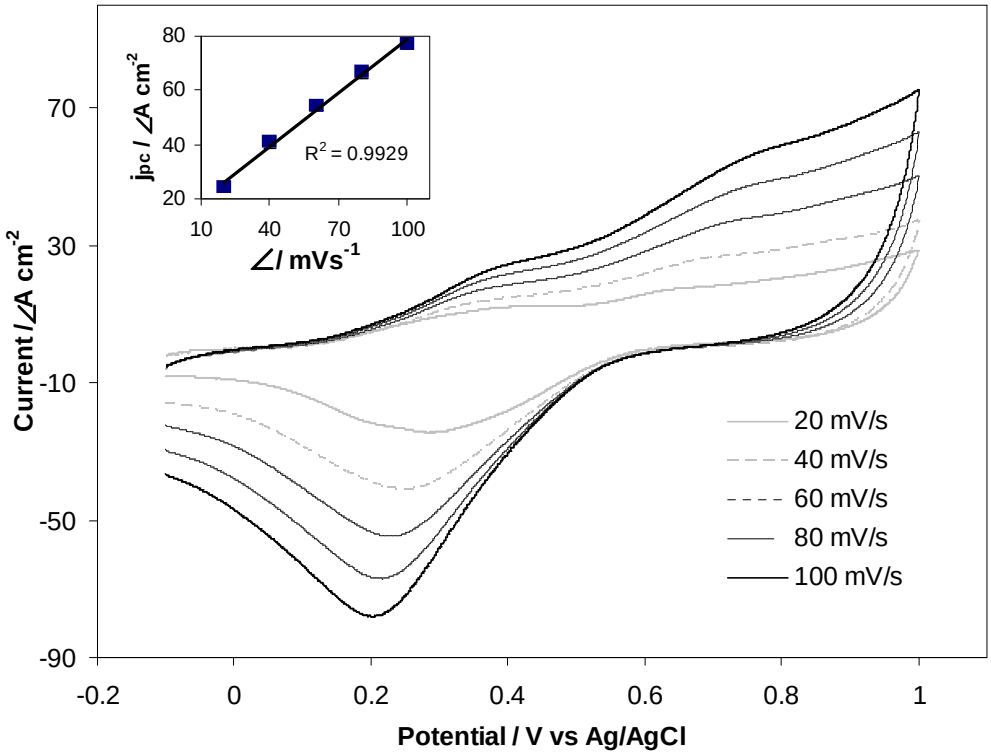

Figure 2.8 Cyclic voltammograms of a PTFA film on ITO in 2 M $HClO_4$ aqueous solution with 16.66 % THF.

In contrast to the data shown in Figure 2.4, the reduction peak current increased linearly with scan rate, indicative of thin layer behaviour [24] (Figure 2.8). An electrochemical study of PTFA in 2 M $HClO_4$ while increasing the THF amount was performed (Figure 2.9). Increasing the amount of THF resulted in increases in the peak current which are associated with increased ion mobility into and out of the film during the redox cycle

(Figure 2.9). It could be seen that for 16.66 % and 20.00 % THF present in solution, the peak currents were definitely greater compared to the others (4.76 %, 9.09 %, 13.04 %) and the reduction peak was well defined.

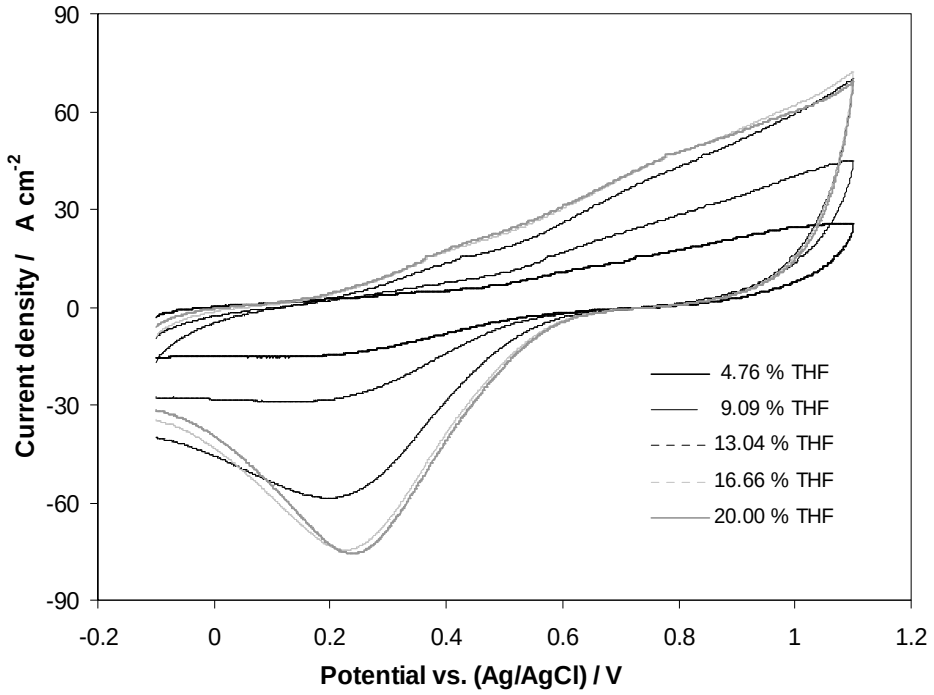

Figure 2.9 Cyclic voltammograms of a PTFA film cycled at 100 mVs^{-1} in 2 M $HClO_4$ aqueous electrolyte while increasing the tetrahydrofuran concentration.

Attempts were made to fully understand the PTFA nature, by describing both ion and electron exchange with the polymer, the polymer matrix and charging of the interfaces.

A more detailed mechanism of spatial and temporal charging was proposed as results of improved electrochemical behaviour of PTFA when THF was present in the solution. In opposition to the behaviour of other conducting polymers such as polypyrrole, polythiophenes that have both significant faradaic and capacitive component, the PTFA polymer suffers from lack of capacitive currents. All these lead to a question: can PTFA be named a conducting polymer? The two diagrams in Figure

2.10 were designed to explain the fundamental process of insertion/ expulsion and transport of charges through this type of electrochemical system.

It was suggested that the hydrophobic nature of PTFA generates the slow redox process in monomer-free solution, as the polymer has a closed structure and does not facilitate the charge transport.

The attention should be focused on the, two-phase distribution of 'deeply trapped' ions in the double layer at the film/electrode interface and 'slightly trapped' ions in the bulk of the films. Addition of different amounts of aprotic organic solvent (THF), caused the PTFA film to swell and as a result the layer was more open to the charge transfer process.

In Figure 2.10.a the film is more closed due to the double-layer from which the ions cannot escape and this was seen previously in Figure 2.5. The improvement of electrochemical faradaic response appeared together with the change of electrolytic media (THF addition) (Figure 2.10.b), where the 'deeply trapped' ions could be more easily expelled (Figure 2.8).

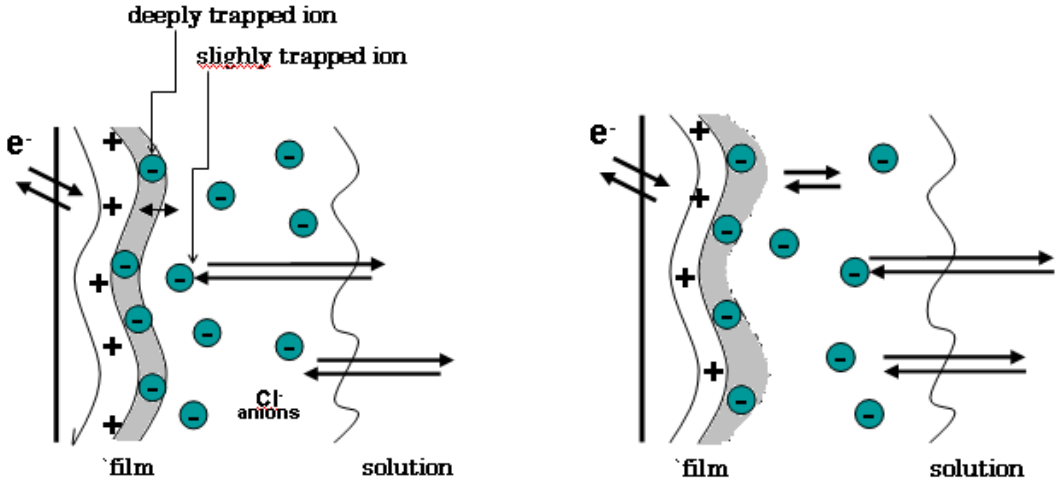

a. b.

Figure 2.10 Ion transport model in PTFA film. a) In absence of THF. b) In presence of THF. The "deeply trapped ions" generate the "low" faradaic process and the "slightly-trapped ions" create the "improved" faradaic process

2.3.3 In-Situ Spectroelectrochemistry of the PTFA Polymer

Spectroelectrochemical analysis was performed in the presence and absence of THF to investigate the optical properties of the polymer. There was a uniform increase in absorbance as a function of potential over the wavelength range 420 nm to 730 nm (Figure 2.11). In addition the spectral band was particularly broad, covering this entire wavelength range. This is reflected in the change from a delicate orange to a much deeper orange colour as the potential was increased [14].

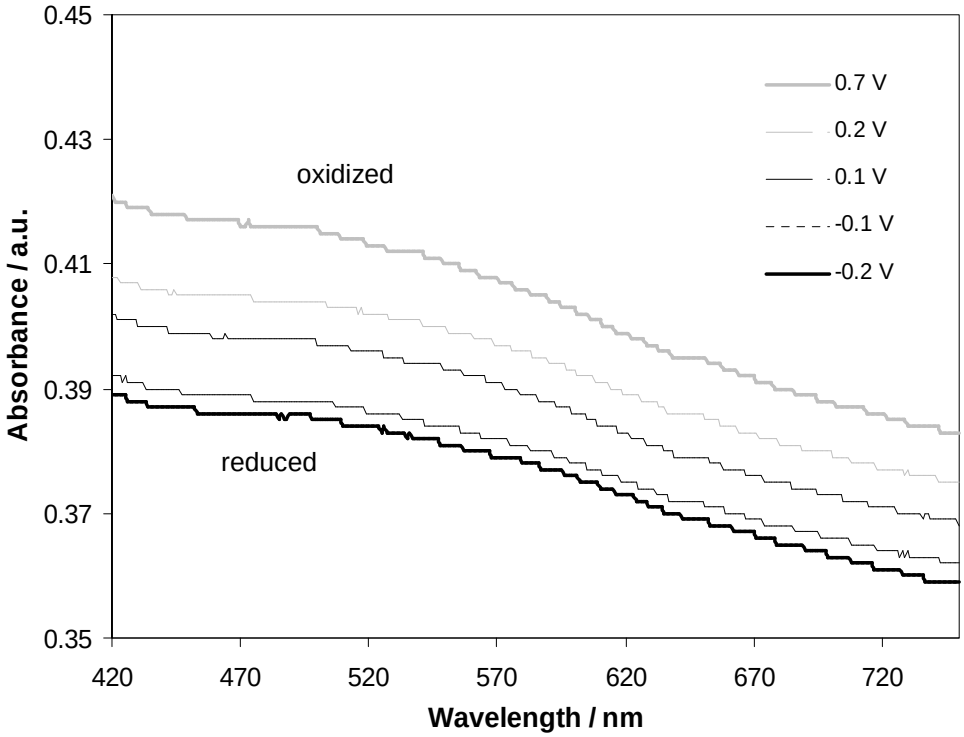

Figure 2.11 UV-Vis spectra of PTFA film in 2 M $HClO_4$ aqueous solution as a function of applied potential.

The changes in absorbance (Figure 2.11) over the visible range correspond to the electronic transition from a neutral (leucoemeraldine) to a polaron (emeraldine) state [7], similar to that seen for monofluorinated anilines [12]. The isosbestic point

related to a simple two stage system is not present, as the neutral polymer electronic transition occured at lower wavelengths, below 420 nm. The band-gap (- *) transition for aniline is generally observed around and sometimes below 300 nm which represents a limitation for electro-optical applications [25]. Compared to spectra of polyaniline, the range of wavelengths associated with the transition in PTFA is very wide, which is due to the presence of the fluorine electron withdrawing groups.

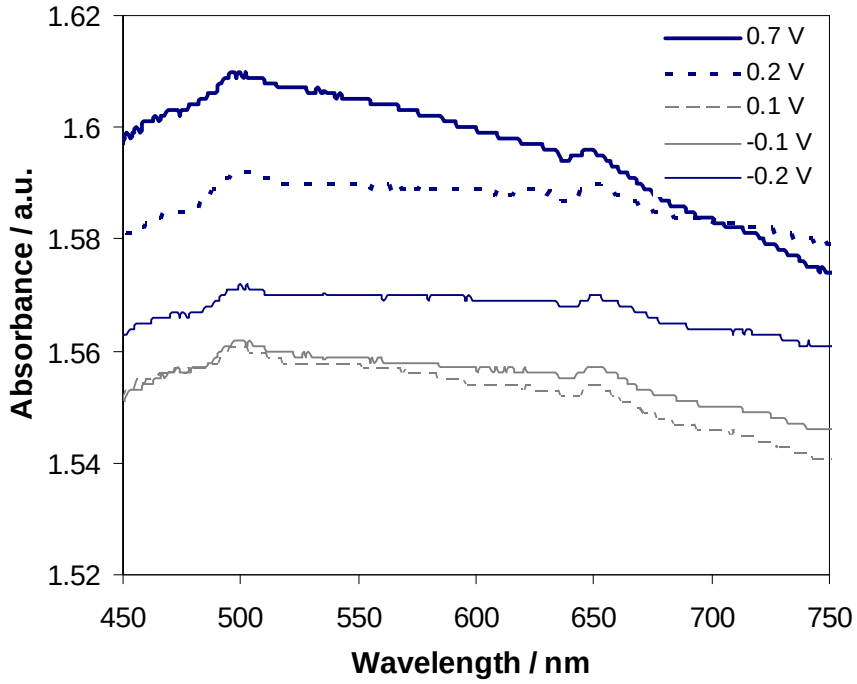

Figure 2.12 UV-Vis spectra of PTFA film in 2 M $HClO_4$ aqueous solution containing 2 % THF as a function of applied potential.

The UV-Vis spectra recorded in the presence of THF can be seen in Figure 2.12. The UV-Vis spectra obtained with addition of THF were not reproducible, and showed only broad absorbance over the visible range. Unfortunately the PTFA films did not exhibit large absorbance changes on oxidation / reduction, even on addition of THF.

2.3.4 Electrochromic Switch

Electrochromic switching studies were performed in order to monitor the ability of the polymer to switch from an oxidized to reduced state and observe the resultant colour changes. For this purpose, the double potential step chronoamperometry technique was used to investigate the oxidation/ reduction switch of the PTFA formed on an ITO substrate.

The response time measured upon switching the polymer film between its neutral and oxidized states was monitored at 450 nm (Figure 2.13). The polymer thickness was controlled by adjusting the number of potential cycles. The film used for this study was a thin film formed during successive oxidation-reduction in the potential range of -0.2 V to 1.4 V. The film thickness was calculated from the total charge passed during oxidation which had a value of 13.6 x 10^{-4} C cm^{-2}.

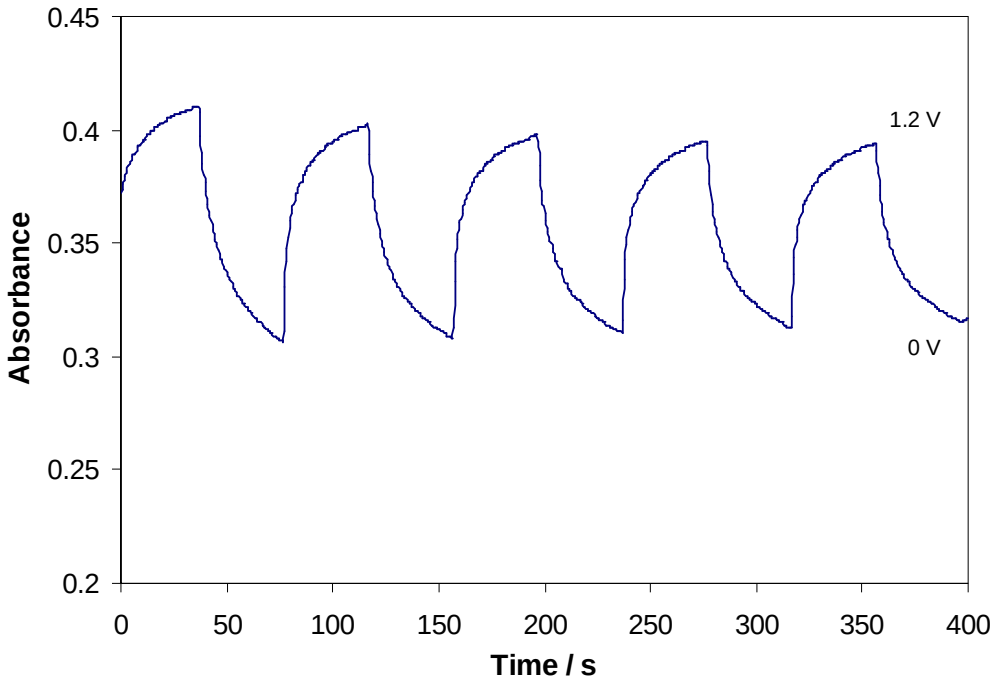

Figure 2.13 Plot of absorbance (= 450 nm) versus time of a PTFA film as the potential was switched between 0 V and 1.2 V. The solution contained 2 M $HClO_4$ and 50 mM monomer. Switching interval of 40 s.

From the charge value obtained for the oxidation of TFA, the moles of monomer deposited were approximately 1.4 x 10^{-8} moles of monomer, which is indicative of a thin film. Also the chronoamperogram for the successive oxidation/ reduction process of PTFA in 50 mM TFA/ 2 M $HClO_4$ solution is represented in Figure 2.14.

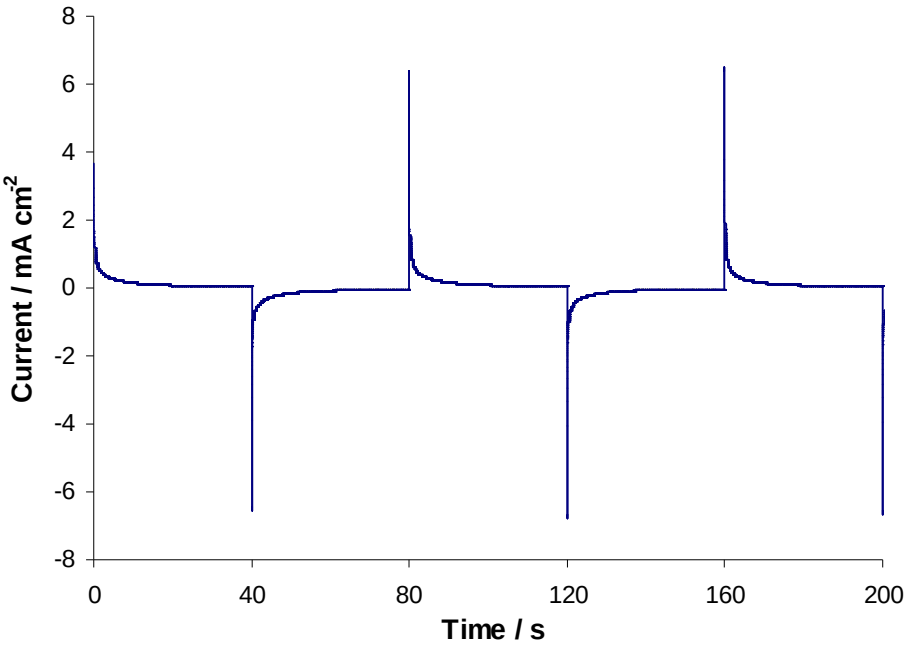

Figure 2.14 Chronoamperogram for oxidation/reduction of PTFA.
Potential limits: 0 V and 1.2 V.

Absorbance variations with time under a step potential stepping between the oxidized and reduced states of the polymer at λ_{max} in the visible range are essential for an electrochromic material. The absorbance change as the polymer is cycled between oxidized and reduced state provides information concerning the film's optical contrast and electro-optical stability [26] .

The polymer film on ITO does not display dramatic colour variations, changing from an orange in the oxidized form to a more bleached orange colour in the reduced form. Consequently, the coloration efficiency had a value of 36.6 cm^2C^{-1} at 450 nm, which is low when compared to other electrochromic materials. For example, a dual electrochromic system containing poly(3,4-ethylenedioxythiophene) (PEDOT) and

poly(3-methylthiophene) had a high coloration efficiency of 460 cm^2C^{-1} at 665 nm [27] where the colours ranged between deep red and deep blue. For other multicoloured electrochromic device based on poly(3-methylthiophene) with zinc hexacyanoferrate / PEDOT:PSS composite as counter electrode, a very good coloration efficiency of 336.8 cm^2C^{-1} was achieved at 750 nm [28].

The rate of colour change recorded at 450 nm wavelength was slow, probably due to the increasing difficulty of inserting ions into the hydrophobic polymer matrix. The hydrophobic nature of PTFA polymer makes the injection of ions on oxidation more difficult in aqueous media, while upon reduction they are more readily released. As stated in the literature the polymer colour depends on the polymer chain-length. An increase in resistivity was observed from cyclic voltammetry (Figure 2.2) and UV-vis spectra (Figure 2.11). The changes in absorbance spectra seen at 450 nm are very small and the rate of the oxidation-reduction process is very slow as the system required 40 s to switch between different oxidation states. Ideally a fast switching time of less than a few seconds is required for most electrochromic device applications.

Still, a slow response time is acceptable for some electrochromic applications known as ‘smart windows’ or ‘switchable windows’. Slow transients have also been reported elsewhere in the literature for a polypyrrole/ polythiophene system (> 20 seconds) [16] and for Tempo/ viologen electrochromic devices (> 50 seconds) [29] [30].

Moreover, in a recent communication [31] the graphene-based electrochromic system with Prussian-Blue nanoparticles deposited on transparent graphene films was presented. The results showed that the response time of the Prussian-Blue material on graphene was mainly influenced by the graphene film thickness loaded with different amounts of Prussian-Blue nanoparticles. In summary, the best response time was achieved for the graphene thin films (response time of 3.3 s) while for the graphene thicker films the response time raised up to 38 s [31].

2.3.5 Morphology Investigation

Morphological investigations were carried out using scanning electron microscopy (SEM) to study the influence of organic solvent (THF) on morphology. The detailed surface morphology of two PTFA polymer films prepared in 2 M $HClO_4$ aqueous solution and deposited on ITO substrate was observed on both cases, with and without THF treatment. Substantial differences in the morphology of PTFA films have been observed.

The SEM micrographs of PTFA films grown from 2 M $HClO_4$ aqueous solution on ITO glass were taken after both films were removed from solution and allowed to dry without any post treatment. Both films were characterised by a porous surface, but differences of pore distribution could easily be seen. The morphological features of PTFA/ITO films obtained in aqueous solution containing 2 M $HClO_4$ without THF addition are presented in Figure 2.15.A. PTFA films had an uneven highly porous structure (Figure 2.15.A) with pore diameters of ca. 50 nm. On addition of a less polar solvent, THF (Figure 2.15.B), the film morphology appears less porous than for the PTFA in aqueous solutions. Previous studies on the polyaniline structure concluded that morphology of aniline based polymers is strongly influenced by the nature of dopant and oxidant used [32] [33]. It is interesting to notice the changes of polymer structure in the presence of 20 % THF which shows reduced number of pores.

In general a less porous structure (Figure 2.15.B) may affect the diffusion of ions into and out of the entire bulk film decreasing the electroactivity [34]. This contradicts the electrochemical study of PTFA / 20 % THF (Figure 2.9) which indicates the presence of a more electroactive layer compared to PTFA / 2 M $HClO_4$ aqueous solution (Figure 2.5). However, SEM images were obtained after the films were removed from solution and completely dried and may not adequately reflect the

structure of the films in solution. The presence of 20 % THF created films with reduced number of pores but with increased pore size which facilitates the insertion/ expulsion of ClO_4^- into/ out of the polymer [34-35].

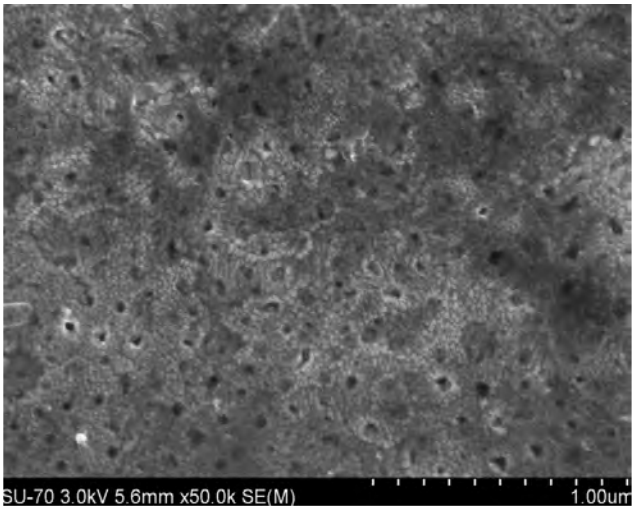

Figure 2.15.A SEM image of PTFA polymer from aqueous solutions.

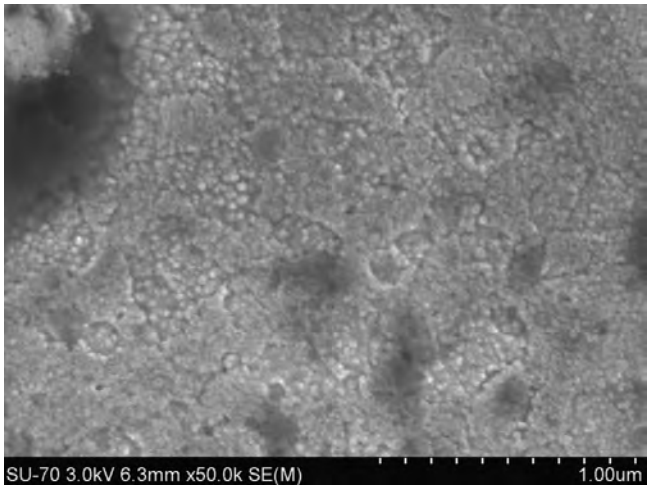

Figure 2.15.B SEM image of PTFA polymer from solutions with tetrahydrofuran (20 %).

The cross-sectional view of PTFA/ ITO (Figure 2.15.C) revealed the compact structure of the film compared to the highly porous network type of polyaniline [32]. The thickness of the polymeric film was 25 nm (Figure 2.15.C), in reasonable agreement with the value of 15.2 nm calculated from the charge passed during polymer oxidation ($Q = 13.6 \times 10^{-4}$ Ccm^{-2}).

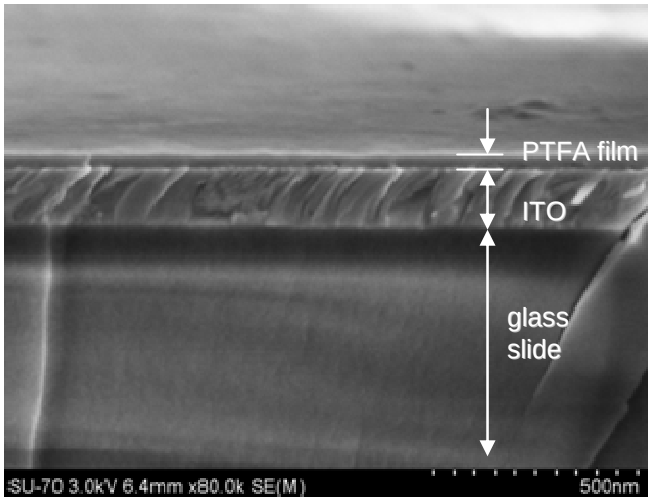

Figure 2.15.C SEM cross-section image of PTFA film run in aqueous solution.

2.3.6 XPS Analysis of PTFA Films

2.3.6.1 Surface Analysis

The chemical composition analysis of PTFA thin films formed by electropolymerization in the potential window -0.2 V to 1.4 V was determined utilizing XPS analysis.

The films used for XPS study were synthesized by cyclic voltammetry as seen in Figure 2.16. Different redox states for PTFA /2 M $HClO_4$ polymer were obtained by use of the appropriate potential, using an oxidising potential (0.9 V) to produce an oxidized film,and a reducing potential (0.5 V) to obtain PTFA in its reduced form. Two samples were prepared, one in the oxidized and the other in the reduced state (Figure 2.16.A and Figure 2.16.B). The film in the reduced state was kept under nitrogen conditions to prevent oxygen access and hence oxidation occurring.

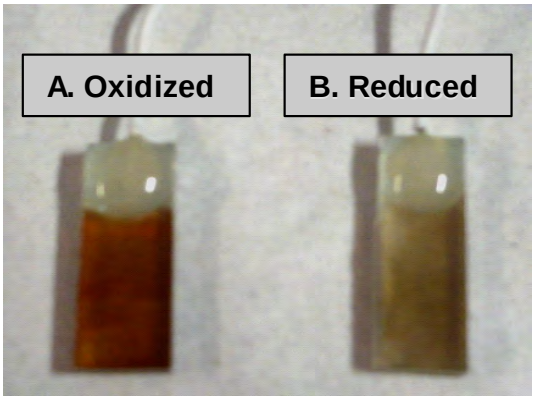

Figure 2.16 PTFA samples used for XPS study. A) Oxidized film; B) Reduced film.

XPS scans for the PTFA films in oxidized and reduced forms are presented in Figure 2.18. The XPS survey scan of PTFA showed the presence of fluorine (F 1s ~ 687.7 eV), carbon (C 1s ~ 284.8 eV), chlorine (Cl 2p ~ 207.6 eV), nitrogen (N 1s ~

400.3 eV), oxygen (O 1s ~ 532.8 eV) and tin (Sn 3d ~ 487.1 eV). In addition to carbon and nitrogen, which originated from the polyaniline backbone, an intense fluorine peak appeared on both XPS scans of the oxidized and reduced states of PTFA (Figure 2.18). Also chlorine element was detected in both PTFA samples, which was a counter ion in the case of oxidized PTFA sample or due to traces of the perchloric acid (2 M $HClO_4$) used during the polymerization process. Similar to Golczak [36] XPS results for polyaniline thin films, the XPS results of PTFA films showed low intensity signal for Cl 2p on both oxidized and reduced forms.

Table 2.1 Composition (at. %) of PTFA samples resulting from XPS quantitative analysis

	F	C	N	O	Cl	Sn	F/Cl	N/Cl	C/N
PTFA oxidized form	21.6	57	6.5	13.8	0.5	0.6	43.2	14	8.8
PTFA reduced form	34.0	55.7	7.2	2.9	0.2	-	170.0	32.6	7.7

at. % = atomic percentage

The relative concentrations of elements F, O, N, C, Cl detected on the film surface, were calculated and showed in Table 2.1. The peak intensity (or peak area) is directly related to the concentration of the element detected on the analysed surface. Clear differences between the XPS survey of the two PTFA samples were observed.

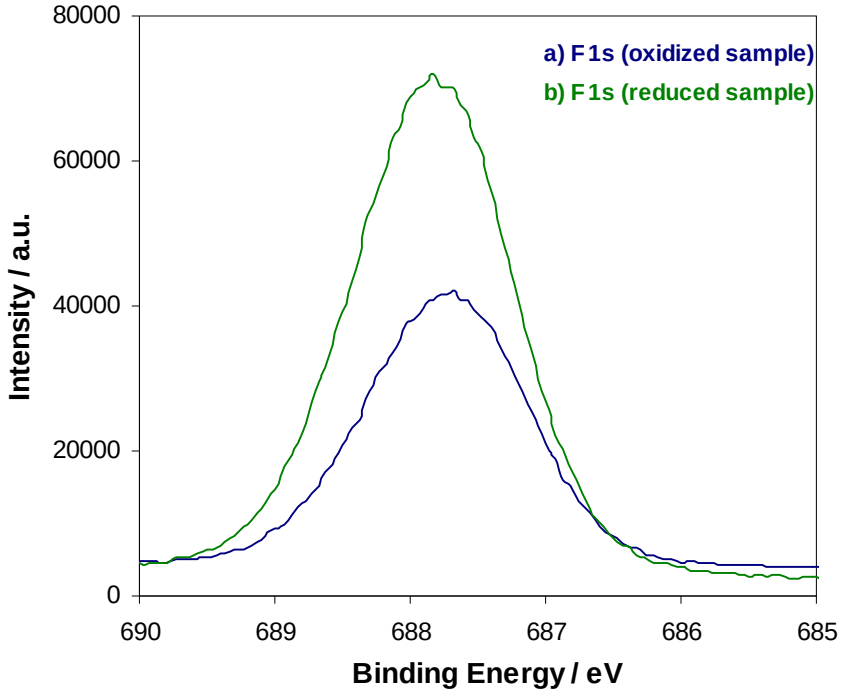

Figure 2.17 High resolution XPS spectrum of F (1s) for a) oxidized sample, and b) reduced sample

The fluorine peak presented a more intense peak for the reduced form of PTFA (Figure 2.17.b), while in the oxidized form the fluorine peak was smaller. On high resolution, the fluorine signal was seen at 687.8 eV for both oxidized and reduced forms of the polymer. The XPS technique can only be used to probe the surface (~ 5-10 nm depth) and can not provide information about the bulk composition. Films used for this analysis had a thickness of approximative 15 nm and for this reason the anomalies were inevitable.

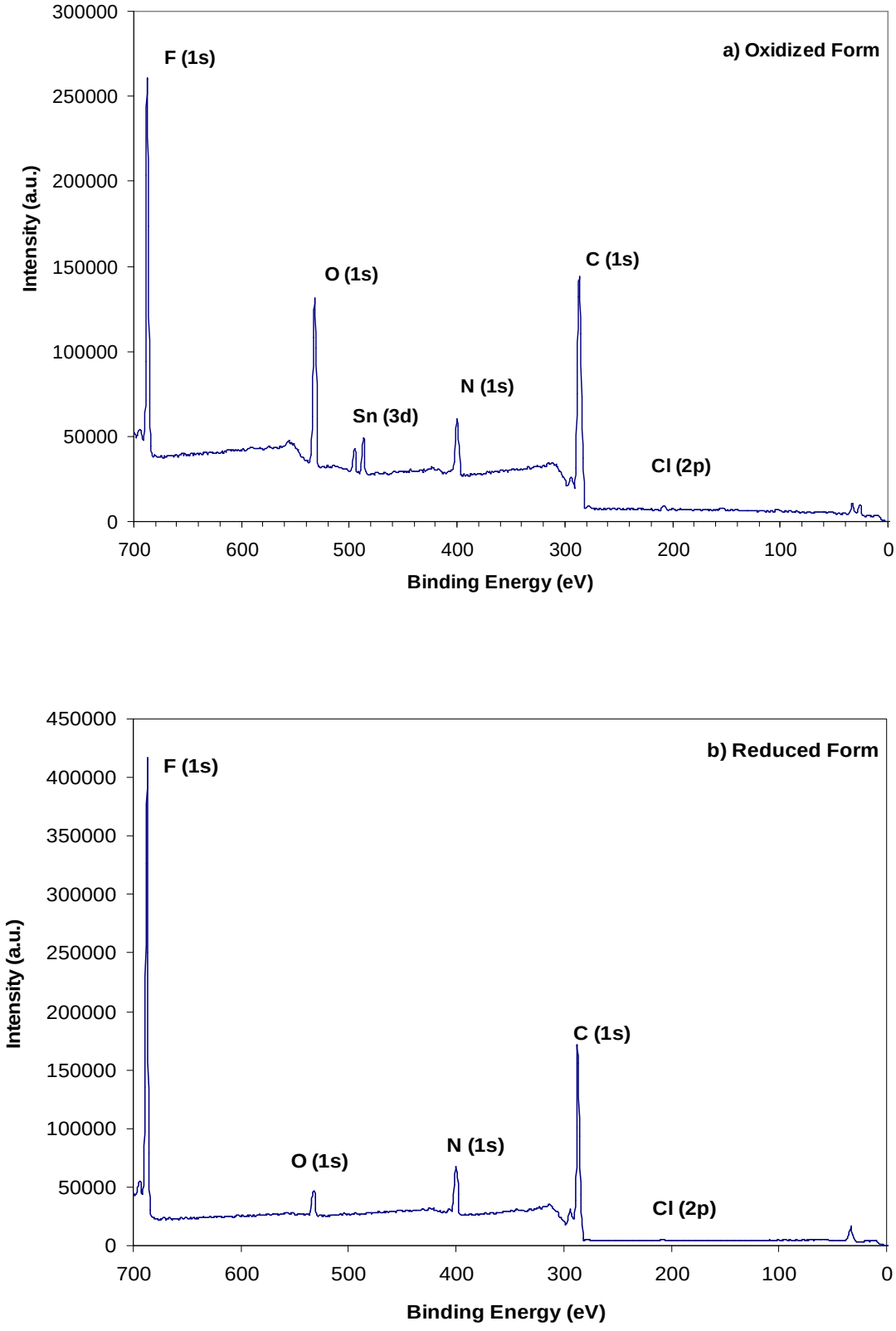

Figure 2.18 XPS wide scan of PTFA. a) Oxidized form of PTFA; b) Reduced form of PTFA.

According to PANI theoretical formula $(C_6H_5N)_n$ the ratio of carbon to nitrogen (C/N ratio) should have a value of 6. For the present study, the C/N ratio was higher than 6 for both PTFA samples (7.7 and 8.8) and did not remain constant. As seen in Table 2.1, for both samples, the ratio between carbon and nitrogen changed. The carbon signal was slightly smaller for the reduced state of PTFA, but the nitrogen peak had increased which indicated that more aniline was formed on the electrode. The present polymer is highly doped with fluorine ions, known as withdrawing group, that have a great influence upon film electropolymerization.

When comparing the results of the two samples, there was great amount of oxygen present in the doped PTFA, and a very small oxygen peak appeared for the reduced PTFA (Figure 2.18). The increased oxygen peak for the oxidised state can be also explained according to A. Sharma [37] from the presence of water molecules. The work done by A. Sharma on the poly(aniline-co-fluoroaniline) copolymer exposed to humid conditions, showed that the copolymer had absorbed the water molecules. The water molecules are of little importance because they were dissociated into H^+ and OH^- at the imine centre. Moreover these ions act as an acidic reagent and increases the effective doping of the poly(aniline-co-fluoroaniline) copolymer [37]. Upon reduction the PTFA had become more hydrophobic, the amount of moisture was reduced and at the end of this process the oxygen content is considerably diminished as in Figure 2.18.b.

2.3.6.2 Use of XPS to Identify Oxidation or Reduction in PTFA

In acidic solution (2 M $HClO_4$), upon oxidation of the film ClO_4^- can enter and then will be expelled on reduction.

By expanding the N 1s peak at 400 eV and using deconvolution to assign a number of overlapping peaks, one can identify N as amine nitrogens (-N-, at 400 eV) or imine nitrogens (=N-, at 401.4 - 401.6 eV) or benzenoid diamine nitrogens (at 398.7-399.2 eV) [36] [37]. However this deconvolution of an XPS high resolution spectrum shown in Figure 2.19 does not clarify the situation. Indeed the intensity for the benzenoid diamiine nitrogens and the imine nitrogens is greater for the reduced form than it is for the oxidized form. This may have happened through the oxidation of the film by air before the spectrum was collected.

The three peak positions were similar to those found by Kang et al. [38] in previous XPS studies on polyaniline films, showing what an elegant method it is for assigning redox characteristics of a conducting polymer. Their study presents the changes in the intrinsic oxidation states of emeraldine base (EM) as a function of treatment time in aqueous-acid during protonation-deprotonation and this quantitatively assessed XPS. As indicated by the angular-dependent XPS data, the changes in the N 1s core-level spectra was obtained at $\alpha = 75°$ and $\alpha = 20°$, for the pristine EM film and a once acid-base cycled EM film when exposed for different length of time in 1 M HCl. A complete deprotonation was achieved by equilibrating the protonated film with deionized water over a period of 24 hours. This was observed in the ratio of imine nitrogens to amine nitrogens which was about unity, taken from the N 1s core-level spectrum obtained at $\alpha = 75°$ [38].

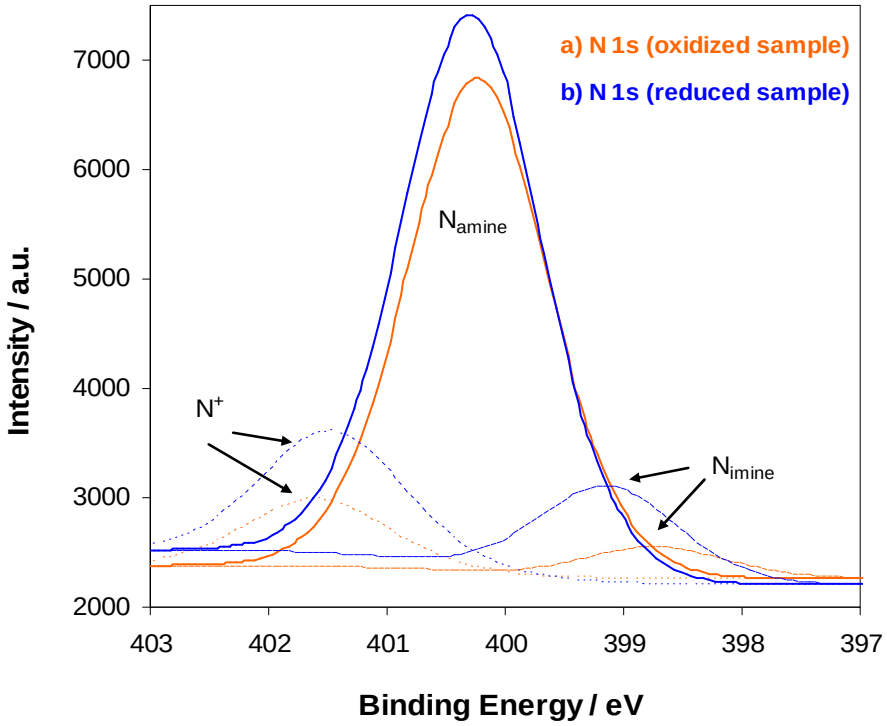

Figure 2.19 High resolution XPS spectrum of N (1s) for a) oxidized sample, and b) reduced sample

According to the study done by Yue and Epstein [39] it was found that small differences might appear in the binding energies for the same species in different samples. The binding energy of C 1s was established at 285 eV [39].

In the case of PTFA/ ITO films the ClO_4^- ions were used as a doping agent. The characteristic peak of perchlorate, Cl (2p) doublet was seen at the binding energy of 207.5 eV. As expected, the atomic percentage (at. %) of Cl had a low value of 0.5 for the doped sample (a) and 0.2 for the reduced sample (b) (Table 2.1). Also the ratios of F/Cl and N/Cl were calculated. Higher values for F/Cl and N/Cl ratios were obtained (F/Cl = 170 and N/Cl = 32.6) for the reduced polymer film, compared to the oxidized state (F/Cl = 43.2 and N/Cl = 14).

2.4 Conclusions

PTFA films were successfully deposited on ITO and FTO substrates and further characterized by electrochemical and spectroscopic methods. The electrochemical study of PTFA/ ITO and PTFA/ FTO have highlighted that films formed on ITO substrate presented improved electrochemical response. However, when the PTFA films were removed from their growth medium, their conductivity was seriously affected. This was manifest in a huge decrease of the peak currents and very broad peak potential. Efforts were made in order to improve PTFA electrochemical behaviour. Results looked promising when PTFA films were kept in their growth media (with monomer), as they exhibited a well defined voltammetry. Addition of THF produced a significant increase of the faradaic peak currents.

Spectroelectrochemical measurements showed a broad absorbance peak over the visible region of the spectrum with an increase in absorbance across the spectrum as the potential was increased. This was very much expected, as according to the UV-Vis spectra of PEDOT treated with 2,3-dichloro-5,6-dicyanobenzoquinone (DDQ) [14], a similar increase in absorbance as a function of potential was observed. Previous work done on fluoro-substituted anilines proved that protonation of aniline makes the electron transfer more difficult [12].

The addition of THF improved the electrochemical response of PTFA films in aqueous solutions. In 2 M $HClO_4$ aqueous solution the films showed a significant decrease in the faradaic response. An increase in the peak currents was observed on addition of THF. The presence of fluorine substituents to form PTFA did not introduce extra stability, as ion movement was hindered and the voltammetric response was more sluggish than that of polyaniline in aqueous solution due to hydrophobic nature of the films. However with PTFA films the neutral to polaron transition was observed from

420 to 730 nm while the neutral transition was moved to lower wavelengths. Furthermore, both in aqueous acidic and with organic solvent addition, the transition from emeraldine (oxidized form) to pernigraniline (reduced form) was not present for fluoro-substituted anilines over visible range [12]. Moreover, for optically active poly(2-fluoroaniline) prepared in organic conditions using DDQ, a hypsochromic shift of the benzenoid π-π* transition and the bipolaron was observed, compared to PANI spectrum [40]. The in situ UV-Vis spectroscopy only confirmed that PTFA films formed by electrochemical oxidation are in oxidized form. A low coloration efficiency of 36.6 cm^2C^{-1} was observed while PTFA polymer exhibited a contrast change of orange to a more transparent orange.

Also the morphology of PTFA polymer with and without THF addition was observed by SEM. The films showed a distribution of pores with pore diameters of ca. 50 nm without THF addition. It was interesting to notice that when THF was added to the electrolyte solution (2 M $HClO_4$), the films exhibited a structure with less pores.

The changes in the intrinsic oxidation states of thin films of PTFA formed in aqueous acidic conditions during successive potential scan were quantitatively assessed by X-ray photoelectron spectroscopy (XPS). The XPS technique is very sensitive as it's possible to scan up to only 5-10 nm depth and sometimes the results may not be reliable to obtain information about the bulk composition. XPS measurements helped in identifying the chemical structure of the PTFA films, but it was not possible to clearly differentiate between oxidized and reduced forms, as the reduced sample was affected by oxygen when exposed to air.

2.5 References

[1] G. Anitha, E. Subramanian, Sensors and Actuators B: Chemical, 92 (2003) 49-59.
[2] B.N. Grgur, V. Ristić, M.M. Gvozdenović, M.D. Maksimović, B.Z. Jugović, J Power Sources, 180 (2008) 635-640.
[3] T.A. Skotheim, R.L. Elsenbaumer, J.R. Reynolds, Handbook of conducting polymers, Marcel Dekker, 1998.
[4] K. Aydemir, S. Tarkuc, A. Durmus, G.E. Gunbas, L. Toppare, Polymer, 49 (2008) 2029-2032.
[5] R.J. Mortimer, Chem Soc Rev, 26 (1997) 147-156.
[6] M. Freund, B. Deore, Self-doped conducting polymers, John Wiley & Sons, 2007.
[7] P.C. Innis, J. Mazurkiewicz, T. Nguyen, G.G. Wallace, D. MacFarlane, Curr Appl Phys, 4 (2004) 389-393.
[8] Reza Ansari, M.B. Keivani, E-Journal of Chemistry, 3 (2006) 202-217.
[9] J. Niessen, U. Schroder, M. Rosenbaum, F. Scholz, Electrochem Commun, 6 (2004) 571-575.
[10] P. Kissinger, W.R. Heineman, Laboratory Techniques in Electroanalytical Chemistry, Second Edition, Revised and Expanded, Taylor & Francis, 1996.
[11] A.H. Kwon, J.A. Conklin, M. Makhinson, R.B. Kaner, Synthetic Met, 84 (1997) 95-96.
[12] A. Cihaner, A.M. Onal, Polym Int, 51 (2002) 680-686.
[13] Jing Zhang, Lian Gao, Jing Sun, Yangqiao Liu, Yan Wang, J. Wang, Diamond & Related Materials, 22 (2012) 82-87.
[14] M.L. Machala, L. Muller-Meskamp, S. Gang, S. Olthof, K. Leo, Org Electron, 12 (2011) 1518-1526.
[15] S.A. Mauger, A.J. Moule, Org Electron, 12 (2011) 1948-1956.
[16] A.J.C. da Silva, F.A. Ribeiro Nogueira, J. Tonholo, A.S. Ribeiro, Solar Energy Materials and Solar Cells, 95 (2011) 2255-2259.
[17] S. Vogel, R. Holze, Electrochim Acta, 50 (2005) 1587-1595.
[18] S. Little, S.F. Ralph, C.O. Too, G.G. Wallace, Synthetic Met, 159 (2009) 1950-1955.
[19] N. Sato, T. Nonaka, NIPPON KAGAKU KAISHI (1997) 451-455.
[20] M. Grzeszczuk, A. Kepas, G. Zabinska-Olszak, Electrochim Acta, 49 (2004) 2405-2414.
[21] A. Lima, P. Schottland, S. Sadki, C. Chevrot, Synthetic Met, 93 (1998) 33-41.
[22] B. Garcia, D. Bélanger, Synthetic Met, 98 (1998) 135-141.
[23] Eric V. Anslyn, D.A. Dougherty, Modern physical organic chemistry, 2006.
[24] A.J. Bard, L.R. Faulkner, Electrochemical methods: fundamentals and applications, Wiley, 2001.
[25] J. Arjomandi, R. Holze, Cent Eur J Chem, 6 (2008) 199-207.
[26] A.V. Rosario, E.D. Rios, A.F. Nogueira, L. Micaroni, Solar Energy Materials and Solar Cells, 94 (2010) 1338-1345.
[27] D.M. Welsh, A. Kumar, E.W. Meijer, J.R. Reynolds, Adv Mater, 11 (1999) 1379-1382.
[28] S.-F. Hong, L.-C. Chen, Electrochim Acta, 55 (2010) 3966-3973.
[29] J.S. Zhao, B. Wang, C.S. Cui, R.M. Liu, J.F. Liu, H.S. Wang, H.T. Liu, Electrochim Acta, 56 (2011) 4819-4827.
[30] C.-W. Hu, K.-M. Lee, K.-C. Chen, L.-C. Chang, K.-Y. Shen, S.-C. Lai, T.-H. Kuo, C.-Y. Hsu, L.-M. Huang, R. Vittal, K.-C. Ho, Solar Energy Materials and Solar Cells, 99 (2012) 135-140.

[31] J.H. Ko, S. Yeo, J.H. Park, J. Choi, C. Noh, S.U. Son, Chemical Communications, 48 (2012) 3884-3886.
[32] Q.L. Hao, W. Lei, X.F. Xia, Z.Z. Yan, X.J. Yang, L.D. Lu, X. Wang, Electrochim Acta, 55 (2010) 632-640.
[33] L. Lizarraga, E. María Andrade, F. Victor Molina, J Electroanal Chem, 561 (2004) 127-135.
[34] M. Gao, Y. Yang, M. Diao, S.-g. Wang, X.-h. Wang, G. Zhang, G. Zhang, Electrochim Acta, 56 (2011) 7644-7650.
[35] B. Sarı, M. Talu, Synthetic Met, 94 (1998) 221-227.
[36] S. Golczak, A. Kanciurzewska, M. Fahlman, K. Langer, J.J. Langer, Solid State Ionics, 179 (2008) 2234-2239.
[37] A.L. Sharma, Thin Solid Films, 517 (2009) 3350-3356.
[38] E.T. Kang, K.G. Neoh, K.L. Tan, Synthetic Met, 68 (1995) 141-144.
[39] J. Yue, A.J. Epstein, Macromolecules, 24 (1991) 4441-4445.
[40] T. Hino, T. Kumakura, N. Kuramoto, Polymer, 47 (2006) 5295-5302.

Chapter 3. Homopolymerization and Copolymerization of Pyrrole and 3,4-Ethylenedioxythiophene in Room Temperature Ionic Liquids Using a Novel Microcell Configuration

3.1 Introduction

As outlined in Chapter 1, conducting polymers have attracted more and more attention because of their potential applications in different fields such as supercapacitors [1], sensors [2], photovoltaic cells [3], electrochromic devices [4], organic light-emitting diodes [5], and actuators [6]. At the same time, huge progress has been made to obtain increased conductivity, stability and processability of conducting polymers. Heterocyclic monomers, such as pyrrole and 3,4-ethylenedioxythiophene (EDOT) have been intensively used for the synthesis of polypyrrole (PPy) and poly(3,4-ethylenedioxythiophene) and their derivatives [7].

The EDOT monomer consists of a five-membered thiophene ring with hydrogens at the 3 and 4 positions replaced with a dioxy-ethyl substituent group. The regularity in its molecular structure yields a polymer with very good chemical stability. Pyrrole has a ring structure composed of four carbon atoms and one nitrogen atom. Due to high electrical conductivity, long term environmental stability and ease of synthesis by chemical or electrochemical means, polypyrrole (PPy) has been widely employed and characterized and can be considered a model for conducting polymers [8-9]. Also poly(3,4-ethylenedioxythiophene) (PEDOT) has received significant attention in commercial applications as an organic electrochromic material because of its rapid switch time and low oxidation potential value [10]. These conducting polymers can be formed and used in a range of solvents, aqueous or organic, but in these conditions they exhibit relatively poor stability which is a major limitation to their applications [11].

Syntheses of conducting copolymers from ionic liquids are considered to be an effective way to compensate for the deficiencies of conducting polymers formed in

traditional solvents. Room temperature ionic liquids (RTILs or ILs) are known to be environmentally benign media. Due to their non-volatility and excellent electrochemical stability, as discussed in Chapter 1, ILs can be used directly as hydrophobic electrolytes for the deposition of both PPy and PEDOT.

In general conjugated polymers have different colours in both the oxidized and reduced states. PPy colours can change from dark blue (oxidized form) to yellow-green (reduced form), while PEDOT can be switched from light blue (oxidized state) to dark blue (reduced state). A variety of methods such as grafting alkyl groups onto the main polymer chain, synthesis of water-soluble precursors and preparation of conducting polymer composites, blends and copolymers can be used to improve the mechanical properties of conducting polymers [12]. One of the strategies that can be used to control and improve the electrochromic properties of electroactive polymers is copolymerization. Copolymerization is generally carried out to combine the diverse physicochemical properties of different polymers to a single polymeric system. Amongst the most widely employed methods of copolymerization are the electrochemical polymerization of the conducting component on a substrate coated with an insulating polymer or electrochemical polymerization of two electroactive monomers.

The reaction mechanism for copolymerization of monomers namely A and B is presented in Figure 3.1:

Step 1: Oxidation of monomers at the electrode surface

$$A \longrightarrow A^{+\bullet} + e^- \quad (3.1.1)$$

$$B \longrightarrow B^{+\bullet} + e^- \quad (3.1.2)$$

Step 2: Coupling of radical cations with the growing radical cation polymer

$$R - A^{+\bullet} + A^{+\bullet} \xrightarrow{k_{AA}} R - A^{+}A^{+\bullet} \quad (3.1.3.a)$$

$$R - A^{+\bullet} + B^{+\bullet} \xrightarrow{k_{AB}} R - A^{+}B^{+\bullet} \quad (3.1.3.b)$$

$$R - B^{+\bullet} + A^{+\bullet} \xrightarrow{k_{BA}} R - B^{+}A^{+\bullet} \quad (3.1.3.c)$$

$$R - B^{+\bullet} + B^{+\bullet} \xrightarrow{k_{BB}} R - B^{+}B^{+\bullet} \quad (3.1.3.d)$$

Step 3: Proton release

$$R - A^{+}A^{+\bullet} \longrightarrow R - AA + 2H^{+} \quad (3.1.4.a)$$

$$R - A^{+}B^{+\bullet} \longrightarrow R - AB + 2H^{+} \quad (3.1.4.b)$$

$$R - B^{+}A^{+\bullet} \longrightarrow R - BA + 2H^{+} \quad (3.1.4.c)$$

$$R - B^{+}B^{+\bullet} \longrightarrow R - BB + 2H^{+} \quad (3.1.4.d)$$

Figure 3.1 Electrocopolymerization mechanism for two monomers (A and B), reproduced from reference [13].

The copolymerization process starts (Step 1) with anodic oxidation of the two different monomers, which can be adsorbed on the electrode surface and radical cations are formed. The main variables taken into account for monomer oxidation refers to the

nature and concentration of each monomer and supporting electrolytes and the polymerization potential [14].

Reactions that occur in Step 2 of the electrochemical copolymerization involve the selective incorporation of monomers into the co-oligomers or the short copolymer chains. The oligomerization can proceed in two ways: the dimerization of one radical cation with a second radical cation [15] and the interaction between a radical cation and a neutral monomer molecule [16]. Step 3 is known to be very fast in comparison to previous steps reactions (Step 1 and Step 2) and therefore not rate controlling [13].

In this work copolymerization of the monomers, Py and EDOT, was performed to obtain one layer, which is expected to have different properties from those of their corresponding homopolymers. The monomer solution for electro-co-deposition contained a mixture of Py and EDOT in an ionic liquid. PEDOT is a very desirable material for electrochromic devices, especially because of its low band-gap which allows the polymer to be almost transparent (very light blue) in the oxidized state [17]. The simple change from light blue to dark blue limits its application to some degree [18]. Copolymerization of EDOT with Py could overcome these drawbacks by creating a material with an improved electrochromic range.

PEDOT and PPy were first formed as thin electroactive layers in 1-butyl-3-methylimidazolium tetrafluoroborate (BMIM BF_4) as supporting electrolyte as well as dopant, using a novel microcell which is described in section 3.2.2. Both the dopant and the solvent have a strong influence upon the electrochemical and physical properties of polymers during potential scanning [19]. Ionic liquids are distinct from traditional solvents, being formed entirely of ions and possessing unique properties (non-volatile, high ionic conductivity, wide potential windows and high thermal/electrochemical stability), as mentioned in Chapter 1. Those properties are extremely advantageous for the electrodeposition of conducting polymers [20].

Copolymerization of PPy with PEDOT will be performed in the same BMIM BF_4 ionic liquid and further characterised electrochemically in monomer-free ionic liquid. The electrochemical copolymerization of PPy with PEDOT will be done by employing three different ratios of monomers which allows formation of three films with different features. The electrochemical behaviour of copolymers will be characterised in neat ionic liquid. This will then be compared to the electrochemical response of the copolymers in aqueous solution. The copolymers will be also characterized spectroelectrochemically using in-situ spectroelectrochemistry, thereby enabling the optical properties of the electrochromic conducting polymers to be investigated upon application of a potential change. This in-situ method will also provide information about the electronic structure of the new copolymers to be obtained. The electrochromic properties of the copolymers will be investigated during successive electrochromic switches between the oxidized and reduced forms. The structure of the new copolymers will be examined using FTIR. The surface morphology of copolymers will be also investigated by scanning electron microscope (SEM).

3.2 Experimental

3.2.1 Materials and Equipment

Pyrrole (Sigma-Aldrich, 98%) (Py) was distilled prior to homo-/co-polymerization as described earlier. 3,4-ethylenedioxythiophene (EDOT) monomer was purchased from Sigma-Aldrich and used without further purification. In order to avoid monomer degradation it was stored in the dark in a refrigerator. Ionic liquids including 1-butyl-3-methylimidazolium tetrafluoroborate (BMIM BF_4) used for copolymerization were received from Sigma-Aldrich and kept in a desiccator to protect them from moisture. Sodium tetrafluoroborate ($NaBF_4$, Sigma-Aldrich) was used without any further purification. All aqueous solutions were prepared from deionised water which had a resistivity of 18.2 MΩ cm (Elgastat Purification system). The electrochemical results were recorded at room temperature with a CHI 600 electrochemical work station, and all potentials were given with respect to Ag/AgCl (3 M KCl) reference electrode in aqueous solution. For experiments performed in ionic liquids as electrolytic media, an Ag wire was used as pseudo-reference electrode. UV-Vis absorption spectra were recorded on a Shzimadzu 1800 UV-Vis spectrophotometer. Film morphology was analysed on a Hitachi SU-70 scanning electron microscope (SEM). The FTIR spectra of the films were recorded on Perkin-Elmer Spectrum 100 FTIR Spectrophotometer with an ATR accessory. All experiments described in this chapter were carried out at room temperature (approximately 18°C).

3.2.2 Novel Microcell Set-up and Electrode Preparation

The cyclic voltammetry experiments were performed using a three electrode cell in a novel set-up. This cell was termed a microcell as it involved the use of very small amounts of ionic liquids (~ 20 l) for polymer formation and further characterization. In the case of polymer deposition, the monomer solution was placed on the ITO working electrode surface using a Gilson pipette and then a flat Pt coil and the Ag wire were placed close to the working electrode surface as shown in Figure 3.2.a) and 3.2.b).

a)

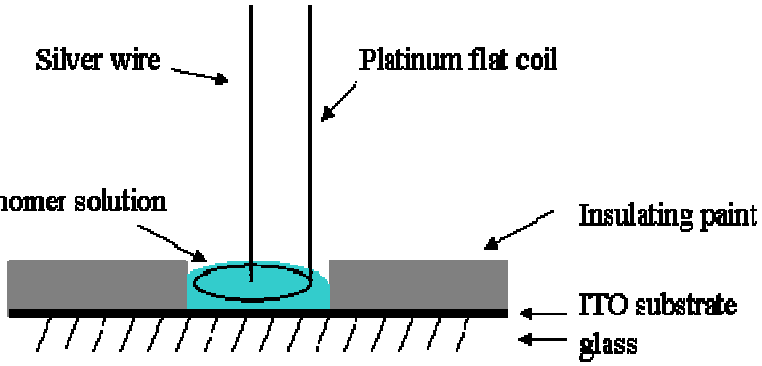

b)

Figure 3.2.a) Schematic diagram showing the cross-section for the microcell set-up. b) Photo of ITO microelectrode

Indium tin oxide coated glass (ITO, Solaronix, Switzerland) with a resistivity of 18 Ω/sq was used as the conducting working electrode. The ITO electrodes were cleaned by successive ultrasonication in deionized water, followed by ethanol and deionized water, prior to electrode connection.

In order to electrically connect the electrode, conductive silver paint (Electrolube, UK) was used. Copper wire was placed at one edge of the ITO conductive surface and next, using a Gilson pipette, a small amount of silver paint (~ 6 l) was attached to form an electrical connection. Then the paint was allowed to dry for 30 minutes before insulating the electrical connection with Araldite glue. The silver paint gave good electrical conductivity, while the glue coverage provided mechanical strength. In order to have a small defined electrode area, the electrode was covered with insulating paint (Dielectric paste, The Gwent Group, UK) leaving a circular shape as electrode surface. Then the electrodes were left in the oven for approximately 15 minutes to allow the paint to dry. A thick layer of insulating paint was built up which defined the working electrode area. The exposed ITO electrode has a diameter of approximately 0.5 cm, which formed a geometrical area of 0.196 cm^2. A flat platinum (Pt) coil was placed on top of the droplet (parallel to the ITO electrode surface) as counter electrode, while a silver (Ag) wire was used as pseudo-reference electrode.

3.3 Results and Discussion

3.3.1 PEDOT Electrodeposition in Ionic Liquids Using the Novel System Configuration: IL Droplet

PEDOT films can be electrodeposited and characterised in imidazolium based ionic liquids such as 1-butyl-3-butylimidazolium hexafluorophosphate (BMIM PF_6) and 1-butyl-3-methylimidazolium tetrafluoroborate (BMIM BF_4) [21]. Damlin et al. [21] presented the electropolymerization of EDOT films on an ITO substrate in two imidazolium based ionic liquids and then conducted electrochemical, spectroelectrochemical and structural characterization. For this study the choice of ionic liquid was BMIM BF_4 as used previously [21] enabling comparison of the differences in electrodeposition of PEDOT films in a bulk cell with the films formed here in a microcell.

PEDOT electrodeposition on ITO was done in a microsystem which involved the use of 20 l total volume of monomer solution. The monomer solution contained 0.15 l EDOT, corresponding to 0.05 M EDOT in the BMIM BF_4 ionic liquid. The PEDOT films formed from a droplet of monomer solution were further characterized in aqueous solution. Use of aqueous solutions as solvent offers a greater variety of supporting electrolytes. One potential cycle between -0.7 V and 1 V (vs Ag wire) was sufficient to form a thin uniform PEDOT film on ITO substrate as seen in Figure 3.3. The cyclic voltammogram showed a clear crossover on the reverse scan indicating nucleation and polymer growth. As expected, the polymer showed a light blue colour in the oxidized form and a dark blue in the reduced form. It displayed good adherence to the electrode surface.

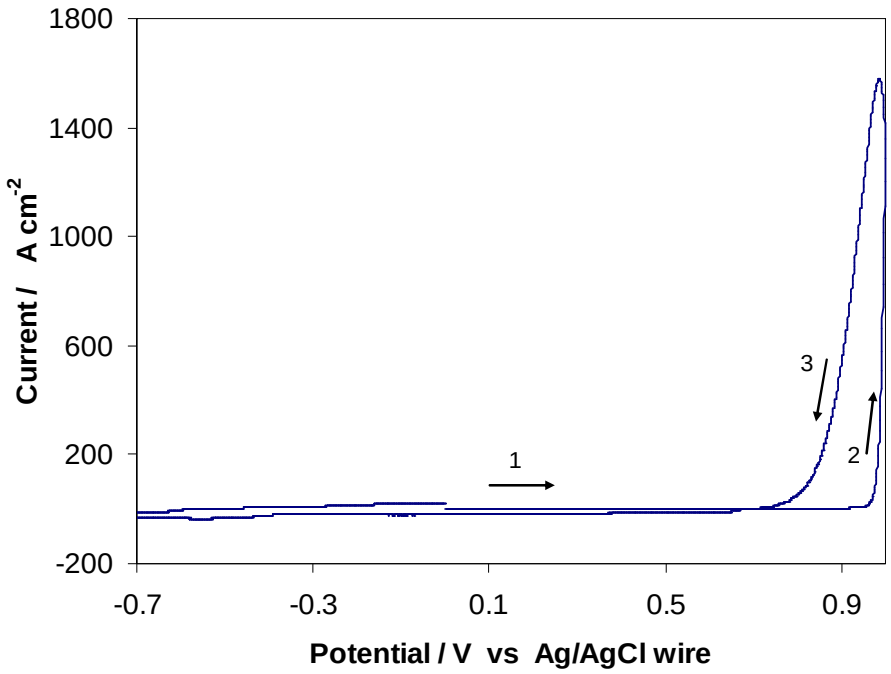

Figure 3.3 Cyclic voltammogram for PEDOT film formation in 0.05 M EDOT/BMIM BF_4 solution. Scan rate: 50 mV s^{-1}.

The PEDOT films formed during potential cycling were successively used in spectroelectrochemical experiments, examining the influence of ClO_4^- and BF_4^- on their electrochemical behaviour. Figure 3.4 shows a reversible spectrum of the PEDOT in 0.2 M $NaBF_4$ aqueous solution, while constant potentials are applied in order to achieve the reduced form of the film. The reduced PEDOT had a $_{max}$ at 540 nm with a dark blue colour at -0.8 V and a very clear isosbestic point at 700 nm. Next the PEDOT film was transferred to 0.1 M $LiClO_4$ aqueous solution in order to obtain a series of UV-Vis spectra for different applied potentials.

The $_{max}$ value for the π-π^* transition in the neutral state for PEDOT was approximately 550 nm (Figure 3.5). At more negative potentials, as the polymer was in the reduced form, the absorbance peaks became broader. Also the bands at longer wavelengths (lower energy) decreased in intensity with application of more negative

potentials, while at 550 nm wavelength the absorbance increased concurrently (Figure 3.3). When switching the dopant anions, from BF_4^- to ClO_4^-, changes in the absorbance spectrum could be observed. As shown in Figure 3.5, the absorbance changes as a function of potential are much greater compared to Figure 3.4. Spectroelectrochemical results of PEDOT films in $LiClO_4$ versus $NaBF_4$ aqueous solution are shown in Figure 3.4 and Figure 3.5. This indicated that ClO_4^- anions could be injected more easily into the polymer matrix in comparison to BF_4^- anions.

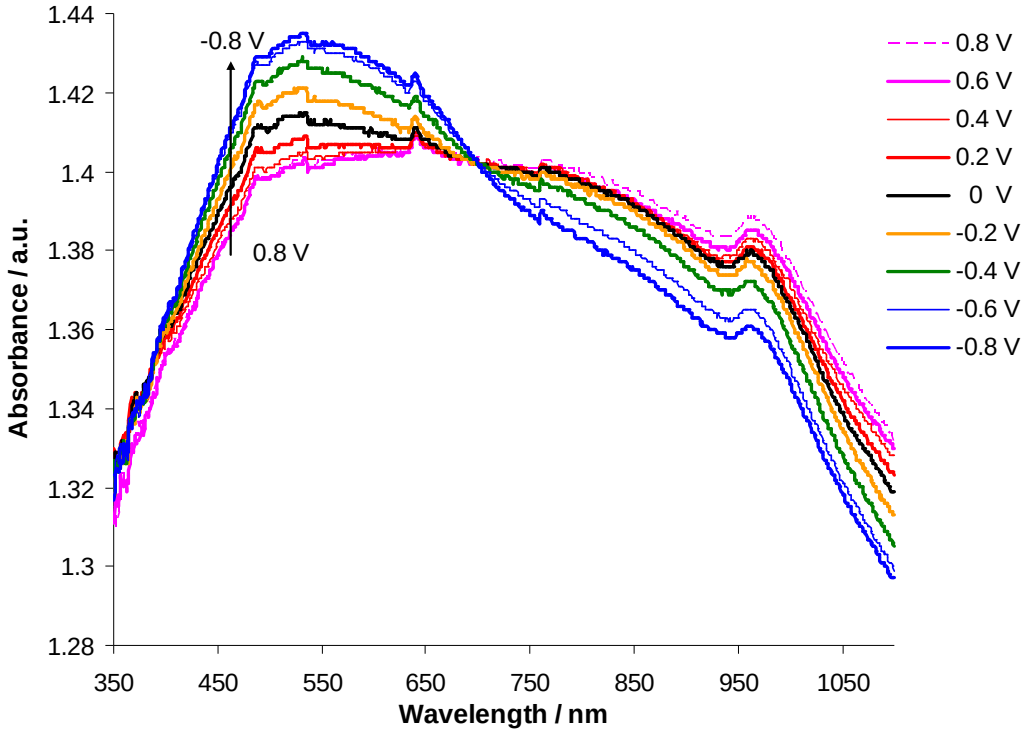

Figure 3.4 In-situ UV-Vis spectroelectrochemistry of the successive reduction of PEDOT/BMIM BF_4 film in 0.2 M $NaBF_4$ aqueous solution in the potential range of 0.8 V to -0.8 V

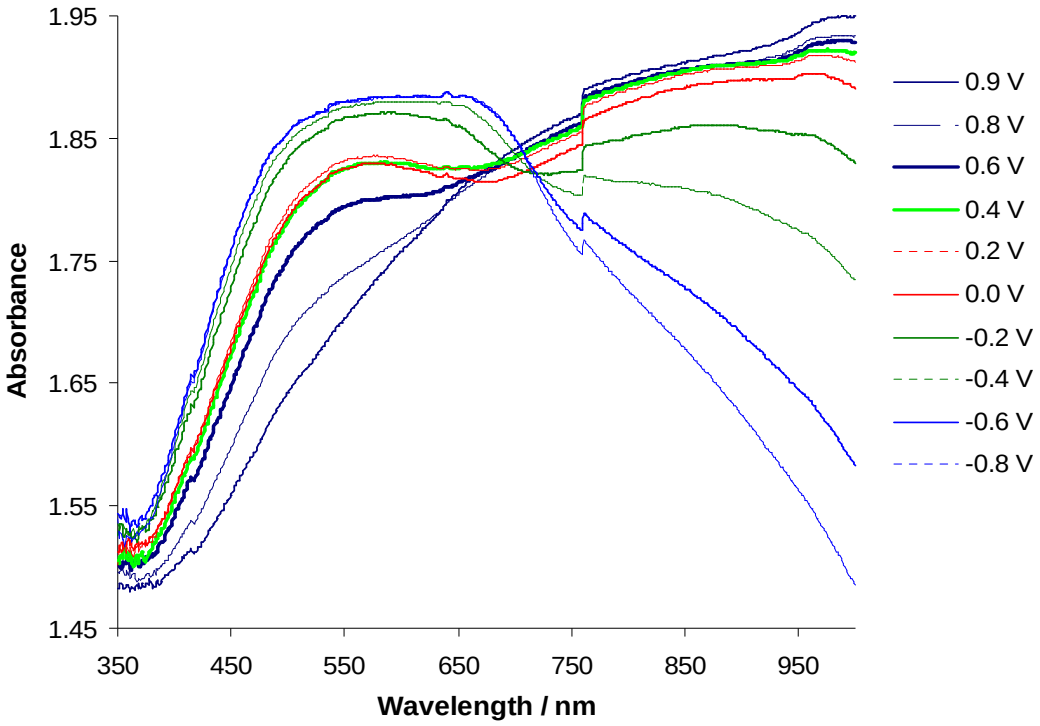

Figure 3.5 In-situ UV-Vis spectroelectrochemistry of the successive reduction of PEDOT/BMIM BF_4 film in 0.1 M $LiClO_4$ aqueous solution for the potential range of 0.9 V to -0.8 V

3.3.2 PPy-co-PEDOT Copolymer Formation and Electrochemical Characterization

Conducting polymers formed in room temperature ionic liquids have been the subject of interest both from the fundamental and application points of view. For copolymerization of PPy with PEDOT, the air stable ionic liquid 1-butyl-3-methylimidazolium tetrafluoroborate (BMIM BF_4) acts as a supporting electrolyte as well as a dopant. Both polypyrrole and poly(3,4-ethylenedioxythiophene) are well-known polymer materials and have been intensively studied because of their high conductivity, relatively low oxidation potential, chemical stability, and atmospheric stability at room temperature [22-23]. In order to improve the electrochromic properties

of CPs and to achieve multichromic materials there are two strategies which can be used: copolymerization or group structural modification [24].

Electrochemical deposition of the copolymers was done from a micro-droplet of ionic liquid which contains the mixed monomers, pyrrole (Py) and 3,4-ethylenedioxythiophene (EDOT). The copolymers were formed during successive cycling in BMIM BF_4.

Thin films of PPy-co-PEDOT copolymers were prepared at different monomer ratios:

- pyrrole : 3,4-ethylenedioxythiophene (1:2), Figure 3.7.
- pyrrole : 3,4-ethylenedioxythiophene (1:1), Figure 3.8.
- pyrrole : 3,4-ethylenedioxythiophene (2:1), Figure 3.9.

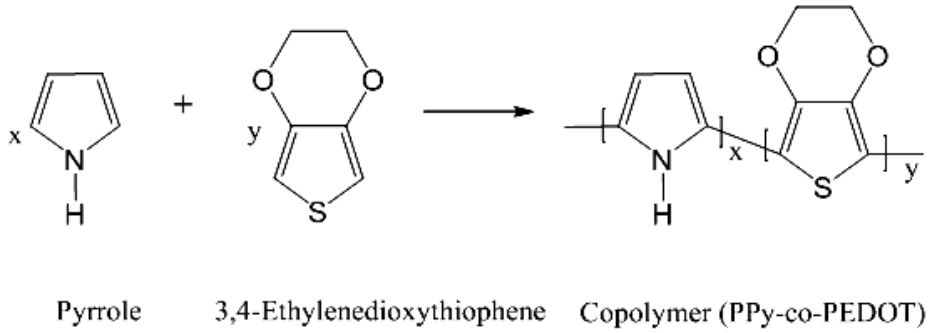

Pyrrole 3,4-Ethylenedioxythiophene Copolymer (PPy-co-PEDOT)

Figure 3.6 Scheme for copolymerization of pyrrole with 3,4-ethylenedioxythiophene

The optimal potential range for copolymer formation was -0.7 V to 0.8 V versus Ag wire (pseudo-reference), which ensured the formation of thin films on the ITO substrate. Potentials higher than 0.8 V lead to formation of overoxidized films with poor adherence at the electrode surface. Copolymerization of pyrrole with 3,4-ethylenedioxythiophene at a molar ratio of 1:2, 1:1 and 2:1 can be seen in Figures 3.7, 3.8 and 3.9, respectively. Film formation starts with nucleation on the first oxidation

step with successive increases in current density on continuous sweeping leading to the formation of a thin film on the ITO substrate.

Polypyrrole is much easier to form than PEDOT, so the EDOT monomer concentration is kept in high concentration for this reason. In each case the ITO electrodes covered with copolymers were studied first in monomer-free ionic liquid BMIM BF_4. Once the films were formed, the solution with the two monomers was removed from the film surface and a fresh drop of ionic liquid applied. In order to study the influence of the electrolyte upon the redox behaviour, the potential scan of the copolymers prepared from different molar ratios was done in both ionic liquid and aqueous solutions.

The copolymer was rinsed with deionized water in order to remove the monomer traces from the modified electrode. A scan rate study over the range 50-150 mV/s was performed for the different ratios of copolymer thin films formed in an ionic liquid droplet. From this experiment a linear relationship between the peak current and the scan rate was seen, indicative of thin layer behaviour [25].

Characterization of both homopolymers and copolymers is necessary when studying the copolymer materials. Separately, the PPy/BMIM BF_4 (Figure 3.10) and PEDOT/BMIM BF_4 (Figure 3.3) films were electropolymerized on ITO glass and then used for electrochemical investigation.

When the potential was cycled in pure BMIM BF_4, cyclic voltammograms of the PPy-co-PEDOT (1:2) film (Figure 3.7.a) showed increases in the peak currents with increased scan rates. The repeated oxidation/reduction process of PPy-co-PEDOT (1:2) was performed in BMIM BF_4 at different scan rates. Linearity of both anodic and cathodic peaks with different scan rates was seen which proved thin layer behaviour. The oxidation peak potential, E_p^f situated at -0.04 V is more defined as the scan rate was increased, while the reduction peak was very broad and shifted to positive potentials.

The electrochemical study of the film was continued in aqueous solution which contains anions of the same size, in this case BF_4^-. During continuous potential scanning in 0.2 M $NaBF_4$ (Figure 3.7.b), both oxidation and reduction peaks appeared broader and smaller, which means that the ion-exchange process was slowed down.

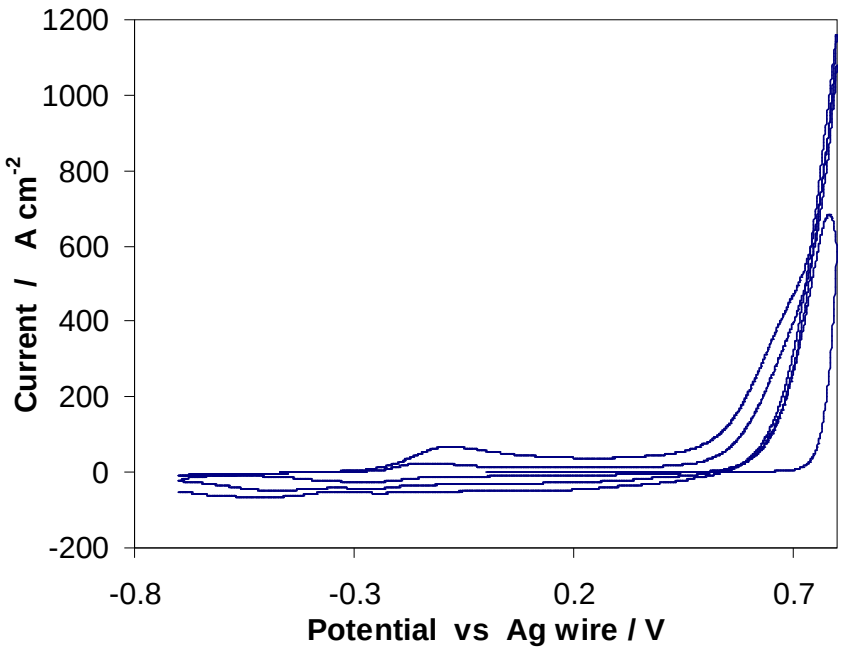

Figure 3.7 Copolymerization of Py-co-EDOT/ BMIM BF_4, ratio 1:2. Film deposition: 3 cycles. Scan rate: 40 mV s^{-1}.

Due to modifications of electrolytic media, significant differences appear when PPy-co-PEDOT was cycled in aqueous solution at the same potential range of -0.5 V to 0.5 V (vs. Ag/AgCl, 3 M KCl). Both anodic and cathodic peak potentials were located in the potential range of -0.2 V and 0 V, while in aqueous solution for high scan rates of 100 or 150 mV s^{-1} the peak potentials shifted to positive values of 0.1 V. When the PPy-co-PEDOT (1:2) was transferred to aqueous solution, the peak currents disappeared and the voltammetry appeared capacitive at 100 mV s^{-1}. This could be explained by the effects of a double layer charging as seen in Figure 3.7.b.

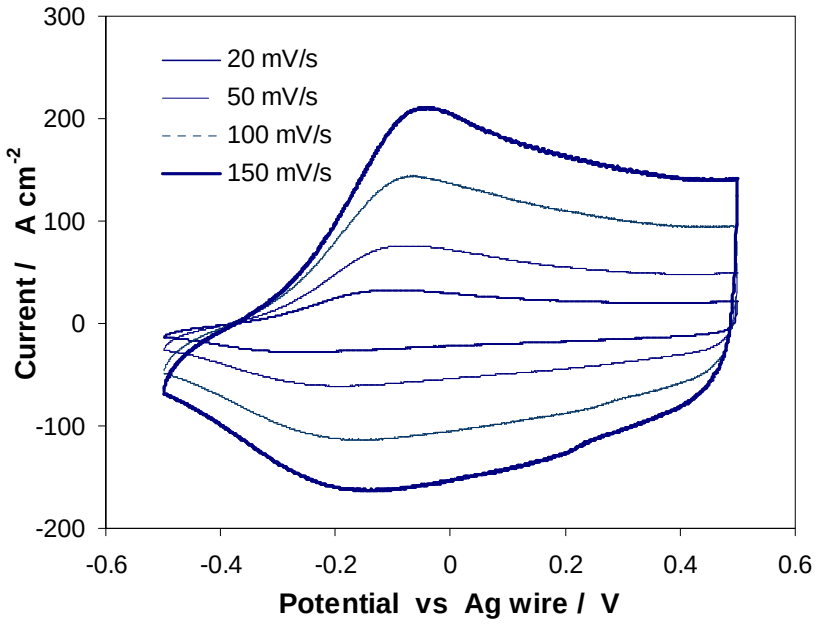

Figure 3.7.a Cyclic voltammogram of PPy-co-PEDOT (1:2) in monomer-free BMIM BF_4.

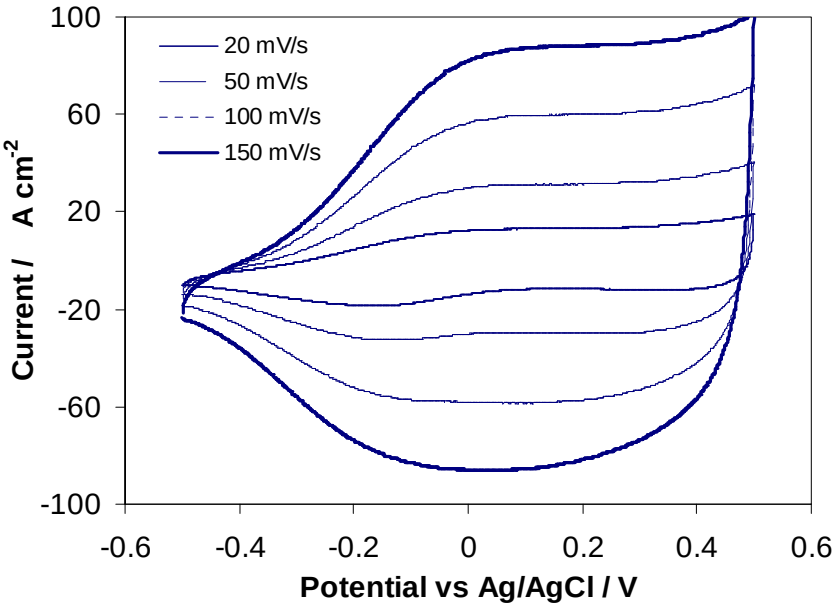

Figure 3.7.b Cyclic voltammogram of PPy-co-PEDOT (1:2) in monomer-free aqueous solution 0.2 M $NaBF_4$.

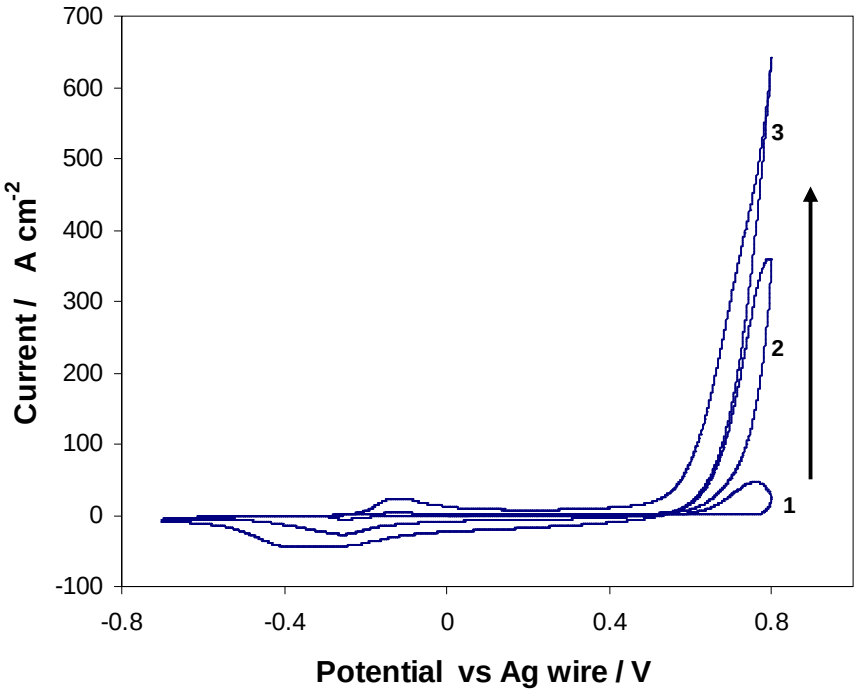

Figure 3.8 Cyclic voltammogram of PPy-co-PEDOT (ratio 1:1)/ BMIM BF_4. Film formation: 3 cycles. Scan rate: 40 mV s^{-1}.

The electrochemical behaviour of PPy-co-PEDOT (1:1) in neat BMIM BF_4 is shown in Figure 3.8.a where both anodic and cathodic peaks become more pronounced with increased scan rate. This means that the reduction and oxidation of copolymer is characterized by faster kinetics which may arise from decreased amounts of EDOT. In addition the oxidation peak current appeared at the same potential position (-0.1 V), while the reduction peak was slightly moved in a positive direction to -0.2 V. The scan rate study showed that ΔE_p was reduced at faster scan rates and the anodic/cathodic peak currents varied linearly with scan rate. The same film of PPy-co-PEDOT (1:1) was subsequently scanned in 0.2 M $NaBF_4$ aqueous solution (Figure 3.8.b). In aqueous solution the copolymer presents a significant increase of the capacitive current component and broad potential peaks.

The currents have a magnitude of 120 A cm^{-2} at 150 mV s^{-1} in BMIM BF_4 (Figure 3.8.a) similar to the values when the films were scanned in 0.2 M $NaBF_4$

(Figure 3.8.b), indicating that the films have preserved their electroactivity. A decrease of ΔE_p value for PPy-co-PEDOT (1:1) copolymer in aqueous solution (ΔE_p = 63 mV) was observed, compared to ΔE_p = 88 mV obtained for the CVs in pure BMIM BF_4.

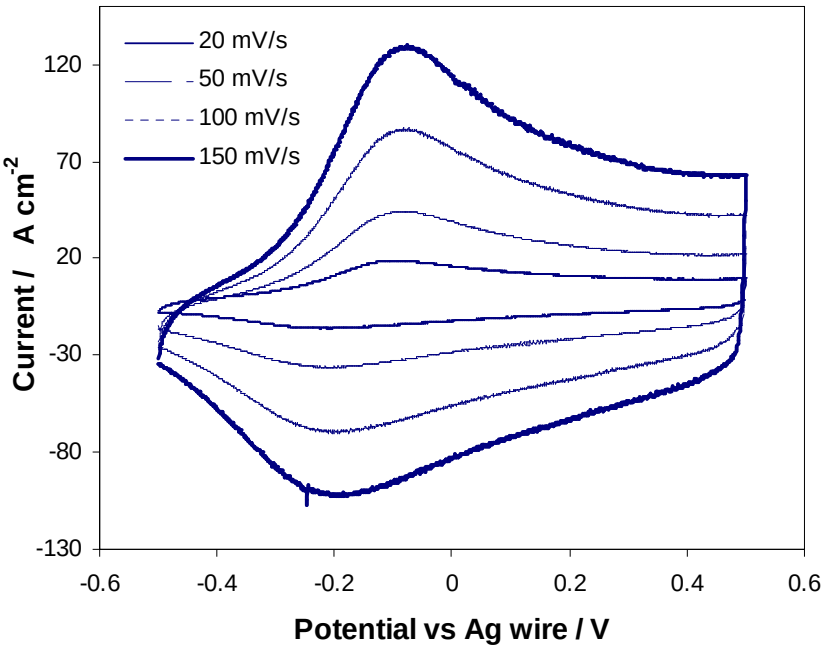

Figure 3.8.a Cyclic voltammogram of PPy-co-PEDOT (1:1) film in monomer-free BMIM BF_4.

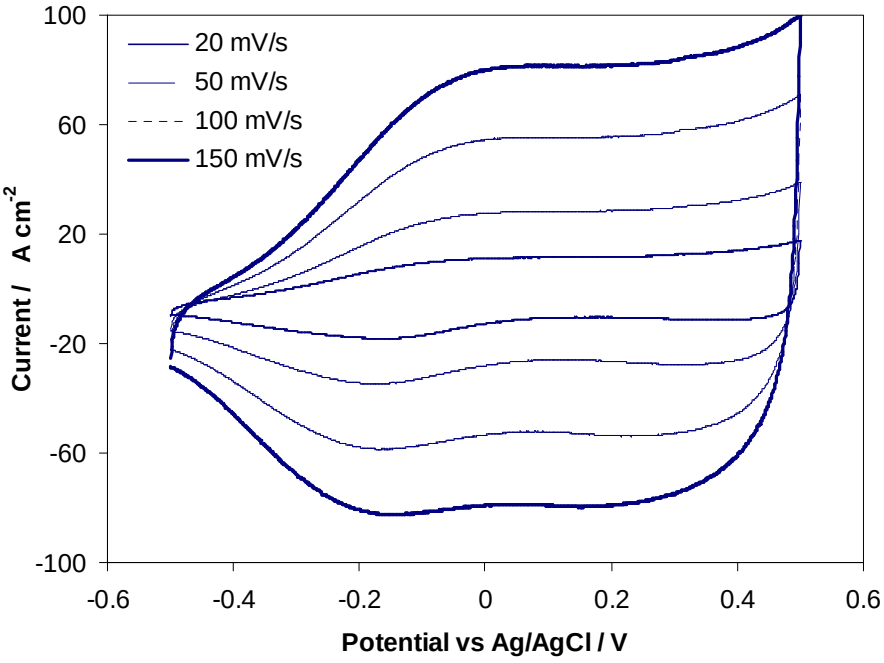

Figure 3.8.b Cyclic voltammogram of PPy-co-PEDOT (1:1) in monomer-free 0.2 M $NaBF_4$ aqueous solution.

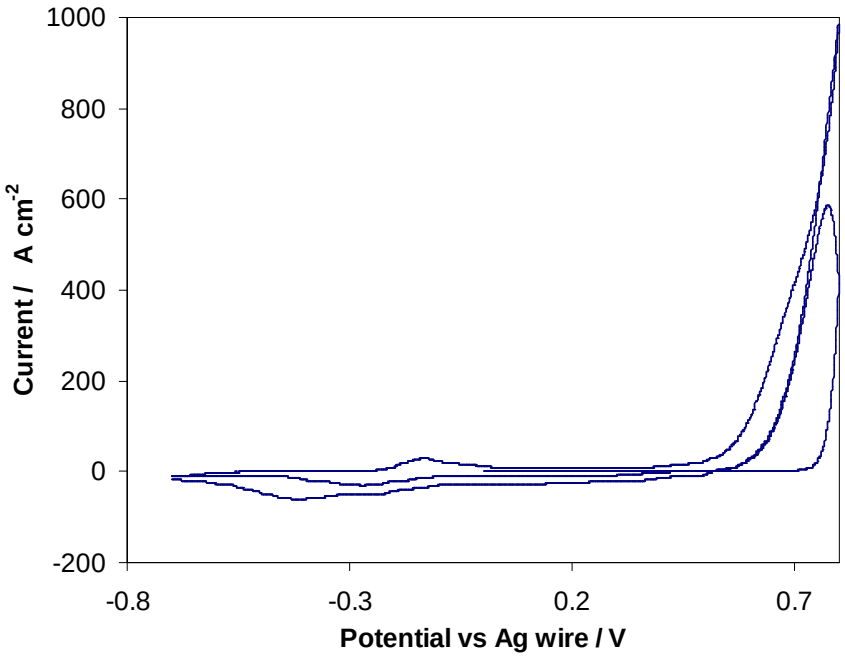

Figure 3.9 Cyclic voltammogram for copolymerization of PPy-PEDOT (2:1) in BMIM BF_4.

For the copolymer film PPy-co-PEDOT (2:1) (Figure 3.9) the electrochemical characterization was done in a similar manner as for PPy-co-PEDOT (1:2) and PPy-co-PEDOT (1:1). The electrochemical response of PPy-co-PEDOT (2:1) showed a clear increase in the peak currents with increased scan rate (Figure 3.9.a). The film exhibited fast kinetics which is evident from the sharp film voltammetry in ionic liquid on successive potential cycling. As expected, when the film was placed in aqueous solution (Figure 3.9.b), on continuous potential scanning the PPy-co-PEDOT (2:1) copolymer presents broad oxidation/ reduction potential peaks. Also the film thickness could be calculated from the total charge passed during oxidation ($Q = 6.34 \times 10^{-4}$ C cm^{-2}).

The resulting copolymer PPy-co-PEDOT thickness, L, was 15 nm, calculated from the relationship:

$$\mathbf{L = QW/(2.25F\ \ A)} \qquad (3.2)$$

where Q (C cm^{-2}) is the charge passed during growth, W (g mol^{-1}) is the molecular weight of the monomer, F (96485 C mol^{-1}) is Faraday's constant, (g cm^{-3}) the density of monomer. Number 2.25 in the relationship (3.2) is the number of electrons transferred. It is assumed that no swelling due to the presence of electrolyte occurred [26].

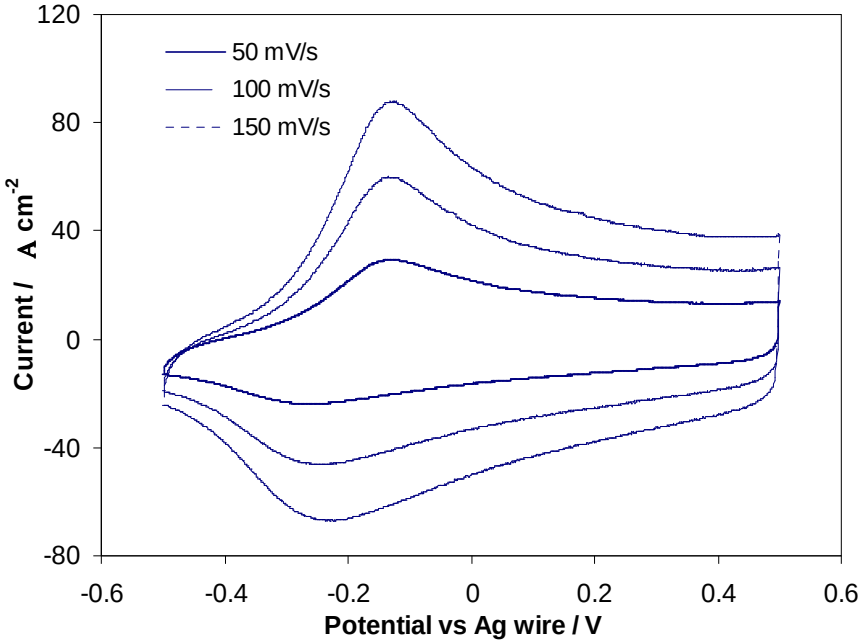

Figure 3.9.a Cyclic voltammogram of PPy-co-PEDOT (2:1) film performed in monomer-free BMIM BF_4.

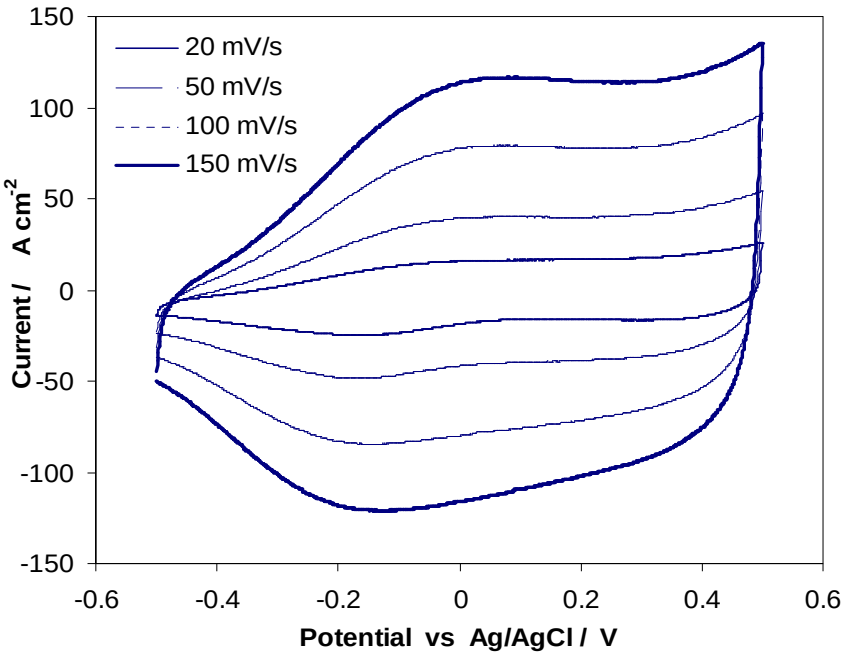

Figure 3.9.b Cyclic voltammogram of PPy-co-PEDOT (2:1), in monomer-free aqueous solution 0.2 M $NaBF_4$.

Consecutively PPy film was formed on ITO from a monomer solution containing BMIM BF_4 (Figure 3.10) which presents a linear relationship between the peak currents and the scan rate, verifying the thin layer behaviour (Figure 3.10.b). Upon oxidation the potential peaks shifted to more positive potentials and similarly upon reduction, the peak potentials shifted towards positive potentials (Figure 3.10.a). Broad peak potentials could be seen for the various scan rates, which could be explained by slow diffusion of the BF_4^- ions into the film.

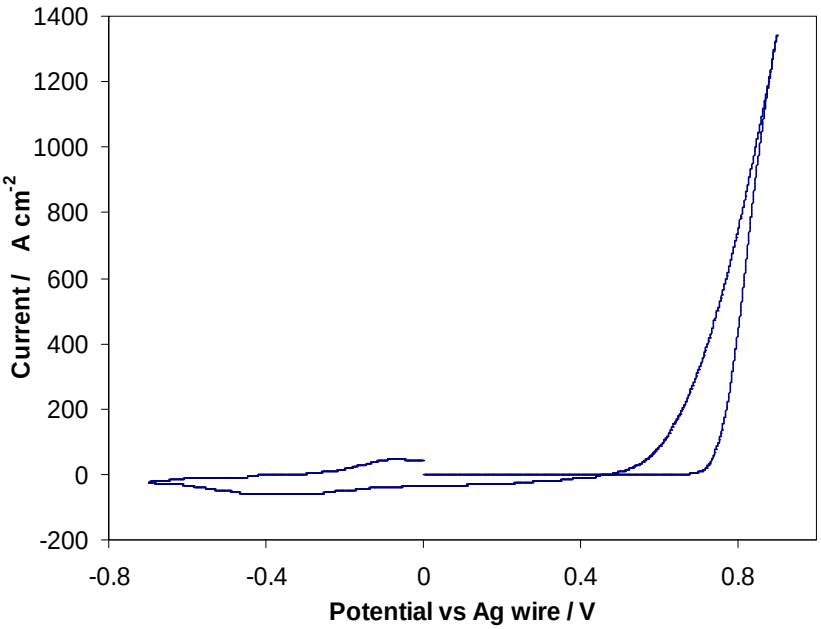

Figure 3.10 Cyclic voltammogram of polypyrrole film formation in BMIM BF_4. Scan rate: 50 mV s^{-1}.

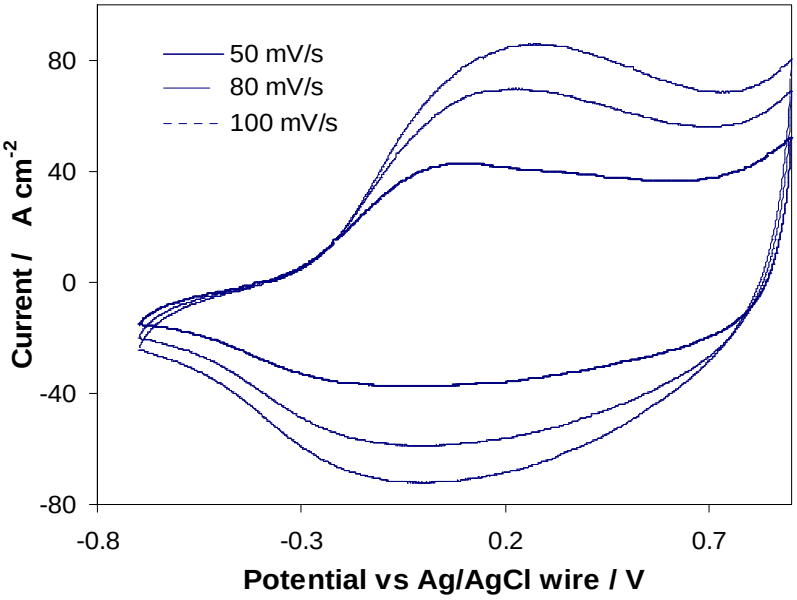

Figure 3.10.a Cyclic voltammogram of polypyrrole film in monomer-free BMIM BF_4

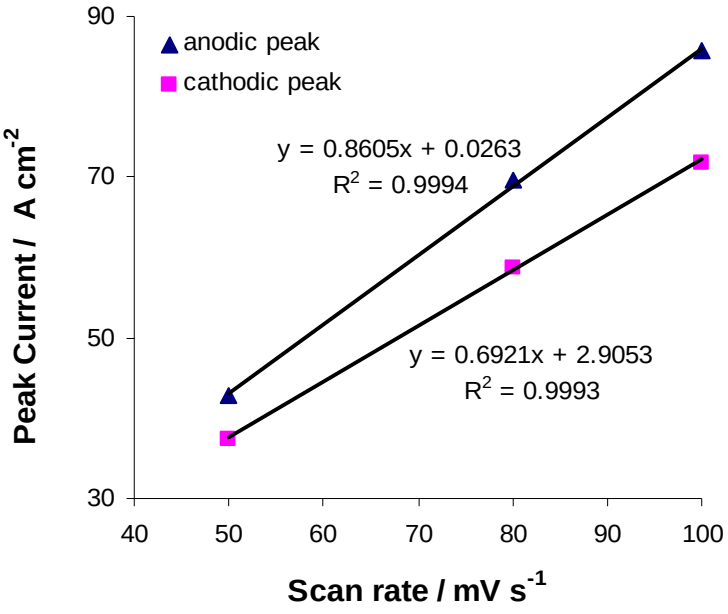

Figure 3.10.b Plot of anodic and cathodic peak currents of polypyrrole as function of scan rate.

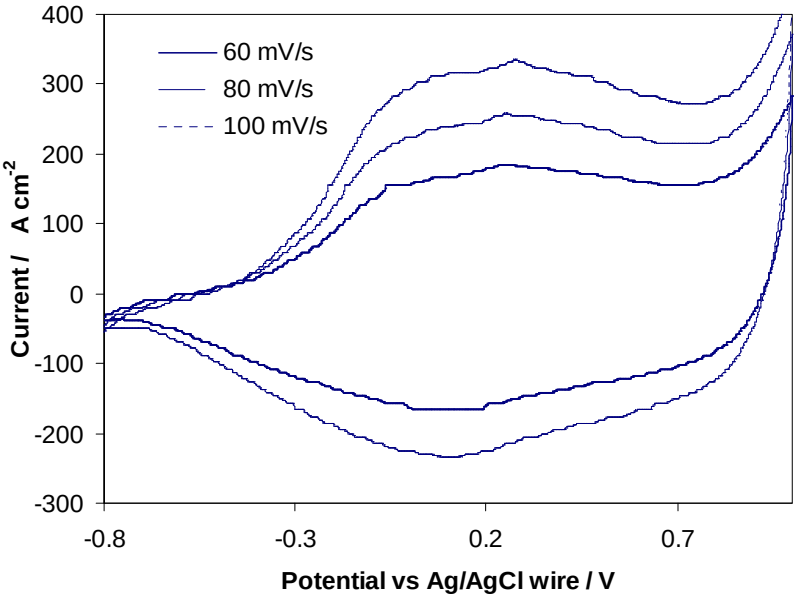

Figure 3.11 Cyclic voltammogram of poly(3,4-Ethylenedioxythiophene) film in monomer-free BMIM BF_4 ionic liquid.

The PPy-co-PEDOT (2:1) was electrochemically characterized in monomer free ionic liquid (BMIM BF_4) in the potential range of -0.5 V to 0.5 V versus Ag wire.

The copolymers present well defined and reversible redox processes. However, a decrease of the currents was seen when copolymer films were cycled in aqueous solution 0.2 M $NaBF_4$. The scan rate dependence of the anodic and cathodic peak currents shows a linear dependence on scan rate as illustrated in Figures 3.7, 3.8, 3.9. This demonstrates that the electrochemical process is a thin layer behaviour. However the ΔE_p for all copolymers is greater than 0 mV as shown in Table 1. Actually all copolymers were electrochemically active with different characters depending on the monomer ratios.

Table 1 Table of forward peak potential (E_p^f) and peaks separation (ΔE_p) of copolymer for different PPy/PEDOT ratios.

PPy ratio	PEDOT ratio	E_p^f	ΔE_p
1	2	> -0.04 V	93 mV
1	1	-0.1 V	88 mV
2	1	-0.15 V	113 mV
1	0	varies	-
0	1	0.1 V	~ 100 mV

It can be seen that as the amount of PEDOT increased, the forward peak potential of the voltammogram in pure BMIM BF_4 also increased. This was an indication of clear increase of PEDOT amount in the copolymer indicating that, it was possible to tune the redox potential of the layer by changing the ratio of monomer concentrations, Py and EDOT respectively.

3.3.3 In-situ Spectroelectrochemistry of PPy-co-PEDOT Copolymers

In-situ UV-Vis spectroelectrochemistry is a useful method for the structural and optical characterization of conducting polymers [27]. Changes in absorption spectra and information about the optical properties as function of applied potential of PPy-co-PEDOT copolymer was studied.

For this purpose, the spectroelectrochemistry of the copolymer films was carried out in monomer-free solution of 0.2 M $NaBF_4$ aqueous solution during successive switching between oxidized to reduced forms. A series of UV spectra were obtained at different potentials. Constant potentials were applied until the current fell to zero and the steady state spectrum was collected. The film had been formed by scanning the potential from -0.7 V to 0.8 V versus Ag/ AgCl/ 3 M KCl..

Figure 3.12 shows the absorbance change with potential starting for 0.8 V (oxidation potential) down to -0.6 V (reduction potential) of the PPy-co-PEDOT (1:2). The film shows very little change in absorbance over the visible range. Upon reduction of the film, a broad absorbance peak was seen at 400 nm, which increased with decreasing potential values and a polaron peak was observed at 507 nm.

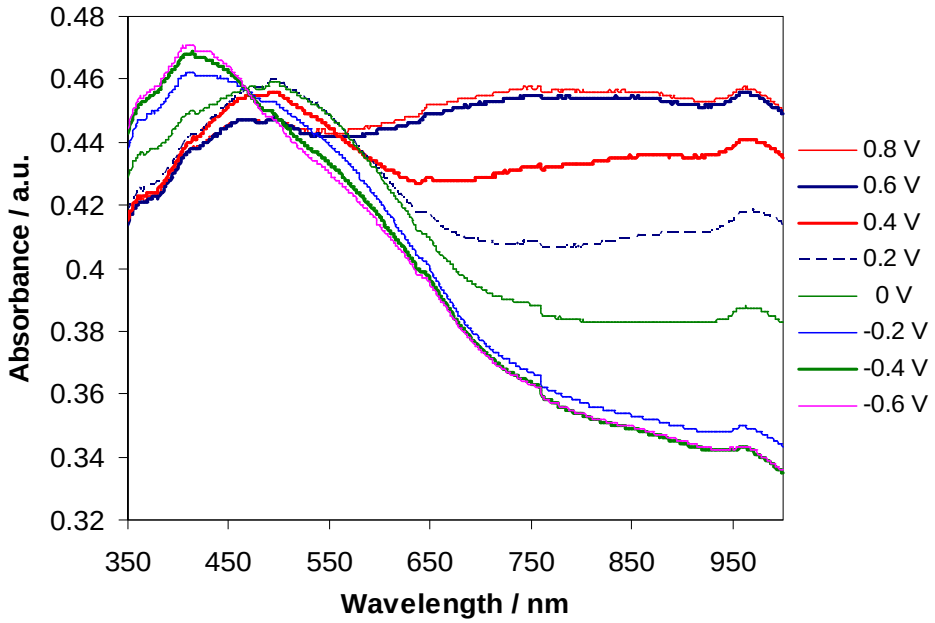

Figure 3.12 UV-Vis spectroelectrochemical spectra of PPy-co-PEDOT (1:2) films on ITO as function of applied potentials from 0.8 V down to -0.6 V in 0.2 M $NaBF_4$ aqueous solution

The potential-dependent change in the peak intensities of the absorbance upon p-doping for PPy-co-PEDOT (1:1) film in 0.2 M $NaBF_4$ aqueous solution is illustrated in Figure 3.13. Similar to PPy-co-PEDOT (1:2), the PPy-co-PEDOT (1:1) films present very little change in the absorbance over the UV-Vis range and the isosbestic point is not very clear. Upon successive reduction of PPy-co-PEDOT (1:1) thin film in an aqueous solution of 0.2 M $NaBF_4$, the π-π^* transition intensity was reduced and the formation of charge carrier bands was observed. The appearance of the broad absorbance peak at 564 nm can be attributed to the presence of a polaron band (Figure 3.13).

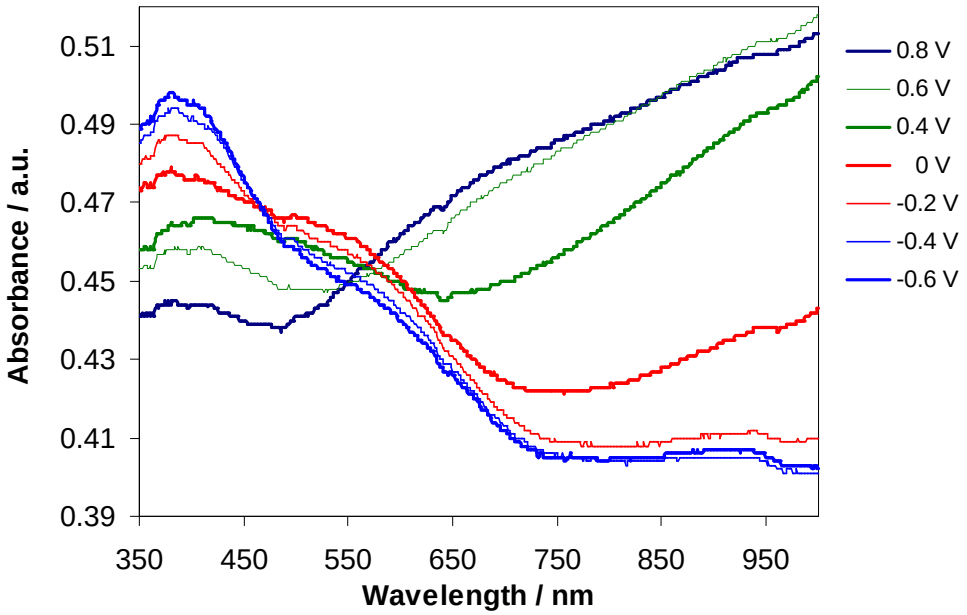

Figure 3.13 UV-Vis spectroelectrochemical spectra of PPy-co-PEDOT (1:1) films on ITO as a function of applied potentials from 0.8 V down to -0.6 V in 0.2 M $NaBF_4$ aqueous solution.

In Figure 3.14 the reduction process of 'polypyrrole dominated' copolymer PPy-co-PEDOT (2:1) in aqueous solution 0.2 M $NaBF_4$, shows a sharp absorbance peak at 380 nm in the oxidized form. As the potential applied to the polymer reached a value of 0 V, the absorbance peak displayed a blue shift to 370 nm. At negative potentials, $_{max}$ occurred at 400 nm and also significant changes in the absorbance were noticed compared to PPy-co-PEDOT (1:2) and PPy-co-PEDOT (1:1). At 560 nm a broad shoulder appeared due to polaron formation [28].

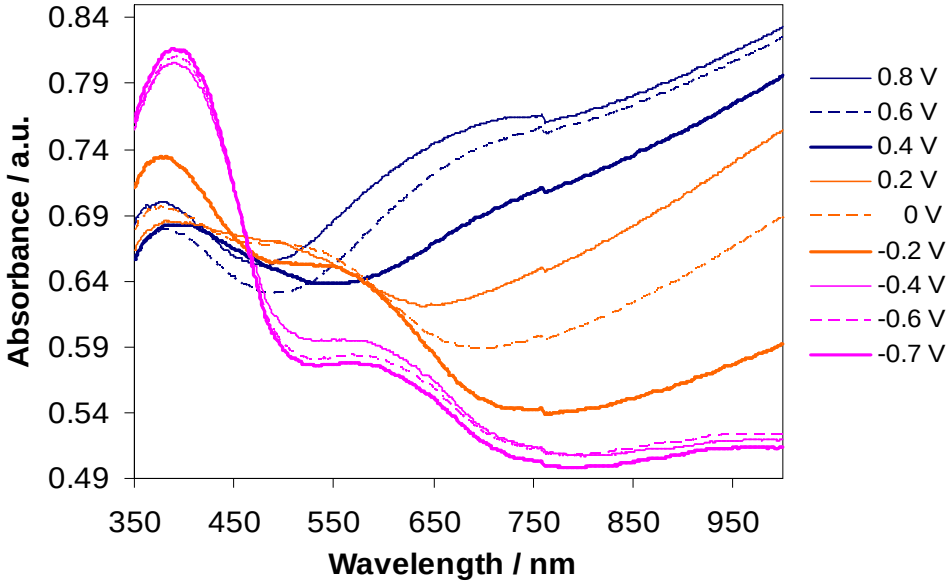

Figure 3.14 UV-Vis spectra of PPy-co-PEDOT (2:1) films on ITO while constant potentials were applied for 50s. Potential range: 0.8 V down to -0.7 V. Intervals of 0.2 V were applied.

Comparing the spectroelectrochemical results of PEDOT and copolymers, the λ_{max} for the neutral PEDOT was found at 520 nm and in Figure 3.14 an isosbestic point appeared indicating the transition between neutral and bipolaron. In figures 3.12, 3.13 and 3.14 no isosbestic point is present and each of the spectra show the presence of neutral, polaron and bipolaron peaks. The absorbance peak in the neutral form is at the same wavelength for all the copolymers and is dominated by pyrrole. The bipolaron peak was broad in each case and the maximum wavelength was difficult to determine.

Table 2 λ_{max} of polaron peak as a function of the ratios of PPy/PEDOT

PPy	PEDOT	λ_{max} (nm)	Figure
1	2	507	3.12
1	1	564	3.13
2	1	558	3.14

The evolution of polaron peak appears to be directly related with the change of Py : EDOT monomer ratio. In all three copolymers the polaron state is stable unlike the PEDOT polymer where the equilibrium lies to the right hand side.

2 polarons ⇌ neutral + bipolaron

Thus it is clear that the polaron band gap can be modulated by changing the Py : EDOT monomer ratio. Even when a small amount of pyrrole such as Py-co-PEDOT of 1:2 (Figure 3.12), the polaron is stabilised compared to Figure 3.5.

3.3.4. Electrochromic Switching Studies

The spectral variation corresponds to a change of colour from oxidized form (grey-blue) to a reduced form (olive-green). The ability of the polymer to change its colour in a reversible manner is of main importance for display applications [17, 29]. The PPy-co-PEDOT copolymer exhibited systematic changes in the visible absorbance spectrum and this was seen as a promising material for electrochromic applications. The PPy-co-PEDOT (2:1)/ BMIM BF_4 system was studied in detail in order to explore its properties as electrochromic material. The copolymer formed from the ionic liquid was used in aqueous solution when spectroelectrochemical experiments were performed.

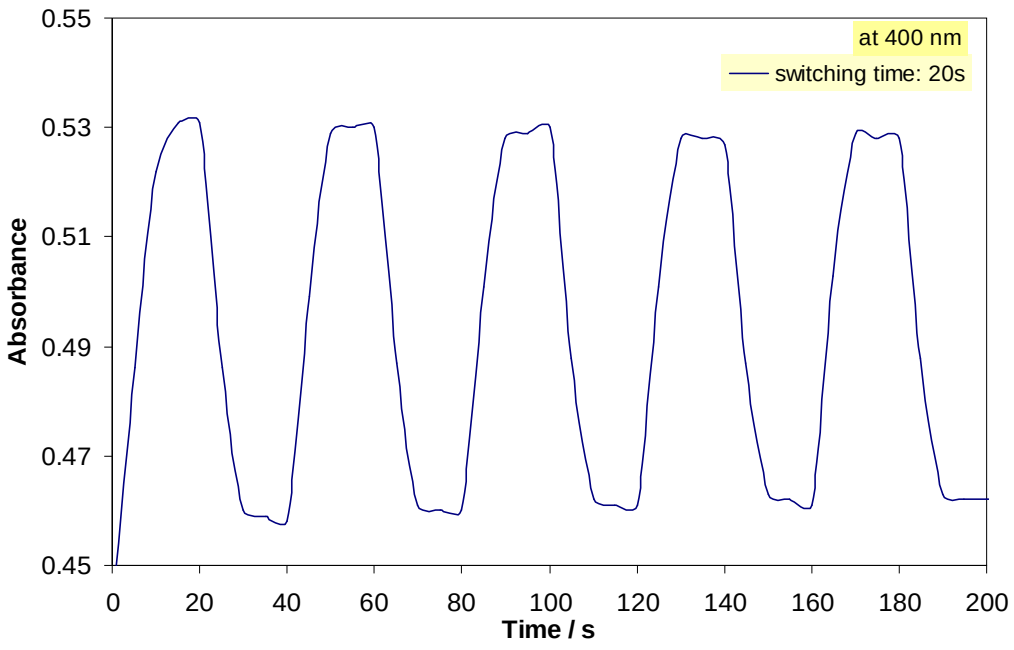

Figure 3.15 Electrochromic switching response for PPy-co-PEDOT (2:1) monitored at 400 nm.Response time: 20 s. Potential limits: -0.7 V to 0V.

The PPy-co-PEDOT (2:1) electrochromic response was performed at 400 nm and 700 nm wavelength, applying a potential between -0.7 V and 0 V (Figure 3.15 and Figure 3.16). The potential was interchanged between -0.7 V (reduced form) and 0 V (oxidized

form) at exact intervals of 20 seconds. The film exhibited reversible behaviour and a relatively fast switching time of 20 seconds [30].

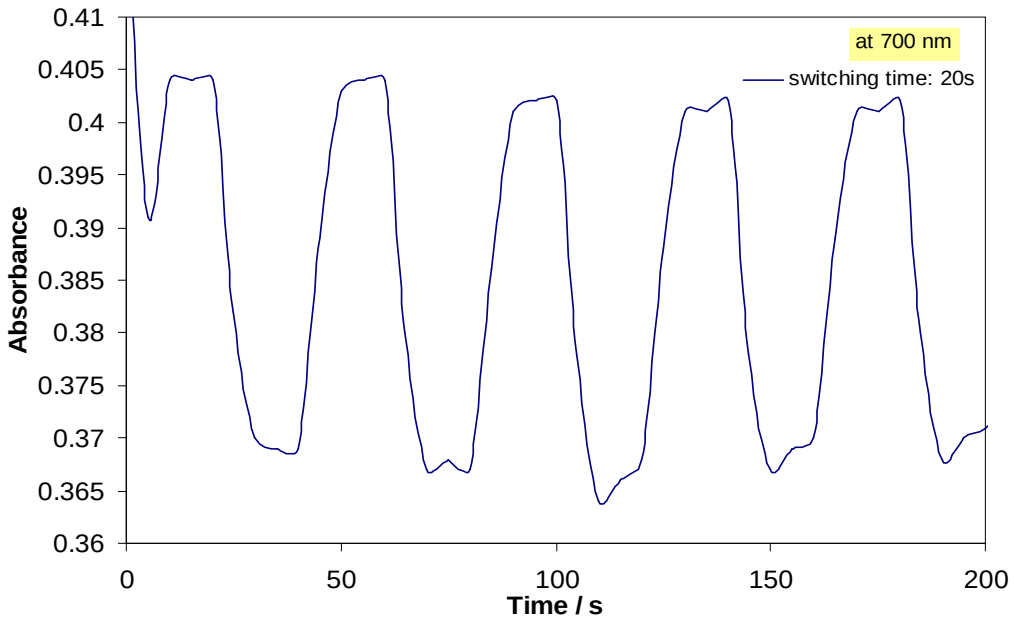

Figure 3.16 Electrochromic switching response for PPy-co-PEDOT (2:1) monitored at 700 nm. Response time: 20 s. Potential limits: -0.7 V to 0V.

The electrochromic switch experiment was carried out also at 700 nm for the same potential interval of -0.7 V to 0 V. The film showed steady and reversible change in absorbance with time also at 700 nm.

A control experiment investigating the electrochromic switching properties was performed at 800 nm, where it can be seen that for a different potential range -0.5 V to 0.5 V, the absorbance range remained constant with time (~ 10 minutes) (Figure 3.17). PPy-co-PEDOT (2:1) films were submitted to consecutive potential steps between -0.5 V and 0.5 V in order to retrieve data about the stability of electrochromic changes.

Another important characteristic of electrochromic films is the coloration efficiency (CE), which is calculated using the following equation derived from Beer-Lamber law [31]:

$$CE = \frac{\Delta A}{Q_d} = \frac{\log\left(\frac{T_{ox}}{T_{neut}}\right)}{Q_d} \qquad (3.3)$$

where Q_d is in C cm^{-2}, CE ( ) is in $C^{-1}cm^2$, and T_{ox} and T_{neut} are the transmittance value of oxidized and reduced state. For the present study ΔA was used, as shown in Figure 3.12 and Figure 3.13.

Colouration efficiency CE ( ) is related to the performance of the electrochromic device and is defined as the ratio between the change in optical density (ΔOD) and the injected/ ejected charge per unit area of the electrode at a specific wavelength ($_{max}$) [32]. The PPy-co-PEDOT (2:1) copolymer had colouration efficiency of 101.3 $C^{-1}cm^2$, which is a reasonable value for an electrochromic material [29] [33].

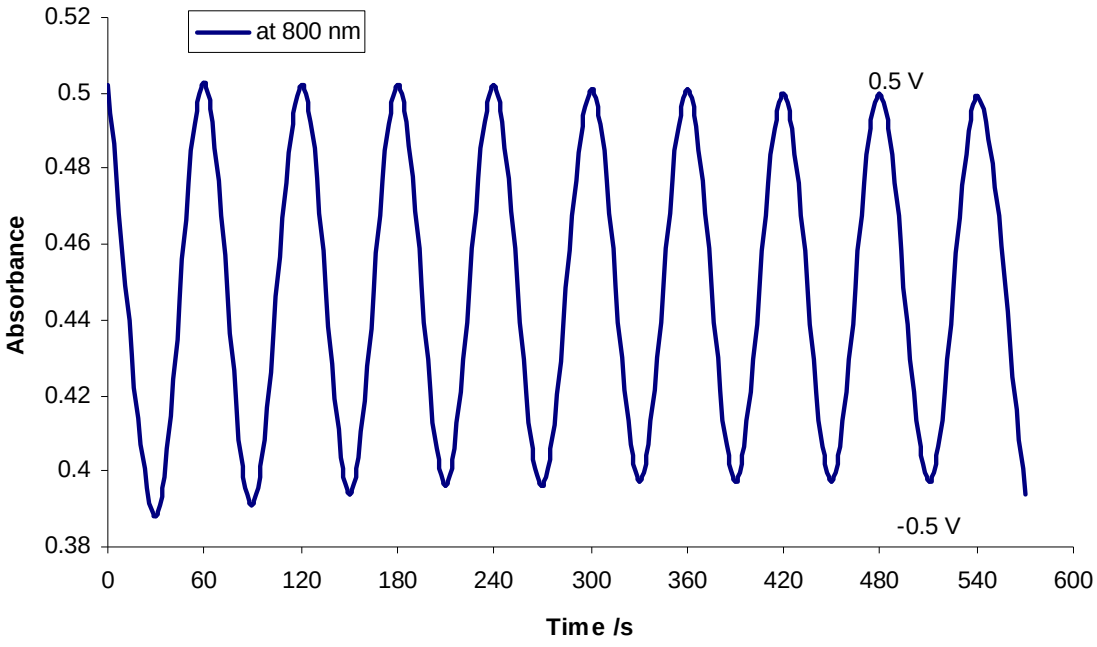

Figure 3.17 Reversible response for PPy-co-PEDOT (2:1) monitored at 800 nm. Potential limits: -0.5 V and 0.5 V

Comparing Figure 3.9.b and Figure 3.18, it can be seen that the absorbance increases well beyond the peak current. This indicates that the region past the peak associated with double layer charging comprises of faradaic current.

Similar results were reported by Kalaji and Peter [34], which indicates that current at higher potentials is not solely due to double layer charging. Their study was done for an 80 nm polyaniline film deposited on ITO glass at 20 mV s^{-1}. The polyaniline optical absorption was observed at 620 nm as a function of potential since polyaniline presents a maximum absorbance at this wavelength upon oxidation. The results showed a continuous increase in absorbance during oxidation, observed beyond the peak in the voltammogram [34]. This was associated with rapid charge transfer which meant that there was a faradaic pseudo-capacitive component. The non-linearity seen in the plot of absorbance versus potential (Figure 3.18) indicated that more than one absorbing species was formed (e.g. polaron and bipolaron species [35]).

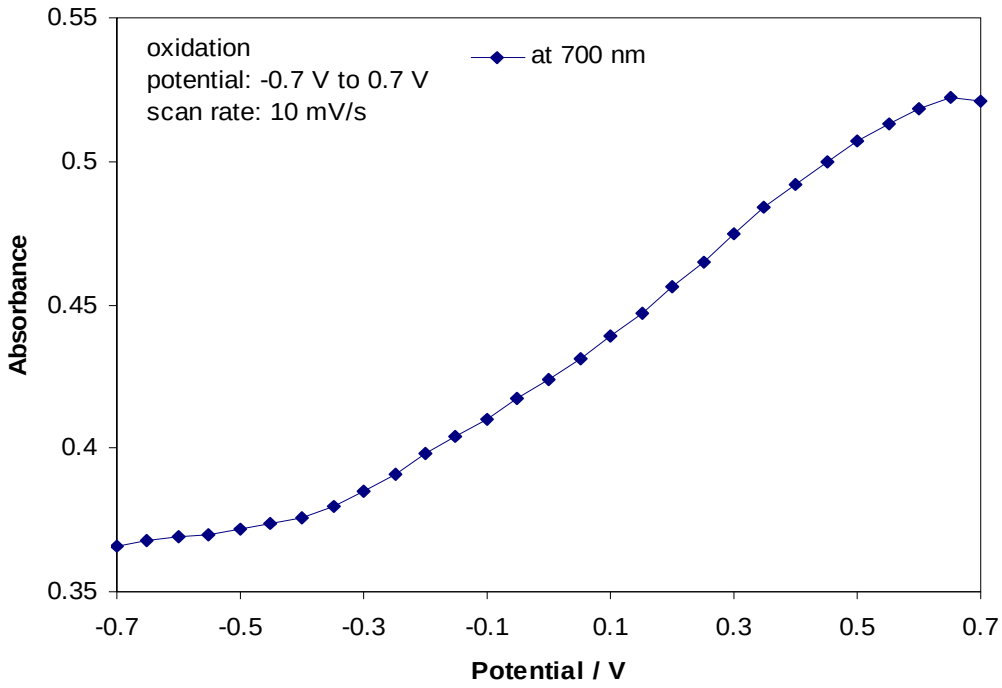

Figure 3.18 Absorbance evolution with time at 700 nm, when PPy-co-PEDOT (2:1) copolymer is cycled in 0.2 M $NaBF_4$ aqueous solution between -0.7 V to 0.7 V.

3.3.5. FTIR-ATR Structural Characterization

Thick films of PEDOT, PPy and PPy-co-PEDOT copolymers were formed on ITO by cyclic voltammetry and analysed by FTIR. The results of the FTIR analysis were rather unclear as the films formed on ITO were quite far from the detector. It is known that PPy and PEDOT polymers have characteristic peaks at 827, 936, 1140, 1182, 1372, 1552, 2677, 2829 cm^{-1} and 813, 1016, 1126, 1192, 1125, 1424, 1571, 1846, 2008, 2663, 2824 cm^{-1}, respectively [36].

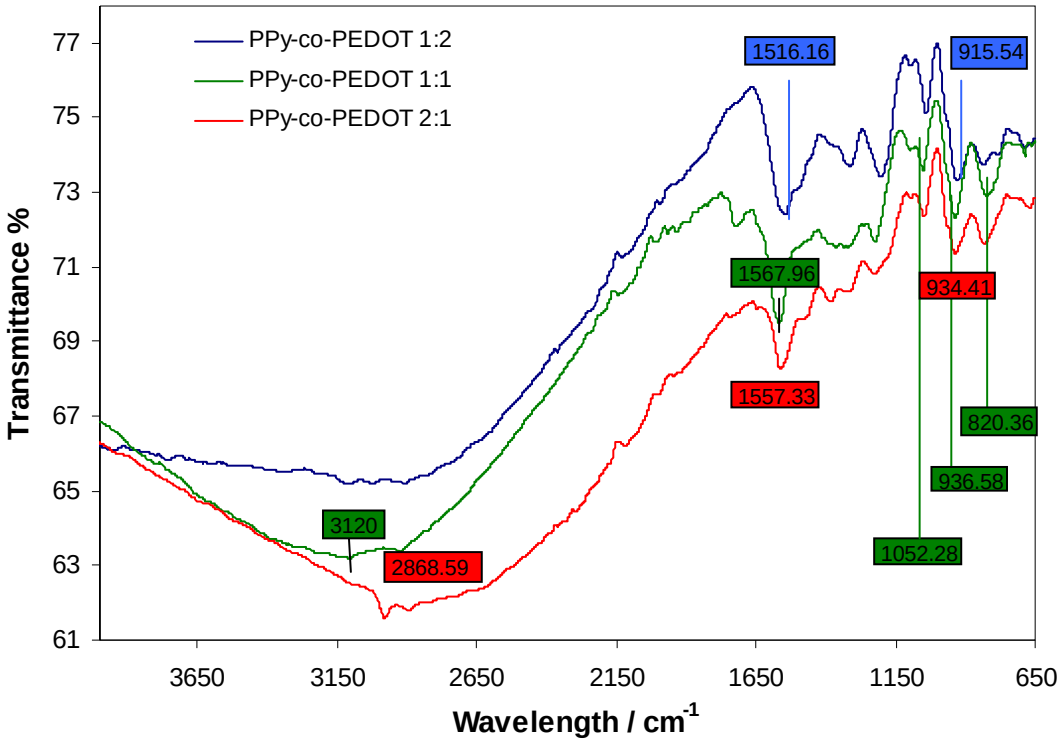

Figure 3.19.A FTIR spectra of PPy-co-PEDOT (1:2), (1:1), (2:1) films on ITO substrate.

In Figure.3.19.A the three copolymers clearly have a dominant pyrrole signature and peaks at 1516.16, 1567.96, 1557.33, and 1052.28 cm^{-1} can easily be seen. The peaks at 1300 cm^{-1} for PEDOT were not evident for the three copolymers. FTIR analysis revealed little difference in the FTIR spectra of the three copolymers, even

though they were prepared in different monomer ratios. All copolymers showed small peaks characteristic to C-S bands at 820 cm^{-1}, that indicated the presence of thiophene in the copolymers. In comparison with the corresponding homopolymers, the PPy-co-PEDOT films had weak bands 820.36, 915.54 and 1054.28 cm^{-1}, indicating the presence of EDOT rings.

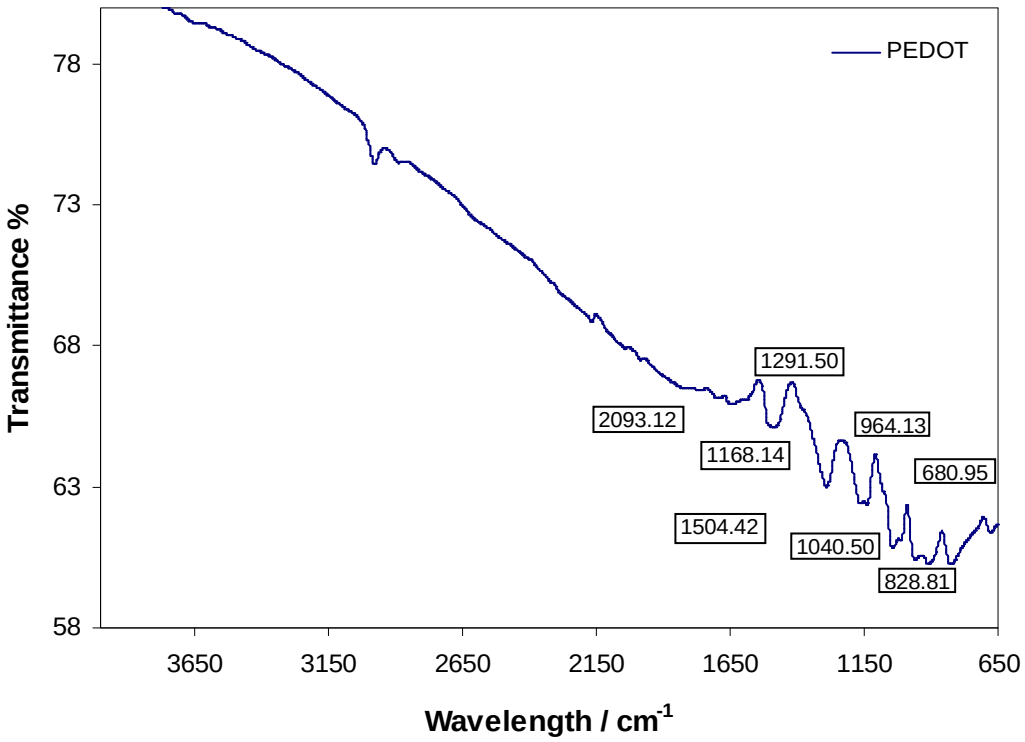

Figure 3.19.B FTIR spectra of PEDOT film formed in BMIM BF_4.

The FTIR spectra of PEDOT films showed bands at 680.95, 828.81 and 964.13 cm^{-1} which originate from the stretching mode of C-S. The bands which appeared at 1040.50 and 1168.14 cm^{-1} are assigned to the stretching modes of C-O-C groups. The vibration modes of the C=C and C-C bonds in thiophene rings could be seen at 1504.42 and 1291.50 cm^{-1}.

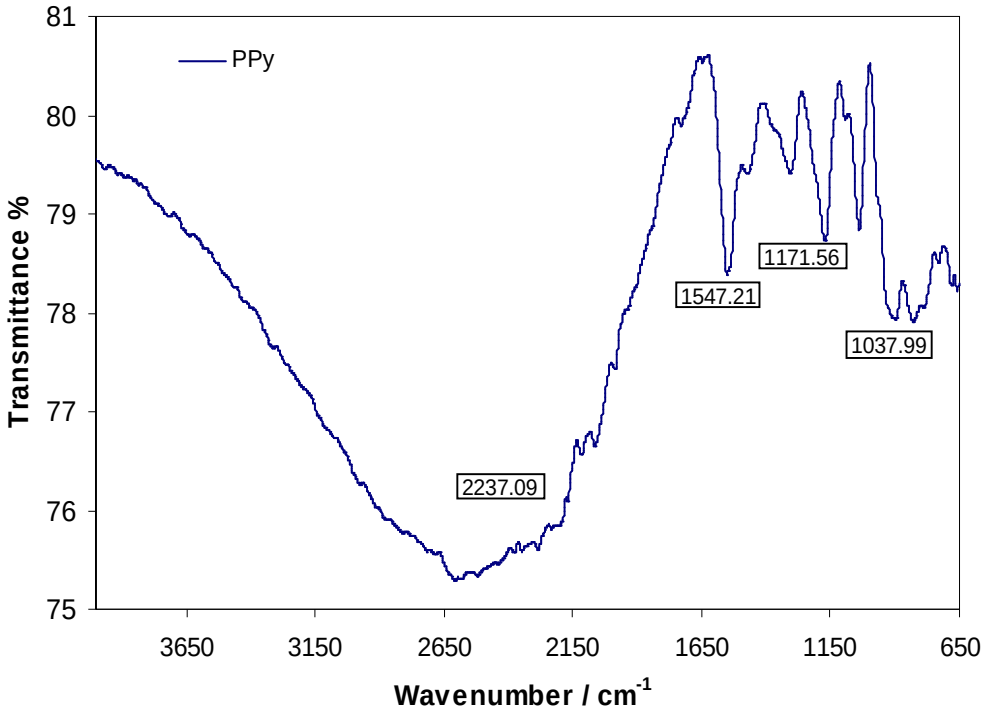

Figure 3.19.C FTIR spectra of PPy film formed in BMIM BF_4.

Characteristic bands of PPy films formed in BMIM BF_4 are presented in Figure 3.19.C. The stretching mode of C-N was located at 1037.99 and 1171.56 cm^{-1}, while the stretching bands corresponding to N-H at 750 and 3400 cm^{-1} were not very clearly defined.

The PEDOT peaks were poorly defined when compared to the spectra of the PPy and PPy-co-PEDOT copolymers. The peaks situated at ca. 1200 cm^{-1} correspond to ring vibrations of pyrrole and EDOT in the copolymers. It can be seen that the intense peaks at 1054 cm^{-1} and 1541 cm^{-1} have appeared due to the influence of PEDOT band at 1040.50 cm^{-1} and PPy band at 1547.21 cm^{-1}. The FTIR spectra demonstrate that the PPy-co-PEDOT films contain features of both pyrrole and EDOT monomer units.

The peak corresponding to -coupling for the pyrrole units in the copolymer was previously located at 770 cm^{-1} [37] and had a very low intensity. The present FTIR study indicates a low intensity peak around 700 cm^{-1} (Figure 3.19.A), which may assigned to copolymer formation.

3.3.6 Morphological Features

Polymer films of PPy, PEDOT, PPy-co-PEDOT (1:2), PPy-co-PEDOT (1:1), PPy-co-PEDOT (2:1) were formed on ITO substrates and characterized by scanning electron microscopy (SEM). The films were rinsed with acetonitrile in order to remove traces of ionic liquid and dried in air before the analysis. All three copolymer films prepared from different monomer ratios and observed on SEM exhibited different morphologies.

The morphologies of new copolymers have different features compared to PPy/ BMIM BF_4 and PEDOT/ BMIM BF_4. PEDOT homopolymers are known to be porous films [38], while PPy films are characterized by a cauliflower appearance [21]. The PPy-co-PEDOT (1:2) film has a distribution of globules, pores and holes which indicated the incorporation of both PPy and PEDOT to produce the new copolymer. It is interesting to observe that the PPy-co-PEDOT (1:1) film has a featureless structure.

The morphological aspect of PPy-co-PEDOT (1:1) is very different since this copolymer shows an array of very small granules. The PPy-co-PEDOT (1:1) morphology is strikingly different from the 'polypyrrole dominated' copolymer PPy-co-PEDOT (2:1), which presents bigger clusters of globules and holes with increased diameter. The SEM analysis of PPy-co-PEDOT (2:1) was interesting to observe since this polymer displayed the best electrochomic properties. The apearance of pores with increased diameter could explain the good electrochemical behaviour, from the perspective of ions which can be injected/ ejected easily into/out of the polymer matrix.

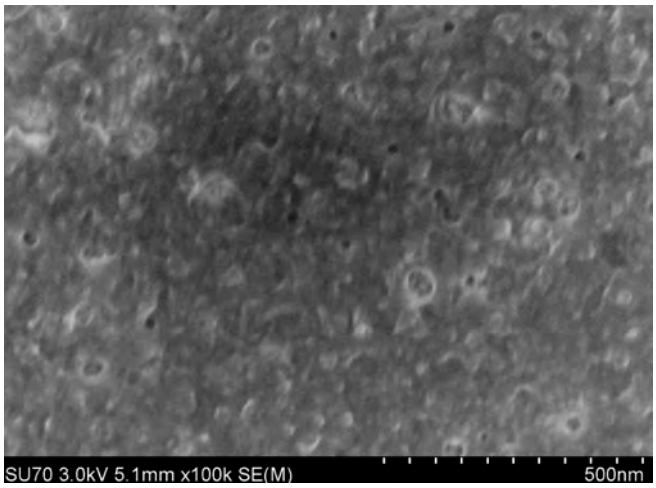

Figure 3.20.A SEM image for PPy-PEDOT (1:2)

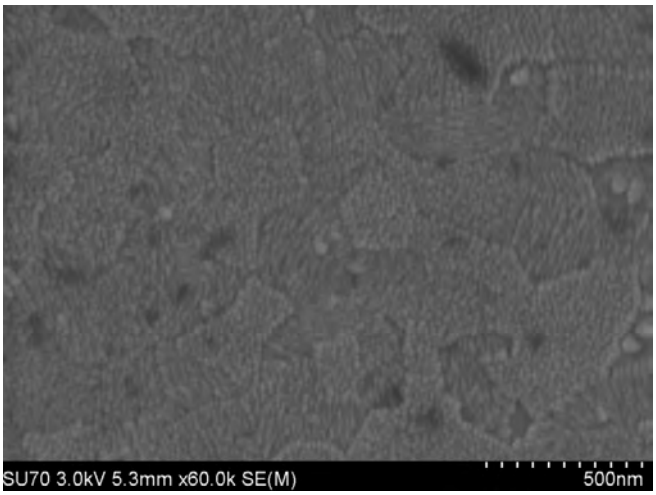

Figure 3.20.B SEM image for PPy-PEDOT (1:1)

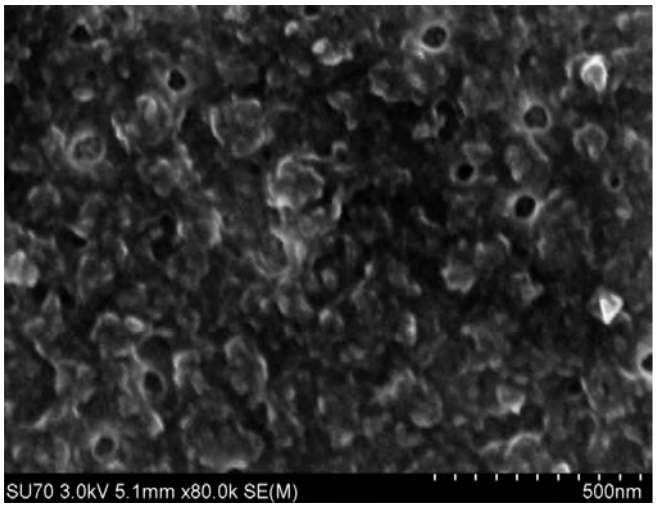

Figure 3.20.C SEM image for PPy-PEDOT (2:1)

3.4 Conclusions

In this study, new PPy-co-PEDOT copolymers were successfully synthesised by electrochemical oxidation of monomer mixtures in BMIM BF_4 ionic liquid using a novel microcell set-up. The copolymers prepared in three different ratios were further characterized by several means such as cyclic voltammetry, in-situ UV-Vis spectroelectrochemistry, FTIR analysis and scanning electron microscopy (SEM). According to the cyclic voltammograms (CVs) of the copolymer film obtained in both ionic liquids and aqueous electrolyte, different electrochemical responses were observed when the copolymers were removed from their growth medium. Actually the copolymers CV curves showed well-defined redox processes comparable to earlier studies done by Tao Yi-Jie et al [37]. The current density was proportional to the applied scan rates indicating the presence of an electroactive thin film.

Spectroelectrochemical analysis of copolymers showed distinct electrochromic properties compared to those of PPy and PEDOT polymers. Changes in the absorbance spectrum of the copolymer film as a function of the applied potential to the electrode were observed upon the evolution of charges for all three copolymers. The in-situ spectroscopic measurement as function of potential helped in detecting PPy-co-PEDOT (2:1) as the best behaved copolymer, as only for this copolymer transitions from neutral to polaron and bipolaron could be seen. These results are comparable to the UV-Vis spectra upon oxidation of PPy-co-PEDOT copolymers in acetonitrile [37].

FTIR was used to confirm the existence of both pyrrole and EDOT rings in the copolymer. FTIR spectra of the polymers and copolymers investigated were not very clear, but according to existent literature [37] on copolymerization it was possible to state that a new copolymer was formed. Previous work reported similar FTIR features for the PPy-co-PEDOT copolymers formed in acetonitrile solutions containing lithium perchlorate [37]. The copolymers study was completed by SEM analysis, which

highlighted the differences in morphology of copolymers to that of homopolymers. In comparison to PPy-co-PEDOT films formed in acetonitrile [37], the SEM test revealed various accumulations of globules and porous appearance, according to the amount of pyrrole existent in the sample. The careful study of copolymers helped in understanding the redox behaviour of these materials. Investigation of the electrochromic properties at two wavelengths, 400 and 700 nm, proved the reversible electrochromic behaviour of copolymer PPy-co-PEDOT (2:1) and the value for the coloration efficiency was 110.41 C^{-1} cm^2. The value obtained for colouration efficiency is in good agreement with those required for display applications reference and suggested that this new material could be used in applications such as smart windows and other ECDs.

Different colours were observed for the oxidized and reduced forms of the copolymers formed in the three monomer ratios. The PPy-co-PEDOT (2:1) colours were different from those of PPy and PEDOT, as they changed from olive-green to blue-grey when switching between oxidized and reduced form. The colours seen for the PPy-co-PEDOT (1:2) had a green-yellowish in reduced state and blue-greenish in the oxidized state. The copolymer prepared in equal monomer ratios (PPy-co-PEDOT, 1:1) exhibited a yellow –greenish colour in the reduced form and a (darker) grey-bluish colour in the oxidized state.

3.5 References

[1] E. Frackowiak, V. Khomenko, K. Jurewicz, K. Lota, F. Beguin, J Power Sources, 153 (2006) 413-418.
[2] S. Aytaç, F. Kuralay, İ.H. Boyacı, C. Unaleroglu, Sensors and Actuators B: Chemical, 160 (2011) 405-411.
[3] C.J. Brabec, N.S. Sariciftci, J.C. Hummelen, Adv Funct Mater, 11 (2001) 15-26.
[4] A.A. Argun, A. Cirpan, J.R. Reynolds, Adv Mater, 15 (2003) 1338-+.
[5] A. Kraft, A.C. Grimsdale, A.B. Holmes, Angew Chem Int Edit, 37 (1998) 402-428.
[6] C. Plesse, F. Vidal, H. Randriamahazaka, D. Teyssié, C. Chevrot, Polymer, 46 (2005) 7771-7778.
[7] T.A. Skotheim, R.L. Elsenbaumer, J.R. Reynolds, Handbook of conducting polymers, Marcel Dekker, 1998.
[8] J.M. Pringle, J. Efthimiadis, P.C. Howlett, J. Efthimiadis, D.R. MacFarlane, A.B. Chaplin, S.B. Hall, D.L. Officer, G.G. Wallace, M. Forsyth, Polymer, 45 (2004) 1447-1453.
[9] D. Kumar, R.C. Sharma, Eur Polym J, 34 (1998) 1053-1060.
[10] A.J.C. da Silva, F.A. Ribeiro Nogueira, J. Tonholo, A.S. Ribeiro, Solar Energy Materials and Solar Cells, 95 (2011) 2255-2259.
[11] J.P. Ferraris, M.M. Eissa, I.D. Brotherston, D.C. Loveday, A.A. Moxey, J Electroanal Chem, 459 (1998) 57-69.
[12] F. Selampinar, U. Akbulut, T. Yilmaz, A. Gungor, L. Toppare, J Polym Sci Pol Chem, 35 (1997) 3009-3016.
[13] W. Plieth, Electrochemistry for Materials Science, Elsevier Science, 2008.
[14] R. Schrebler, P. Grez, P. Cury, C. Veas, M. Merino, H. Gómez, R. Córdova, M.A. del Valle, J Electroanal Chem, 430 (1997) 77-90.
[15] G. Engelmann, W. Jugelt, G. Kossmehl, H.-P. Welzel, P. Tschuncky, J. Heinze, Macromolecules, 29 (1996) 3370-3375.
[16] Y. Wei, J. Tian, D. Glahn, B. Wang, D. Chu, ChemInform, 25 (1994) no-no.
[17] P. Camurlu, L. Toppare, J Macromol Sci Pure, A43 (2006) 449-458.
[18] F. Tran-Van, L. Beouch, F. Vidal, P. Yammine, D. Teyssie, C. Chevrot, Electrochim Acta, 53 (2008) 4336-4343.
[19] G. Sonmez, P. Schottland, J.R. Reynolds, Synthetic Met, 155 (2005) 130-137.
[20] P.S. Murray, S.F. Ralph, C.O. Too, G.G. Wallace, Electrochim Acta, 51 (2006) 2471-2476.
[21] P. Damlin, C. Kvarnstrom, A. Ivaska, J Electroanal Chem, 570 (2004) 113-122.
[22] S. Tarkuc, E. Sahmetlioglu, C. Tanyeli, I.M. Akhmedov, L. Toppare, Opt Mater, 30 (2008) 1489-1494.
[23] A.S. Ribeiro, A.U.d. Silva, M. Navarro, J. Tonholo, Electrochim Acta, 51 (2006) 4892-4896.
[24] C. Pozo-Gonzalo, M. Salsamendi, J.A. Pomposo, H.J. Grande, E.Y. Schmidt, Y.Y. Rusakov, B.A. Trofimov, Macromolecules, 41 (2008) 6886-6894.
[25] A.J. Bard, L.R. Faulkner, Electrochemical methods: fundamentals and applications, Wiley, 2001.
[26] P.A. Christensen, A. Hamnett, Techniques and mechanisms in electrochemistry, Blackie Academic & Professional, 1994.
[27] C.L. Gaupp, J.R. Reynolds, Macromolecules, 36 (2003) 6305-6315.
[28] J.L. Bredas, G.B. Street, Accounts Chem Res, 18 (1985) 309-315.
[29] E.d.C. Rios, A. Viana Rosario, A. Flávia Nogueira, L. Micaroni, Solar Energy Materials and Solar Cells, 94 (2010) 1338-1345.

[30] M. Deepa, A. Awadhia, S. Bhandari, S.L. Agrawal, Electrochim Acta, 53 (2008) 7266-7275.
[31] W.A. Gazotti, G. Casalbore-Miceli, A. Geri, M.A. De Paoli, Adv Mater, 10 (1998) 60-+.
[32] K.C. Chen, C.Y. Hsu, C.W. Hu, K.C. Ho, Solar Energy Materials and Solar Cells, 95 (2011) 2238-2245.
[33] B. Wang, J.S. Zhao, C.S. Cui, J.F. Liu, Q.P. He, Solar Energy Materials and Solar Cells, 98 (2012) 161-167.
[34] R.S. Hutton, M. Kalaji, L.M. Peter, J Electroanal Chem, 270 (1989) 429-436.
[35] E.M. Genies, M. Lapkowski, Synthetic Met, 24 (1988) 61-68.
[36] A.S. Sarac, G. Sonmez, F.C. Cebeci, J Appl Electrochem, 33 (2003) 295-301.
[37] T. Yi-Jie, C. Hai-Feng, Z. Wen-Wei, Z. Zhao-Yang, J Appl Polym Sci, (2012) n/a-n/a.
[38] G.G. Min, S.B. Kim, S.M. Park, J Electrochem Soc, 158 (2011) F92-F99.

Chapter 4. Model For Thin Layer of Ionic Liquid Coating on an Electrode

4.1 Introduction

For many years electrochemistry at the interface of two-phase liquid system has represented a fascinating subject of study for electrochemists. The interface of two immiscible electrolyte solutions (ITIES) continues to be an intriguing subject in electrochemistry. This is illustrated by a range of publications presenting the processes generated by the ion transfer across ionic liquids/ water interface such as migration, solvation /desolvation, complex formation and adsorption/desorption. Examples within ITIES include ion transport across biological membranes [1], drug delivery [2], extraction processes in oil recovery [3] [4] and the list with other applications in electroanalytical or applied chemistry is long.

The class of ionic liquids (ILs) named also the 'green solvents' [5], previously described in Chapter 1, are preferred as new reaction media. ILs can be used for a wide range of electrochemical reactions because of their negligible vapour pressure and relatively high thermal stability. However, most of ILs are hydrophobic and are characterized by increased viscosity, which can curtail their application on an industrial scale. The viscosity decreases with increasing temperature, but room temperature is the desirable condition for most experimental work.

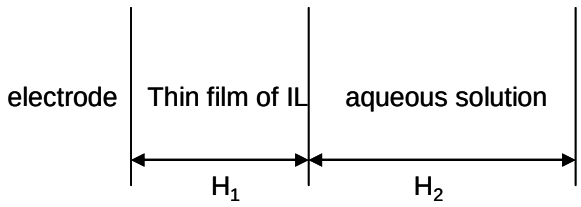

Figure 4.1 A thin film of IL of thickness H_1 and the distance H_2 out into solution.

The transfer of the ferricenium (Fc) ion at the interface of an hydrophobic ionic liquid (IL) with aqueous solution interface was observed on successive cyclic voltammetric experiments and also simulations using a Fortran program were run. The present work was done using manufactured ITO micro-electrodes previously described in section 3.2.2 of Chapter 3.

The ionic liquid chosen for this study was 3-methyl-1-propylpyrridinium bis(trifluoromethylsulfonyl)imide [MPyr TFSO], which has increased hydrophobicity [6]. The bis(trifluoromethylsulfonyl)imide ion is described as one of the most efficient anions because of features such as being weakly interacting with water and being flexible [7]. In order to prepare a stable hydrophobic layer, a composite of MPyr TFSO and PVC was employed.

This chapter describes the charge transfer process at the interface between a polar (aqueous solution) and nonpolar solution (ILs). For the present study, both experimental work and computer simulations were performed in order to understand the ion transfer across liquid/liquid interface using a model redox couple namely ferrocene.

In order for ion transport to occur across ionic liquid/ water interface the ferrocene-ferricenium couple was used. Ferrocene is soluble in ionic liquids and insoluble in the aqueous phase, while ferricenium is soluble in aqueous phase. SEM analysis was performed in order to observe the PVC film morphology and to estimate the film thickness.

4.2 Model For Thin Layer of Ionic Liquid Coating on an Electrode.

Mass transport controlled model

This consists of a thin layer of ionic liquid containing ferrocene coated on an electrode in an aqueous solution. The ferrocene is soluble in the ionic liquid but not soluble in the aqueous solution. When oxidised, the ferricenium ion is soluble in the aqueous solution. For the general system:

$$O + ne = R \qquad (4.1)$$

Diffusion equations are solved for within the IL, which is region 1 and where the diffusion coefficient is D_1 and the aqueous solution where the diffusion coefficient is D_2 as can be seen in Figure 4.1. There are 4 diffusion equations to be solved. The diffusion coefficient for ferrocene in aqueous solution is 1.2×10^{-5} cm^2s^{-1}, while in an ionic liquid BMIM TFSI is 3×10^{-7} cm^2s^{-1} [8]. Thus there is a requirement to differentiate between the two media.

$$\frac{\partial C_{O1}}{\partial T} = D_1 \frac{\partial^2 C_{O1}}{\partial x^2} \qquad (4.2)$$

$$\frac{\partial C_{R1}}{\partial T} = D_1 \frac{\partial^2 C_{R1}}{\partial x^2} \qquad (4.3)$$

$$\frac{\partial C_{O2}}{\partial T} = D_2 \frac{\partial^2 C_{O2}}{\partial x^2} \qquad (4.4)$$

$$\frac{\partial C_{R2}}{\partial T} = D_2 \frac{\partial^2 C_{R2}}{\partial x^2} \qquad (4.5)$$

All the parameters are made dimensionless as follows. The concentrations are normalised to the initial ferrocene concentration C_o. In region 1 the distance is normalised to the thickness H_1.

For region 2, at a distance sufficiently far from the electrode, the concentrations of O and R will always be zero. This distance is taken to be $6(D_2t_c)^{1/2}$ [9] and the distance in

region 2 is normalised to this.t_c is the total time of the experiment, determined by the difference between the initial and final applied potentials and the scan rate and D_2 is the diffusion coefficient of ferricenium in aqueous solution.

The dimensionless diffusion coefficient D_M is calculated as follows [10] where Δt is the time increment and Δx is the distance increment.

$$D_M = \frac{D\Delta t}{(\Delta x)^2} \qquad (4.6)$$

The initial conditions at time = 0 are:

The concentration of the oxidised form in region 1 is C^o, (the bulk concentration). The concentration of the reduced form is zero. In region 2, the concentrations of the oxidised and reduced forms are both zero.

The boundary conditions are as follows:

At the electrode surface the concentrations of O and R are set by the applied potential, E.

$$\frac{C_o}{C_R} = \exp\left(\frac{nF(E - E^o)}{RT}\right) \qquad (4.7)$$

Where E_o is the standard potential for the couple in equation (4.1) and n, F, R and T have their usual meanings.

Also at the electrode surface the slope of the concentration profiles for the oxidised and reduced forms are equal and opposite in region 1.

$$\frac{dC^R}{dx} = -\frac{dC^O}{dx} \qquad (4.8)$$

At the edge of the IL film, between region 1 and region 2, the oxidised form cannot diffuse outside the film and

$$\frac{dC^O}{dx} = 0 \qquad (4.9)$$

At the edge the reduced form can diffuse outside the film, and so for R,

$$D_1 \frac{dC^1}{dx} = D_2 \frac{dC^2}{dx} \qquad (4.10)$$

The concentration profiles on either side of the edge are equal.

The equations are solved by the Crank Nicholson implicit method where there are N distance increments and L time increments. The advantage is that the implicit method is not limited to values of D_M less than 0.5.

The input file to the program reads in the 2 diffusion coefficients, the layer thickness and the scan rate and the rate constant k. The initial and final potentials are 0.3 and -0.3 and the standard potential is 0.0 V. The concentrations are in FRNW1, FRNW2, FONW1 and FONW2 and the current is dimensionless PCHI, as outlined in the program attached in the appendix.

When the program was run under simple conditions to check that the output was accurate, the following behaviour was obtained as seen in Figure 4.2.

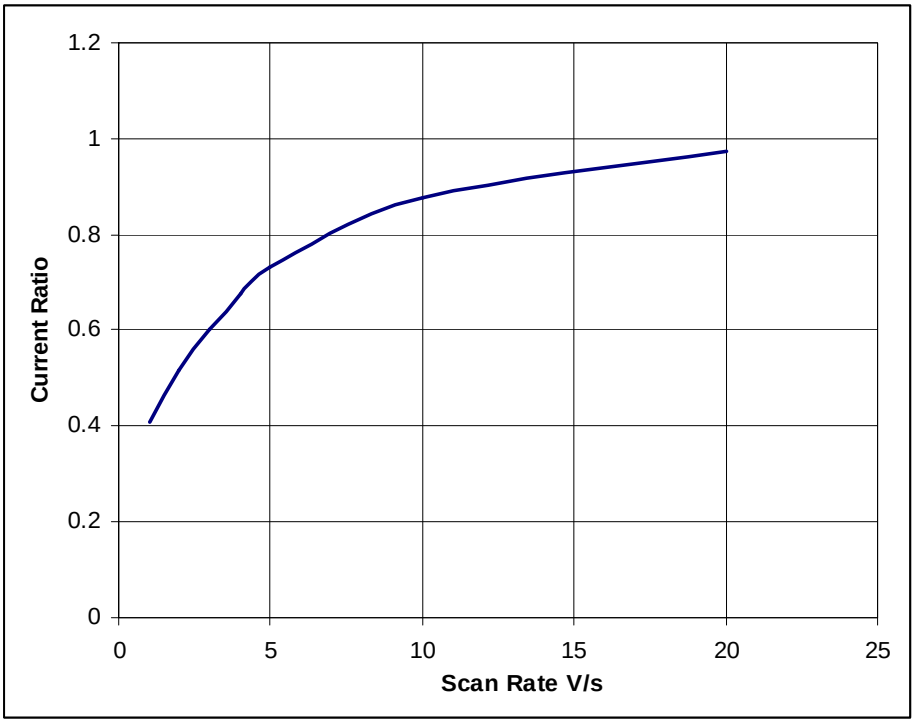

Figure 4.2 The corrected peak current ratio as a function of scan rate.
Ratio is 1 at high scan rates.

The conditions used were: the diffusion coefficient is 3 x 10^{-6} cm^2 s^{-1}, the thickness is 0.001 cm, the number of time increments is 500 and the number of distance increments is 500. The scan rates were in volts per second.

The dimensionless current is $\sqrt{\quad}$ (at) where

$$\sqrt{\quad}(at) = i/(nFAC^o \sqrt{aD}) \qquad (4.\ 11)$$

where a = nF ν /(RT). The ideal dimensionless peak current is 0.4463 [10] [9] [11]. This dimensionless current includes the electrode area, the concentration, the diffusion coefficient of the species. It can be seen from the Table 4.1 and Figure 4.2 that at scan rates greater than 10 V/s, the dimensionless peak current is close to the literature value. This is an indication that the iron is oxidised and reduced fast enough that it does not have a chance to migrate outside the film. However at slower scan rates it can be seen

that the ferricenium diffuses out and so the corrected peak current on the backward scan decreases where the corrected peak current ratio is given by [10] [9] :

$$\frac{i_{pb}}{i_{pf}} = \frac{i_{pbo}}{i_{pfo}} + \frac{0.485 * i_{\gamma}}{i_{pfo}} + 0.086 \qquad (4.12)$$

Where i_{pb}/i_{pf} is the corrected peak current ratio and

i_{pfo} is the forward peak current

i_{pbo} is the reverse peak current

i_{γ} is the current at the switching potential [11]

Table 4.1 Results obtained by running the programme. Conditions are as in Figure 4.3. Data in table and in the figure is in V/s.

Scan rate V/s	i_{pfo}	i_{γ}	i_{pbo}	i_{pb}/i_{pf}
1	0.186	0.022	-0.0496	0.410
2	0.261	0.027	-0.099	0.515
3	0.312	0.04	-0.142	0.603
4	0.347	0.056	-0.178	0.677
5	0.372	0.0719	-0.206	0.733
10	0.427	0.123	-0.278	0.876
20	0.442	0.157	-0.316	0.973

The oxidation peak currents do not vary linearly with the square root of scan rate as when the scan rate decreases; there is a transition between the bulk cyclic voltammetric behaviour and the thin layer voltammetry. This can be seen as while the currents decrease with scan rate, the shape also become more symmetric, indicative of thin layer behaviour as seen in Figure 4.3.

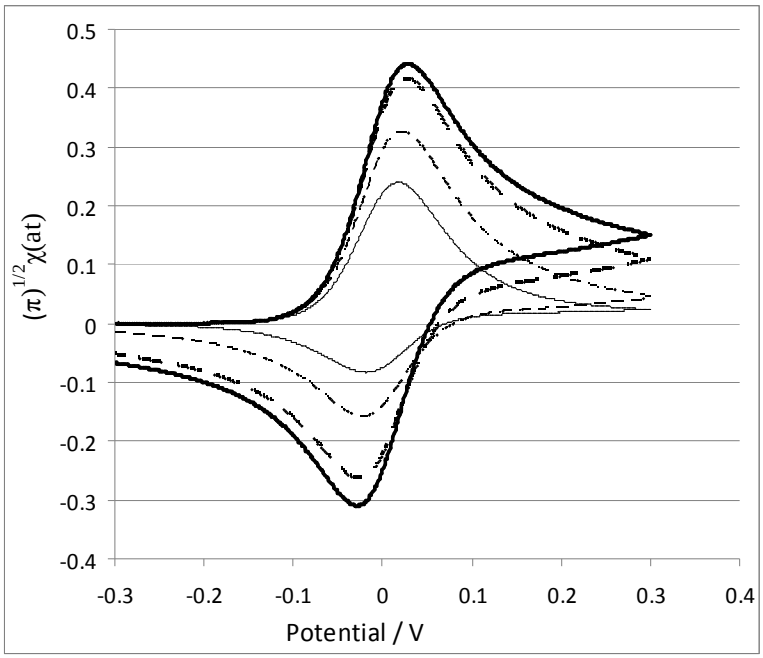

Figure 4.3 Predicted cyclic voltammograms for ferrocene at different scan rates from the PROGRAM 6 using $D_1 = D_2 = 3 \times 10^{-6}$ cm^2/s and $H_1 = 0.001$ cm.

4.3 Experimental

Ferrocene was obtained from Merck and poly(vinyl-chloride) (PVC, M_w = 62,000), tetrahydrofuran (THF, anhydrous, 99.9 %) and 3-methyl-1-propylpyrridinium bis(trifluoromethylsulfonyl)imide ([MPyr TFSO], 97 %, HPLC) were purchased from Sigma-Aldrich, Germany. The electrolyte used for aqueous solution was potassium chloride (KCl, 99+ %) was obtained from Fisher Scientific. The water used for electrochemical experiments was purified by deionization using the Elgastat Maxima machine with a measured resistivity of 18.2 MΩ cm. All chemicals were stored in tightly closed containers to protect from humidity; especially the ionic liquids which were always kept in a dessicator.

A three electrode cell was employed for all electrochemical experiments: ITO electrode as working electrode, platinum wire (0.5 mm, Alfa-Aesar, UK) as counter electrode and reference electrode Ag/AgCl [3 M KCl]. The electrochemical measurements were performed with CH Instruments three-electrode potentiostat. The aqueous solution used for electrochemical experiments was of 10 ml total volume containing 0.1 M KCl.

A phosphate buffer solution, pH = 7 was prepared. Electrochemical experiments were performed in two different solutions, 0.1 M KCl aqueous solution and 10 mM phosphate buffer (pH = 7.0).

4.3.1 Electrode Preparation

The indium-tin oxide (ITO) glass substrate (Solaronix, Swizerland) microelectrodes (Figure 4.4) were used for all electrochemical measurements. As described in Chapter 3, the geometry of the electrodes surface is a circle of 0.4 cm diameter and calculated geometric area of 0.125 cm^2.

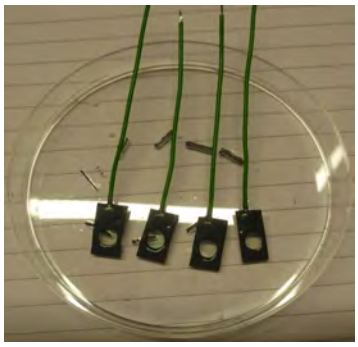

Figure 4.4 Picture of manufactured ITO electrodes.

The 3-methyl-1-propylpyrridinium bis(trifluoromethylsulfonyl)imide [MPyr TFSO] ionic liquid is highly hydrophobic, so in order to achieve formation of a thin layer of on the ITO surface, a supporting material was needed. The poly(vinyl chloride) (PVC) was used as a support for immobilization of the ionic liquid layer [12]. PVC polymer represented the best option as support for the hydrophobic ionic liquid because of its spongy morphology observed on SEM analysis (Figure 4.5). First a PVC stock solution was prepared which contained 0.05 g PVC, 3 ml THF and 5 mM ferrocene. From the PVC stock solution, a volume of 20 l was removed using a Gilson pipette, and further mixed with 2 l [MPyr TFSO] ionic liquid. The solution of PVC and [MPyr TFSO] was cast on the ITO surface and allowed to dry under the fumehood.

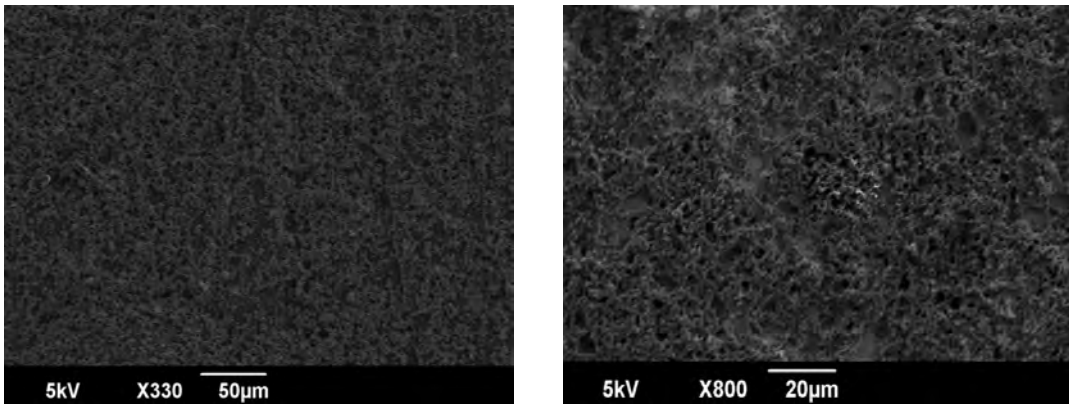

Figure 4.5 SEM images of the PVC cast film on ITO electrode

The PVC film thickness was determined by SEM. The sample was scratched and tilted at 90° in order to examine the film in cross-section. From the cross-section, a film thickness 10 m was determined (Figure 4.6).

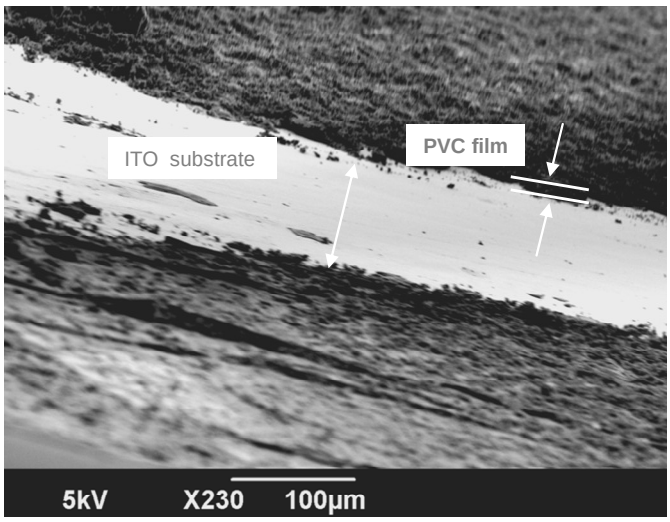

Figure 4.6 SEM cross-section image of the PVC film on ITO electrode

4.4 Results and Discussion

The cyclic voltammetry experiments were performed over the potential range of -0.1 V to 0.8 V vs Ag/AgCl. Various scan rates were applied in order to get a better insight of ion transfer process between ionic liquid and water phase. All cyclic voltammetric experiments were run on different scan rates, starting from high scan rates (Figure 4.7) and successively decreasing the scan rate (Figure 4.8-10).

The starting point was at 300 mV/s scan rate which seemed to be too high for the Fc mobility and this resulted in a response typical of bulk- voltammetry (Figure 4.7). Similar results were seen at 200 and 100 mV/s, where the cyclic voltammograms exhibited slow kinetics with broad peak potential (Figure 4.7). The successive decreases in the scan rate (50 mV/s) did not bring much improvement in peak to peak separation (ΔE_p). ΔE_p had values of 600 and 500 mV at 300 mV/s and 50 mV/s, respectively (Figure 4.6).

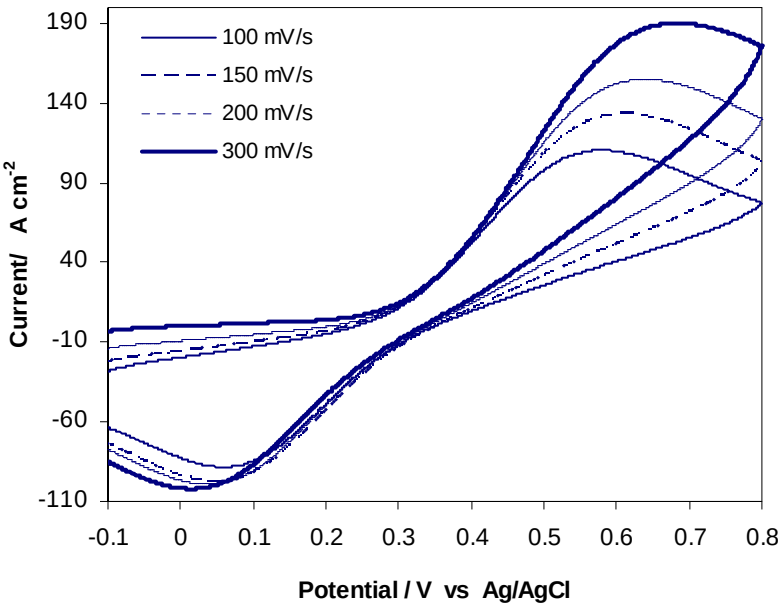

Figure 4.7 Cyclic voltammogram of Fc/Fc^+ couple in 0.1 M KCl aqueous solution

The reason for the large peak to peak separation in Figure 4.7 may be due to a combination of resistance and slowness of ion transfer. When ferrocene is initially oxidized in the film, either an anion has to penetrate the film or a cation has to exit to preserve charge neutrality. By comparing Figure 4.8 and Figure 4.7, this can be seen to be a sluggish process.

When lower scan rates of 20 or 10 mV/s were used (Figure 4.8) an improvement in the electrochemical response, with well defined peak potentials appears. The peak potentials which were seen at 0.65 V (anodic) and 0.05 V (cathodic) in Figure 4.5, were shifted to 0.45 V (anodic) and 0.15 V (cathodic) in Figure 4.8.

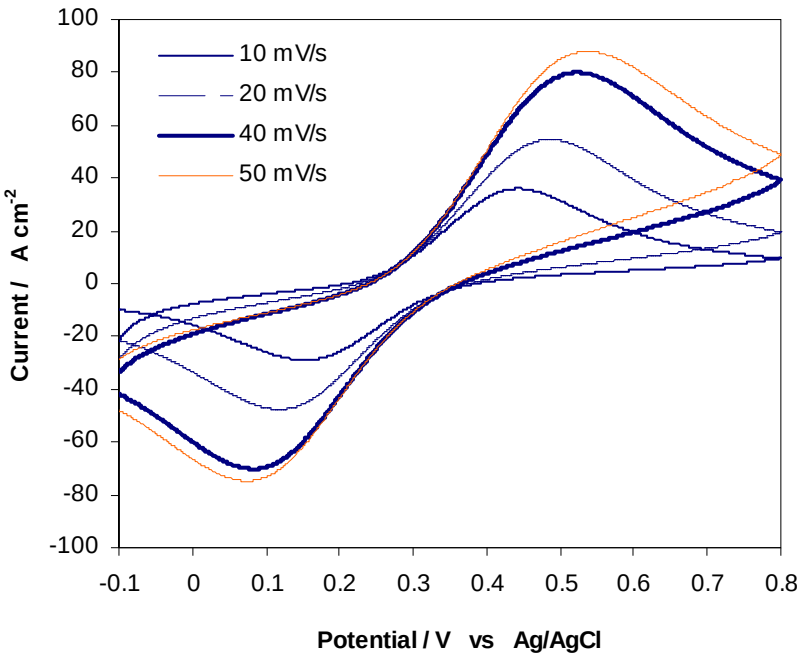

Figure 4.8 Cyclic voltammogram of Fc/Fc^+ couple in 0.1 M KCl aqueous solution

From the CV shape in Figure 4.8, can be clearly seen a decrease of both oxidation and reduction peak potential when the scan rates were successively lowered. Beside successive decrease in the peak potential separation, a reduction of the cathodic peak current is observed and this is due to decreased concentration of Fc^+. Reduction of the cathodic peak current is more evident when approaching lower scan rates of 5 or 2

mV/s, where more Fc is oxidized to Fc^+ (Figure 4.9). Fc^+ has diffused out in the aqueous solution, but not all Fc^+ amount has been reduced, as some of the Fc^+ is lost in the aqueous phase. At these slow scan rates the Fc^+ has time to diffuse out of the ionic liquid film and a smaller reverse peak is seen.

In Figure 4.9 at 5mV/s the forward peak is quite symmetric indicating thin layer behaviour, but the peak to peak separation is greater than 0 V due to resistance and/or slow kinetics.

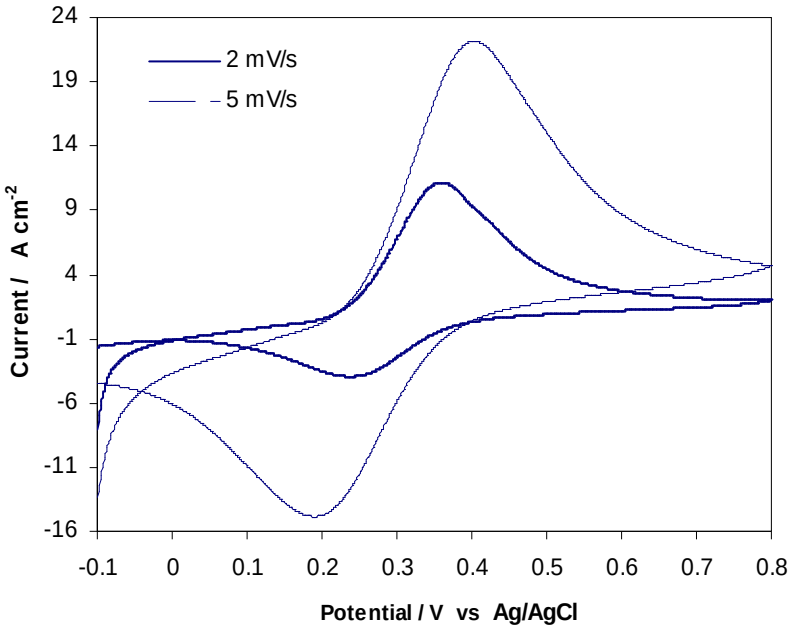

Figure 4.9 Cyclic voltammogram of Fc/Fc^+ couple in 0.1 M KCl aqueous solution.

At very low scan rate such as 1 mV/s (Figure 4.10), the reduction peak current is significantly diminished compared to anodic peak current. This occurs because higher amount of Fc species are transformed into Fc^+ species which diffuse into the aqueous solution.

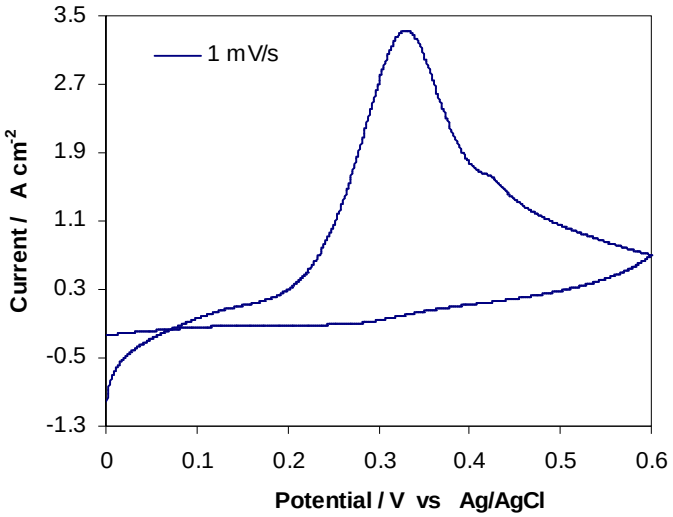

Figure 4.10 Cyclic voltammogram of Fc/Fc^+ couple in 0.1 M KCl aqueous solution

When calculating the dimensionless peak current ratio of Nicholson and Shain, most of the values were greater than unity (Figure 4.11.a). For the scan rates above 10 mV/s, the values of corrected dimensionless peak current ratio (reverse peak/ forward peak) were always higher than 1.

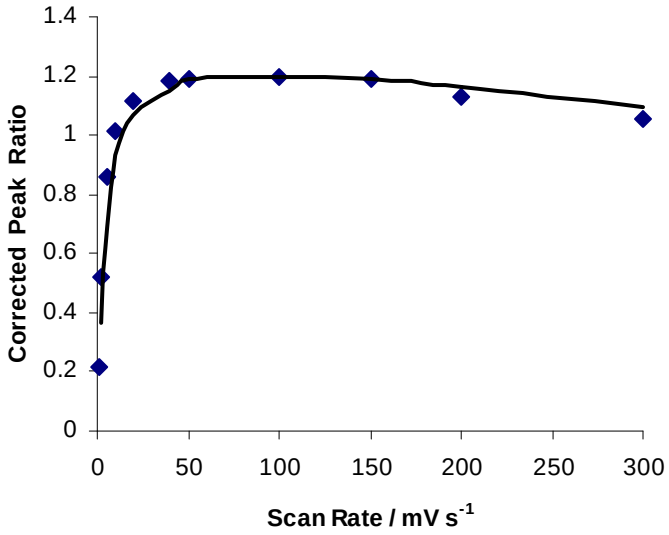

Figure 4.11.a Plot of dimensionless peak current ratio as function of scan rate.
Data from Figure 4.7, 4.8, 4.9 and 4.10.

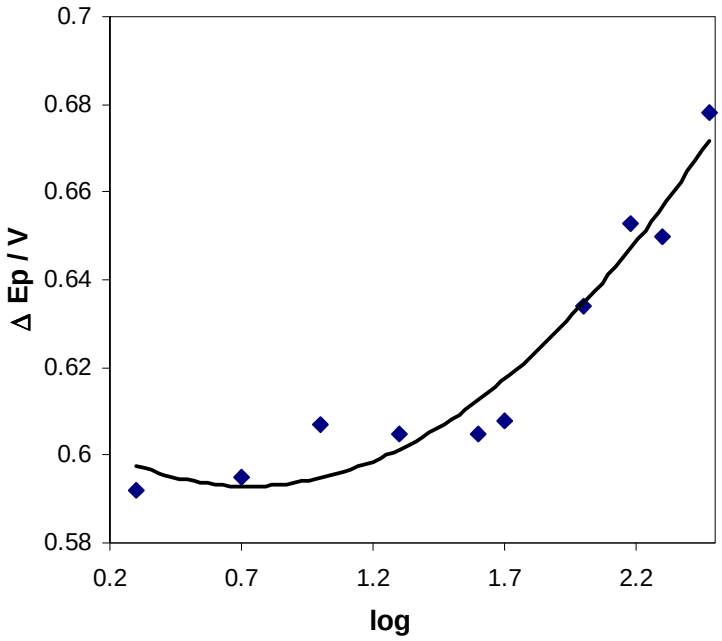

Figure 4.11.b Plot of peak potential difference as a function of logarithm of scan rate for the cyclic voltammograms obtained in 0.1 M KCl.

Because Figure 4.7 to 4.10 were all performed on the same film, the initial concentration of Fc was different for each cyclic voltammogram . However this factor is corrected for by using current ratios as shown in Figure 4.11.a.

The experimental results are quite different when compared to the designed model for thin film layer of ionic liquid, as the ideal value for dimensionless peak current ratio should be 0.4463 [10] [9] [11].

From the CVs obtained experimentally can be seen a gradual increase of peak to peak separation with increasing scan rate. According to literature the difference in peak to peak separation should have the value of 57 mV for a reversible process [9].

However under conditions where the kinetics is slow the peak to peak separation follows the equation [13] , as can be seen in Figure 4.11.b

$$\Delta E_p = \frac{59}{\quad}\log_{10}(\ ) + constant\ , \quad \text{at 298 K} \quad (4.13)$$

Where is the scan rate and the transfer coefficient.

Table 4.2 Conditions for simulations with PROGRAM 6 [8] [14]

Fc diffusion coefficient		film thickness
in Mpyrr TFSO	2.31 x 10^{-11} m^2s^{-1}	10 μm
	3.77 x 10^{-11} m^2s^{-1}	100 μm
in aqueous solution	7.17 x 10^{-10} m^2s^{-1}	

Results obtained from simulations with PROGRAM.6 of the model are presented in Figure 4.12 and 4.13, using the conditions presented in Table 4.2.

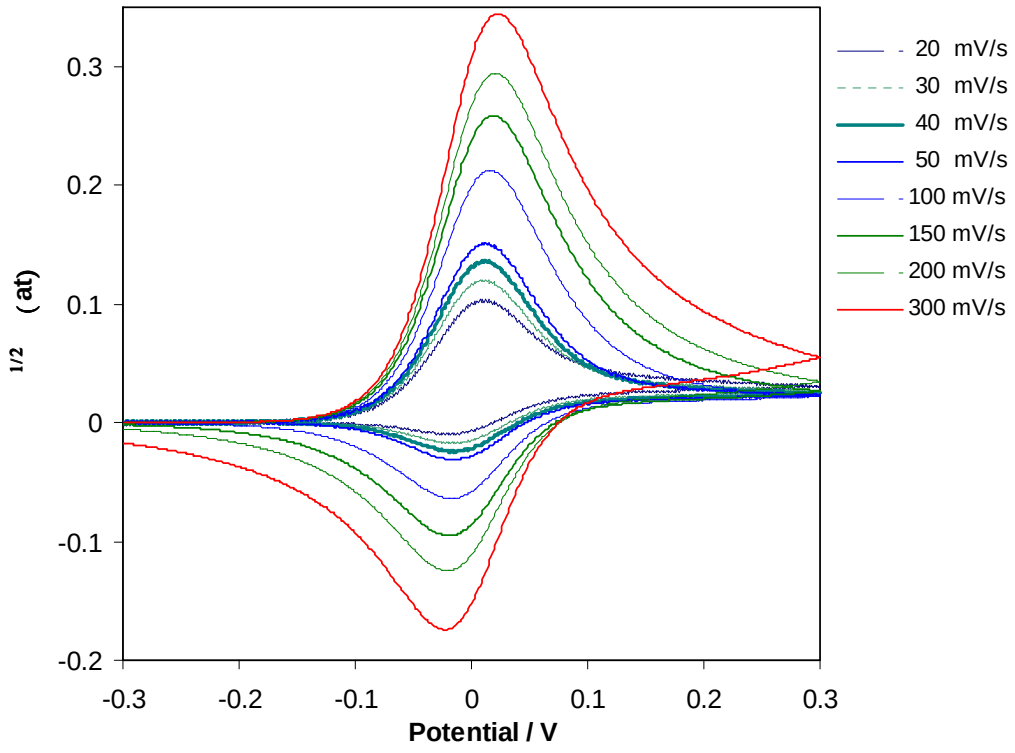

Figure 4.12 Cyclic voltammogram of Fc/Fc^+ couple in 0.1 M KCl aqueous solution, simulated by PROGRAM 6. IL film thickness: 10 m.

The results from simulations (Figure 4.12) are showing that for a thin film of IL (10 m), below 20 mV/s the program is going into oscillation, while for higher scan rates the thin layer behaviour can be seen and at even higher scan rates again bulk CV

behaviour is seen. In Figure 4.12 the peak width around half height is 106 mV for 20 mV/s, which is bigger than 90/n mV expected.

In Figure 4.13, the results from simulations are shown for a thicker film of ionic liquid (100 m), the electrochemical behaviour of this thick film is more similar to experimental results shown in Figures 4.7, 4.8 and 4.9.

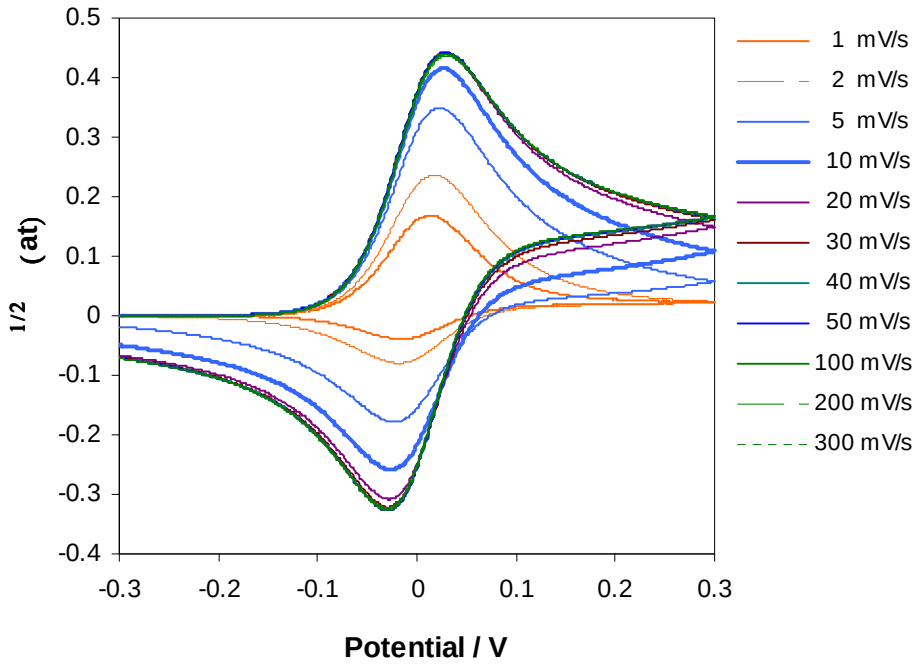

Figure 4.13 Cyclic voltammogram of Fc/Fc^+ couple in 0.1 M KCl aqueous solution, simulated by PROGRAM 6. IL film thickness: 100 m.

It can be stated that for the thicker layer, at fast scan rates the function equals 0.4463 as expected from Nicholson and Shain.

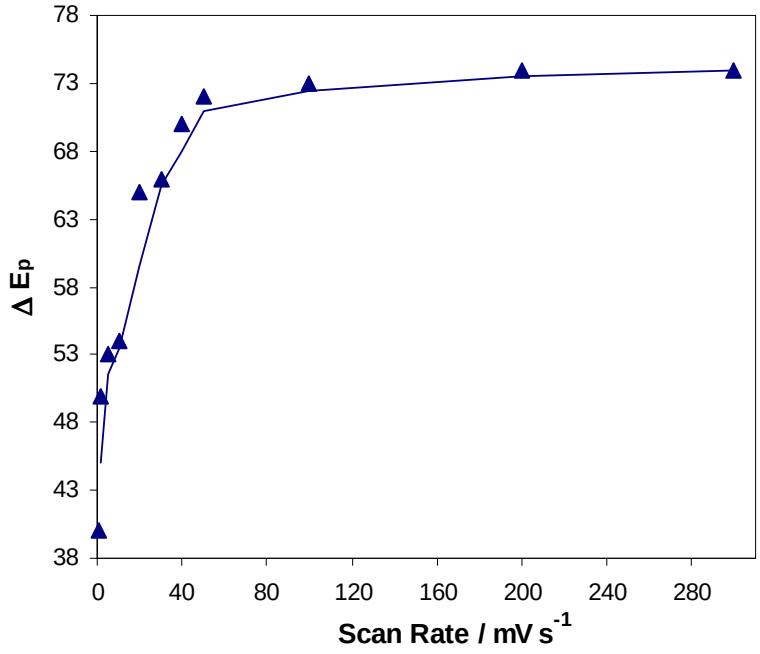

Figure 4.13.a Plot of peak potential difference as a function of scan rate for the simulated cyclic voltammogram. IL film thickness: 100 m.

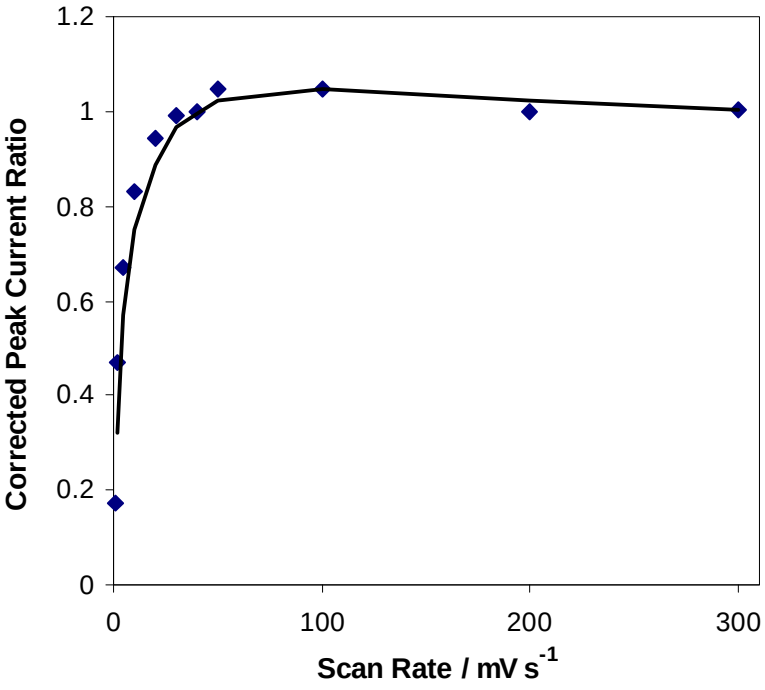

Figure 4.13.b Plot of corrected peak current ratio as function of scan rate for the simulated cyclic voltammogram. IL film thickness: 100 m.

Other workers in the field have used recessed microelectrodes where the cavity was filled with IL and have used cylindrical coordinates to solve the diffusion equations [8] . Several authors [8] [14] have included kinetic terms associated with equations 4.2, 4.3, 4.4, and 4.5. An additional kinetic term is due to the reaction between ferricenium which reacts further with oxygen or tetraphenyl borate.

Another term which has been included in the diffusion equations and which applies to the surface of ionic liquids is:

-AkC/V (4. 14)

Where A is the area, V is the volume of the liquid, k is the rate of movement of the ferricenium from the ionic liquid in cm/s and C is the concentration.

This term is made dimensionless by dividing by the bulk concentration and multiplying by the layer thickness. This term has been included in the diffusion equations only at the interface. It is curious that this has not been included as a boundary condition. The term is included to model the movement of ferricenium from the ionic liquid to the aqueous solution. This happens when the liquid junction potential at the IL/water interface is more negative that the standard liquid junction potential.

The liquid junction potential at the interface is set by the concentration of the cation in the aqueous solution as

$$\Delta\emptyset = constant - \frac{RT}{nF}\ln\left(C_{aq}^{+}\right) \qquad (4.15)$$

As the concentration of the electrolyte cation increases the liquid junction potential becomes more negative. This happens because as the electrolyte cation concentration increases, it can exchange more readily with the ferricenium as it exits the IL increasing the rate at which the ferricenium exits the IL. In fact the rate of removal of the IL can be modelled by the Butler-Volmer equation

$$k = k^{o}\exp\left(\frac{-\alpha nF}{RT}\left(\Delta\emptyset - \Delta\emptyset^{o}\right)\right) \qquad (4.16)$$

Where the rate is dependent on how far the liquid junction potential is away from the standard liquid junction potential value. This term has been included in the program as RKR2(1) and RKR1(N). However for small values of k, there was no change seen in the voltammetry. At larger values of k, the program went in to oscillation and thus the kinetic term was neglected.

Further electrochemical studies involving ion diffusion at the interface of a thin film ionic liquid with phosphate buffer solution were performed. The cyclic voltammetry was carried out in similar manner to experiments performed in 0.1 M KCl, starting from high scan rate of 300 mV/s and successively reducing to 1 mV/s.

The cyclic voltammograms obtained when experiments were performed in phosphate buffer, pH = 7.0 are presented below in Figure 4.14.a to Figure 4.14.f.

The electrochemical response of ferrocene/ferricenium in contact with phosphate buffer solution showed an increase in the peak potential separation (ΔE_p). The characteristic shift of the peak potential (upon oxidation/ reduction) indicated the effect of anion present in the aqueous solution in the oxidation of ferrocene to ferricenium. Presence of PO_4^{3-} anion generated a change in the peak potentials which were moved towards more positive values upon oxidation and down to more negative values when reduction occurred (Figure 4.15).

At very high scan rates of 150, 200 and 300 mV/s, there was seen an extremely high peak potential separation of 1 V was found. The voltammetric behaviour of Ferrocene is far from bulk layer behaviour, as the ΔE_p value was higher than 57 mV. This could be caused by increased hydrated radius and ionic radius of the PO_4^{3-} anion [15], compared to Cl^-. The values presented in literature for PO_4^{3-} anion were 0.223 nm and 0.339 nm [16] for ionic radius and hydrated radius respectively. For Cl^- anion, the values found were 0.167 nm (ionic radius) and 0.324 nm (hydrated radius) [17], which are smaller than for PO_4^{3-} anion. However, the difference in size for ionic radius, is not

very dramatic and cannot be a determining factor for permeation of Ferrocene ions in the phosphate solution.

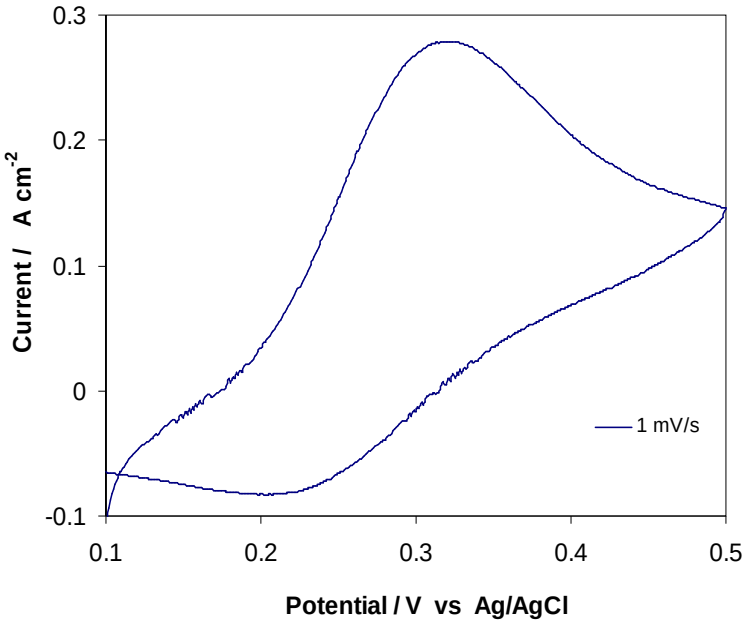

Figure 4.14.a Cyclic voltammogram of Fc/Fc^+ couple in phosphate buffer (pH = 7.0) solution.

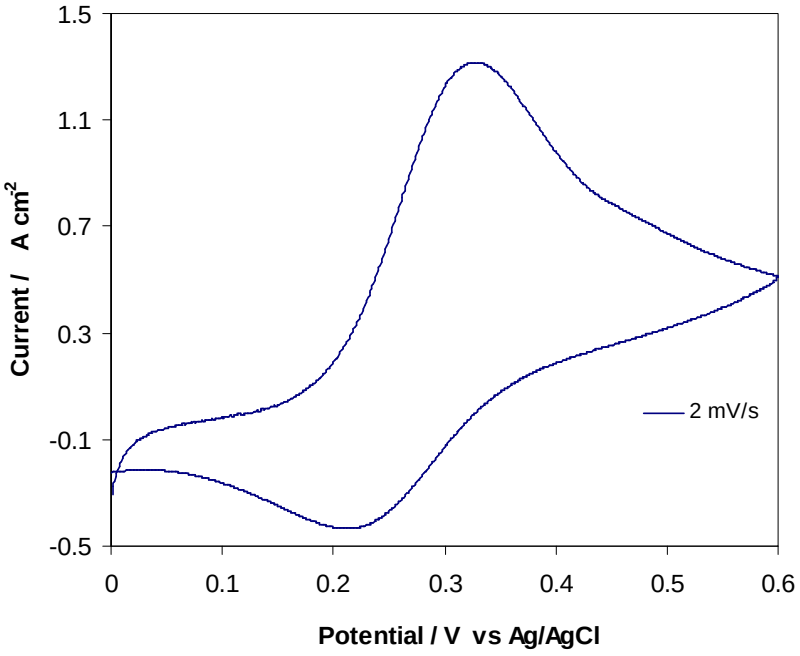

Figure 4.14.b Cyclic voltammogram of Fc/Fc^+ couple in phosphate buffer (pH = 7.0) solution.

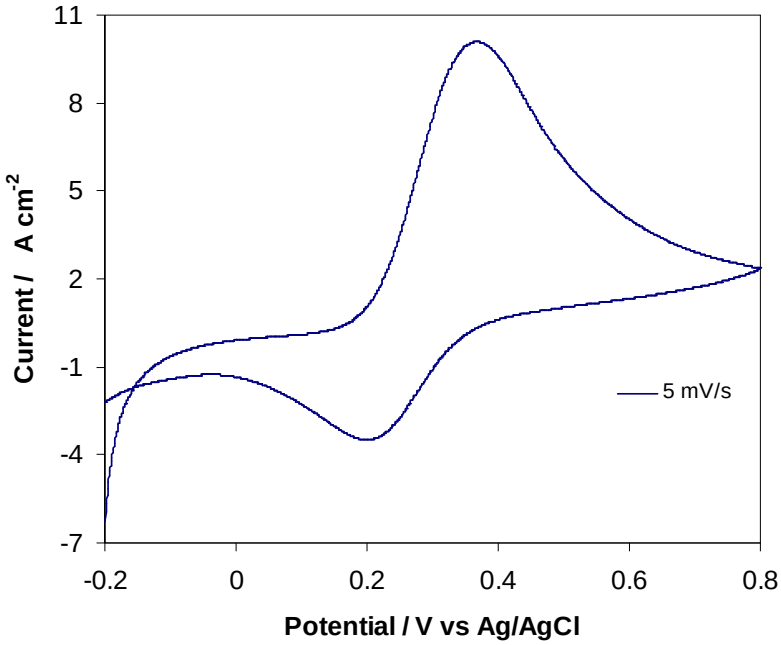

Figure 4.14.c Cyclic voltammogram of Fc/Fc^+ couple in phosphate buffer (pH = 7.0) solution.

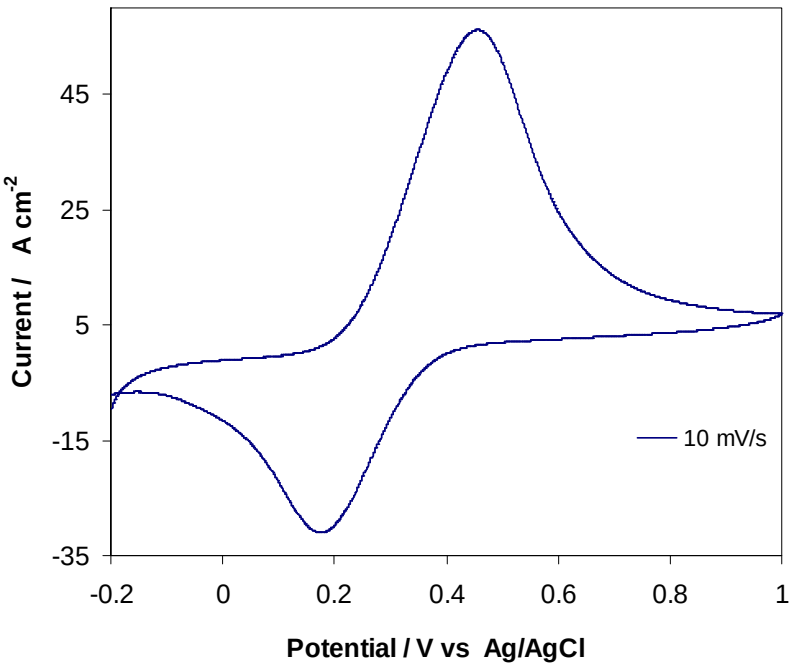

Figure 4.14.d Cyclic voltammogram of Fc/Fc^+ couple in phosphate buffer (pH = 7.0) solution.

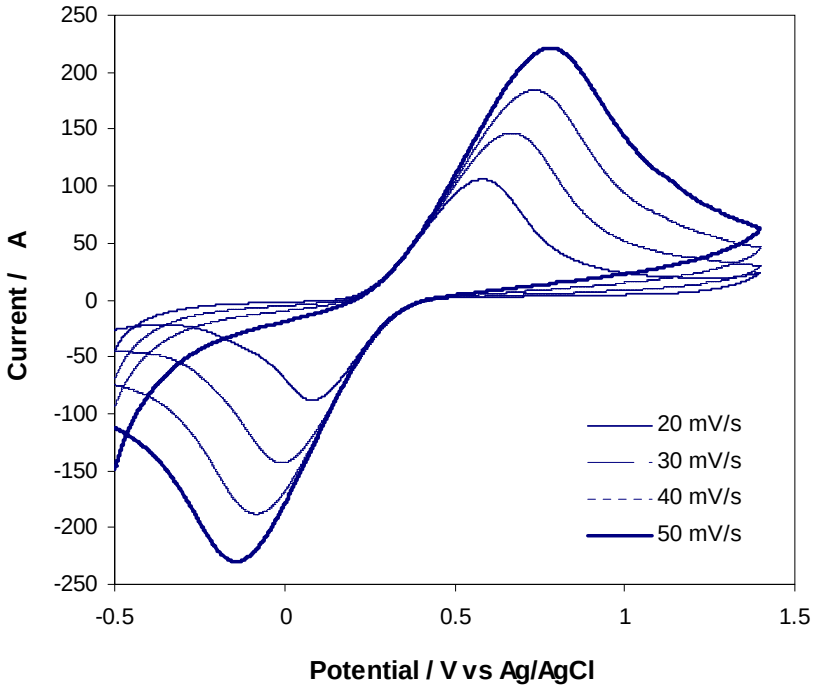

Figure 4.14.e Cyclic voltammogram of Fc/Fc^+ couple in phosphate buffer (pH = 7.0) solution.

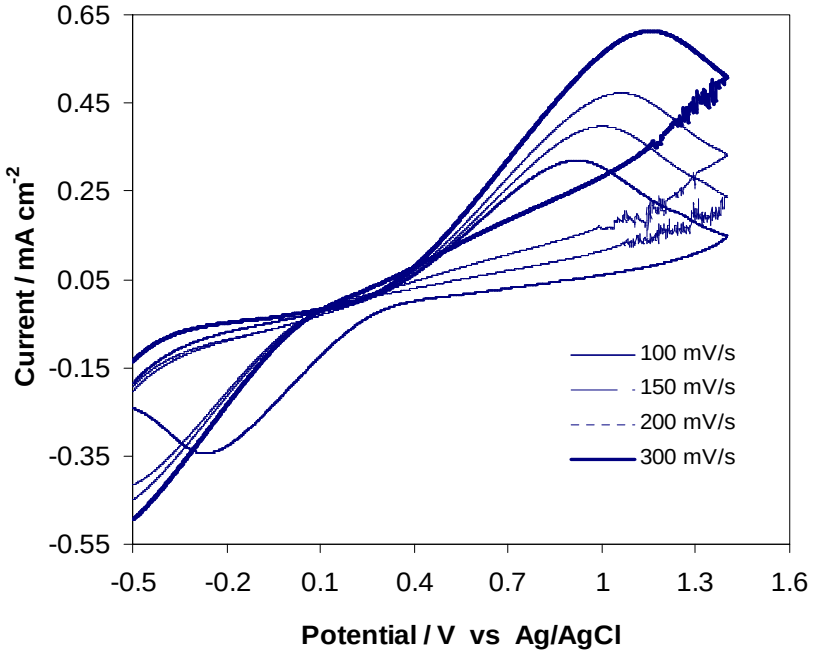

Figure 4.14.f Cyclic voltammogram of Fc/Fc^+ couple in phosphate buffer (pH = 7.0) solution.

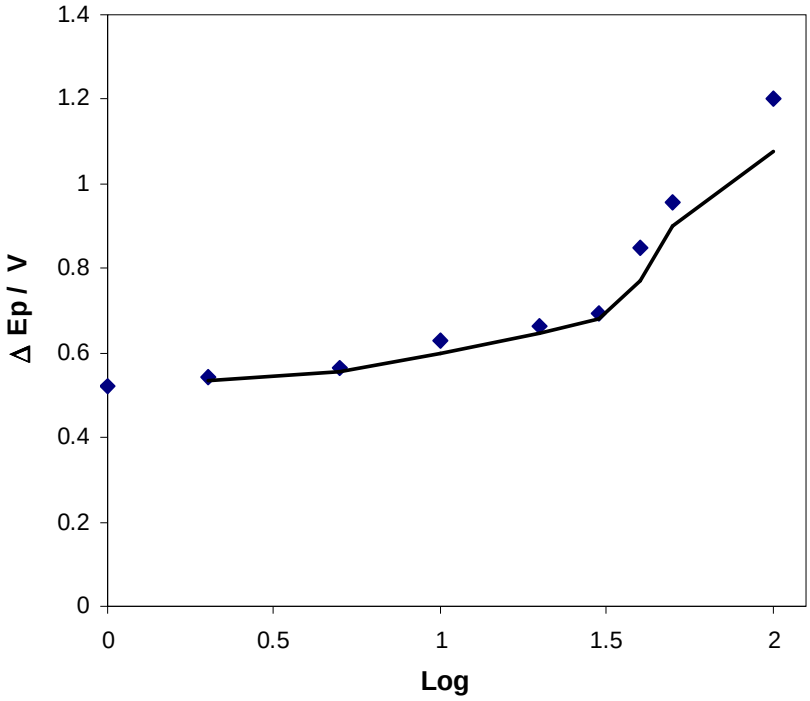

Figure 4.15 Plot of peak potentials difference as a function of logarithm of scan rate for the cyclic voltammograms obtained in phosphate buffer solution pH = 7.0.

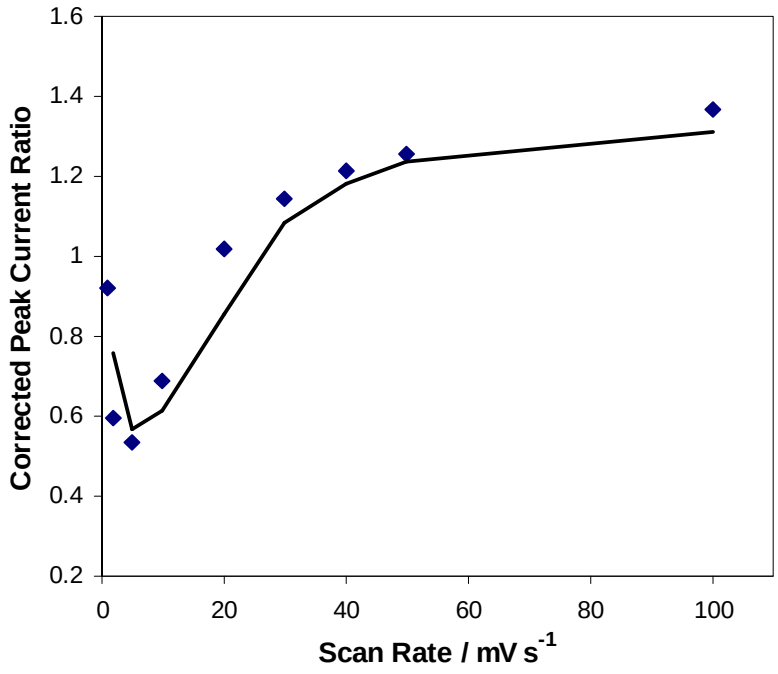

Figure 4.16 Plot of dimensionless peak current ratio as function of scan rate for the cyclic voltammograms preformed in phosphate buffer solution pH = 7.0.

4.5 Conclusions

Certain difficulties were encounted when measuring the Fc concentration for the PVC cast solution, but it was possible to measure approximately 5 mM Fc (0.003 g Fc). The Fc^+ ion transfer at the ionic liquid /water interface was studied by cyclic voltammetry at various scan rates. The ionic liquid thickness was difficult to measure, but it was possible to obtain an approximated film thickness from SEM analysis. The results obtained from experimental work were slightly different when compared to those from simulations performed with PROGRAM 6 designed by John Cassidy.

At high scan rates of 100, 200, 300 mV/s, the peak to peak separation was very large, reaching values of approximately 500-600 mV. At lower scan rates the peak to peak separation decreased to approximately 100 mV. Still, when compared to ideal value for ΔE_p= 57 mV, the peak to peak separation for CVs obtained experimentally was very high.

Finally it was possible to model the behaviour of Fc in a thin layer of ionic liquid using only diffusion controlled conditions without resorting to kinetics at the IL/aqueous interface.

Additional investigations on the diffusion process of ferrocene from an IL layer to a buffer solution at pH = 7.0 were performed for various scan rates. Electrochemical results showed changes in the oxidation potential of ferrocene which were associated with lower solubility of ferricenium in the phosphate buffer.

In conclusion, comparing the experimental results and the modelled plots:

- The corrected peak height ratio (i_{pb}/i_{pf}) is independent of the initial ferrocene concentration.
- The corrected peak height ratio (i_{pb}/i_{pf}) for the model and experimental are close to 1 at fast scan rates and drop below 1 at lower scan rates due to the ferricenium diffusing out of the film. As the scan rate decreases for the model there is a

transition from bulk CV behaviour and thin layer behaviour as the peak to peak separation drops below 57 mV.

- At low scan rates in the experimental plots the peak width at half height is greater than 90/n mV, though the voltammetry looks a little more symmetrical . For example in Figure 4.10 the peak width at half height is 141 mV.

Comparing the peak to peak separation for the model and the experimental, the peak to peak separation increases with scan rate. However in the experimental the peak to peak separation is much greater, perhaps due to slow ion transport across the interface. Thus the diffusion controlled model would require the input of slow kinetics to explain fully the experimental plots.

Comparing Figure 4.13 (b) and Figure 4.16, the corrected peak current ratio for the model and experimental are quite similar in that both drop at about 40 mV/s. However this is unexpected as the layer thickness is estimated at 10 microns rather than 100 microns.

4.6 References

[1] B.C. Pressman, N.T. DeGuzman, Annals of the New York Academy of Sciences, 264 (1975) 373-386.
[2] V. Jaitely, A. Karatas, A.T. Florence, International Journal of Pharmaceutics, 354 (2008) 168-173.
[3] T. Harington, M.M. Hossain, Desalination, 218 (2008) 287-296.
[4] S.H. Chang, T.T. Teng, I. Norli, Chemical Engineering Journal, 173 (2011) 352-360.
[5] M. Petkovic, K.R. Seddon, L.P.N. Rebelo, C. Silva Pereira, Chem Soc Rev, 40 (2011) 1383-1403.
[6] M. Galinski, A. Lewandowski, I. Stepniak, Electrochim Acta, 51 (2006) 5567-5580.
[7] D.R. McFarlane, J. Sun, J. Golding, P. Meakin, M. Forsyth, Electrochim Acta, 45 (2000) 1271-1278.
[8] K. Nakatani, M. Suto, J Electroanal Chem, 659 (2011) 101-106.
[9] A.J. Bard, L.R. Faulkner, Electrochemical methods: fundamentals and applications, Wiley, 2001.
[10]T. Vandernoot, Journal of Electroanalytical Chemistry and Interfacial Electrochemistry, 258 (1989) 479-480.
[11] R.S. Nicholson, I. Shain, Anal Chem, 36 (1964) 706-723
[12] Y. Saeki, T. Emura, Progress in Polymer Science, 27 (2002) 2055-2131.
[13] R.G. Compton, C.E. Banks, Understanding Voltammetry: 2nd Edition, Imperial College Press, 2011.
[14] N. Terui, K. Nakatani*, N. Kitamura, J Electroanal Chem, 494 (2000) 41-46.
[15] B. Tansel, Sep Purif Technol, 86 (2012) 119-126.
[16] M.Y. Kiriukhin, K.D. Collins, Biophys Chem, 99 (2002) 155-168.
[17] J. Zhou, X.H. Lu, Y.R. Wang, J. Shi, Fluid Phase Equilibr, 194 (2002) 257-270.

Chapter 5. Conclusions and Future Work

5.1 General Conclusions

The aim of this project was to make conducting polymers (CPs), in conjunction with Room Temperature Ionic Liquids (RTILs) in order to produce electrochromic films for possible use in electrochromic devices.

Novel electrochromic conducting polymers were prepared and their electrochemical behaviour examined in detail. The results presented in this thesis include a detailed kinetic study of PTFA modified ITO electrodes, the formation and characterization of a new co-polymer: PPy-co-PEDOT and also a detailed characterization of electrochemical behaviour of an ionic liquid thin film in contact with an aqueous solution.

The electrochemical deposition and response of PTFA from an aqueous acidic solution is described in Chapter 2. The faradaic response of PTFA showed a decrease in background electrolyte. When THF was present in the electrolyte solution, PTFA showed improved faradaic response. However, no significant change was observed in the UV-Vis spectrum even on THF addition. Results obtained during electrochromic switch at 450 nm indicated a slow transient interval of 40 seconds between oxidized and reduced forms of PTFA. The morphology of PTFA films was characterised by a less porous structure when THF was added, while in absence of THF the PTFA appeared more porous. In addition, an XPS study indicated the presence of PTFA film on the ITO electrode. Overall the addition of fluorines on the polyaniline backbone affected the redox behaviour and colour of the film dramatically. The PTFA polymer proved good stability according to Niessen et al [1], but does not represent the best choice for an electrochromic device due to slow kinetics. A possible application could be smart windows, as these devices can have a response time up to 60 s.

Copolymerization of two homopolymers (Py and EDOT) in an ionic liquid was the strategy used to make a novel material with improved phsysico-chemical properties (Chapter 3). However, ionic liquids are very costly and a novel micro-cell was designed for electrochemical deposition of the polymers. Formation and electrochemical characterization of PPy-co-PEDOT polymers were performed for three different monomer ratios (PPy : PEDOT 1:2, 1:1, 2:1). PPy-co-PEDOT copolymers showed a more capacitive voltammetry when analysed in Na BF_4 aqueous electrolyte, than CVs obtained in pure BMIM BF_4. The spectroelectrochemical results showed that 'polypyrole dominated' PPy-co-PEDOT (2:1) was the best copolymer combination for an electrochromic material. On redox cycling the PPy-co-PEDOT (2:1) showed a reversible switching time of 20 s at 450 nm seconds and the coloration efficiency value was in good agreement with values required for fast electrochromic devices. The response time of 20 s obtained for 'polypyrrole dominated' copolymer was higher than the value obtained by Yi-Jie et al. (10 s) [2]. This could be a consequence of switching from ionic liquid media to aqueous solutions, which was also seen in the decreased current density of the copolymers in 0.2 M $NaBF_4$. Differences in PPy-co-PEDOT (1:2, 1:1, 2:1) FTIR spectra were less evident, but they displayed different morphology when analysed by SEM. Colours seen in visible region like grey-blue (oxidized form) and olive-green (reduced form) which render the PPy-co-PEDOT (2:1) copolymer a promising material for an electrochromic application.

Both aqueous solutions and ionic liquids proved their use as environments for the production of novel electroactive materials. However, the PPy-co-PEDOT copolymers formed in an ionic liquid had dramatically different electrochemical behaviour when switching to aqueous solutions (0.2 M $NaBF_4$).

Since ionic liquids are expensive one possibility is to have a thin layer of ionic liquid (perhaps with monomer) in contact with a bulk aqueous solution in a

traditional three electrode cell. In order to assess this arrangement, a model redox couple was employed. Ferrocene was incorporated in the mixture 3-methyl-1-propylpyrridinium bis(trifluoromethylsulfonyl)imide and PVC, which allowed formation of drop-cast thin films on ITO substrate. Diffusion of ferricenium ions into the aqueous phase was observed during cyclic voltammetry and the experimental cyclic voltammetric results were modelled using PROGRAM 6. The thickness of the ionic liquid layer was hard to control and it was approximated to 10 m from the SEM images obtained for PVC films. The voltammetric response of Fc/Fc^{+} when the ionic liquid layer was in contact with phosphate buffer solution pH = 7, demonstrated that ion transfer across the interface was slower in phosphate buffer than in potassium chloride solution. The reason for the extremely broad potential peak separation in phosphate buffer (~ 900 mV) was attributed to increased hydration of PO_4^{3-} ions compared to Cl^{-} ions. Experimental results were different than simulations obtained with PROGRAM 6, which was designed for the 'Model for Thin Layer of Ionic Liquid Coating on an Electrode'. In order for the model to be improved a kinetic term should be incorporated to account for the slow ion transfer across the interface. Experimental results did not reflect the simulations done using PROGRAM 6, as this model was designed for a reversible system.

In conclusion, the formation of novel polymeric materials with electrochromic properties was achieved from both aqueous solutions and ionic liquid media, using relatively inexpensive and non-toxic compounds. This work has provided information concerning the electrochemical formation, optical and electrochemical performance and also physical properties of systems such as CPs/aqueous (Chapter 2) solutions and CPs/ILs (Chapter 3).

5.2 Future Work

The most valuable aspect of the present work is represented by the possible use of the PPy-co-PEDOT (2:1) copolymer as part of an electrochromic device. In order to fabricate a display-oriented 'micro-sandwich cell'[3], PPy-co-PEDOT (2:1) was employed as working electrode and PEDOT as counter electrode (Figure 5.1.a and Figure 5.1.b).

Insertion of a small drop of ionic liquid between the modified electrodes represented a problem, as the drop of ionic liquid may leak. This issue was resolved by replacing the ionic liquid with an 'ion jelly' electrolyte [4]. This 'ion jelly' was prepared by simply mixing gelatin with ionic liquids in various ratios (Figure 5.2).

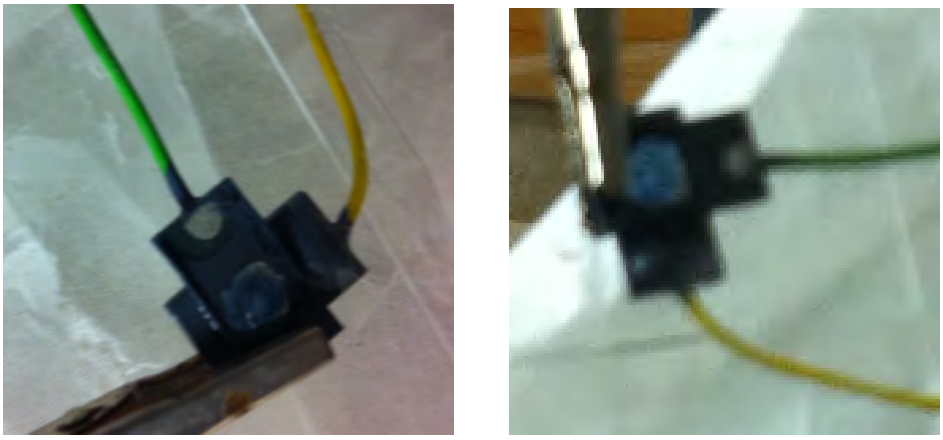

Figure 5.1 Images of the 'micro-sandwich cell' based on 'ion-jelly' electrolyte.
a. Image obtained at -0.7 V. b. Image obtained at 0.8 V.

A cyclic voltammetric experiment was performed in order to observe the colour switch at the oxidation/ reduction potentials. The 'micro-sandwich cell' changed colours from dark-bluish (at -0.7 V) to light-blue (at 0.7 V), thus showing that such a device containing solid state electrolyte was made and could have potential use in an electrochromic device.

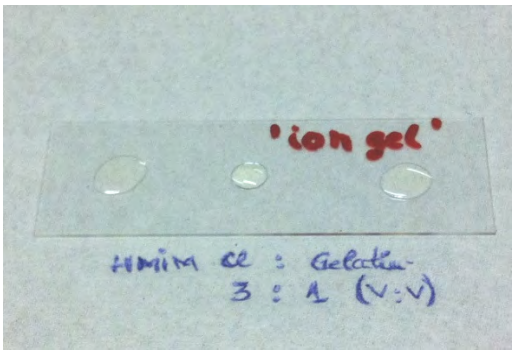

Figure 5.2 Image of 'ion gel' droplets of 1-Hexyl-3-Methylimidazolium Chloride and gelatin (3:1, v:v)

The following issues are recommended for further investigation:

- To optimise the 'micro-sandwich cell' configuration while manufacturing the appropriate 'ion jelly' based electrolyte, to ensure a fast electrochromic switch. This optimisation will entail performing a series of experiments using the 'ion-jelly' electrolytes prepared in different ratios.
- To prepare different film thickness for the polymers and choose the best candidate which will offer high stability and high visual contrast.
- To perform additional in-situ spectroelectrochemical experiments which will indicate the attractive characteristics such as high coloration efficiency, rapid and reversible switch time, and vivid colour/ multi colour change.
- To test the electrochemical stability over an extended period of time, as this characteristic is demanded in the field of electrochromic devices.

To sum up, these recommendations are proposing a new, cost-effective proto-type of 'micro-sandwich electrochromic cell' that can be optimised in order to obtain the desirable features of an electrochromic device, that can be made in a more environmentally-friendly manner.

5.3 References

[1] J. Niessen, U. Schroder, M. Rosenbaum, F. Scholz, Electrochem Commun, 6 (2004) 571-575.
[2] T. Yi-Jie, C. Hai-Feng, Z. Wen-Wei, Z. Zhao-Yang, J Appl Polym Sci, (2012) n/a-n/a.
[3] A.J.C. da Silva, F.A. Ribeiro Nogueira, J. Tonholo, A.S. Ribeiro, Solar Energy Materials and Solar Cells, 95 (2011) 2255-2259.
[4] P. Vidinha, N.M.T. Lourenco, C. Pinheiro, A.R. Bras, T. Carvalho, T. Santos-Silva, A. Mukhopadhyay, M.J. Romao, J. Parola, M. Dionisio, J.M.S. Cabral, C.A.M. Afonso, S. Barreiros, Chem Commun, (2008) 5842-5844.

LIST OF TABLES

LIST OF FIGURES

Program 6

```
  PROGRAM 6
C   MODIFICATION OF PROGRAm5  ( dec 2012)
C      CYCLIC VOLTAMMETRY FOR BULK SOLUTION IMPLICIT METHOD
C      for a thin layer of ionic liquid of thickness d H1 in contact
C      with aqueous solution
       IMPLICIT REAL*8(A-H,O-Z)
C      IMPLICIT REAL*4(Z)
       DIMENSION W(500),RL1(500000),RR1(500000),G(500),PCHI(25000)
       DIMENSION FONW1(500),FOOL1(500),FRNW1(500),FROL1(500)
       DIMENSION FONW2(500),FOOL2(500),FRNW2(500),FROL2(500)
       DIMENSION RKO2(500),RKR2(500),RL2(500000),RR2(500000)
       DIMENSION RKO1(500),RKR1(500),RNEW(500),RK(500),WZ(25000)
       DIMENSION RMAT(500000)
      OPEN (UNIT=5,FILE='BZ1.DAT',STATUS='OLD')
      OPEN (UNIT=6,FILE='BK2.DAT',STATUS='NEW')
C    SET POTENTIAL LIMITS
       VI=0.3D0
       VF=-0.3D0
       EI=VI/0.02569D0
       EF=VF/0.02569D0
      READ (5,60)DIFF1,SCAN,H1
      READ (5,62)DIFF2,RKFTW,RES
      READ(5,61)N,L
      LT2=2*L
      TIMEL=2.D0*(VI-VF)/SCAN
      RES=RES*0.0000001
      DIST=6.D0*DSQRT(TIMEL*DIFF2)
      H2=DIST/FLOAT(N)
      RK1=TIMEL/FLOAT(LT2)
C   TO MAKE THE ION TRANSFER RATE DIMENSIONLESS
      RKFTW1=RKFTW*RK1/H2
      H1=H1/FLOAT(N)
      RKFTW2=RKFTW*RK1/H1
      DM2=DIFF2*RK1/H2**2
      DM1=DIFF1*RK1/H1**2
      BETA=H2/H1
      WRITE(6,70)DM1,DM2,RK1
   70 FORMAT('   DM1 = ',E11.6,'   DM2=',E10.5,' RK1 = ',E10.5)
      WRITE(6,71)TIMEL,DIST,BETA
   71 FORMAT(' TIMEl = ',F11.6,'  DISTANCE= ', E11.5,' BETA',F10.2)
   60 FORMAT(3F12.8)
   62 FORMAT(3F12.8)
```

```
  61 FORMAT(2I6)
     DELTAE=(EF-EI)/FLOAT(L)
     EMOD=EI
C     INITIAL CONDITIONS
     DO 10 J=1,N
     FOOL1(J)=1.D0
     FROL1(J)=0.D0
     FROL2(J)=0.D0
     FOOL2(J)=0.D0
  10 CONTINUE
C      THE TOTAL NUMBER OF INCREMENTS IS 2l
     NX=N-1
C SET UP THE RIGHT HAND SIDE
     DO 16 LL=1,N
     DO 16 K=1,N
  16 RR1((LL-1)*N+K)=0.D0
     DO 17 LL=1,N
  17 RR1((LL-1)*N+LL)=2.D0*(1.D0-DM1)
     DO 14 LL=1,NX
     RR1((LL-1)*N+LL+1)=DM1
  14 RR1(LL*N+LL)=DM1
C CALCULATE THE MATRIX FOR THE LEFT HAND SIDE
      DO 26 LL=1,N
      DO 26 K=1,N
  26 RL1((LL-1)*N+K)=0.D0
     DO 27 LL=1,N
  27 RL1((LL-1)*N+LL)=2.D0*(1.D0+DM1)
     DO 24 LL=1,NX
     RL1((LL-1)*N+LL+1)=-DM1
  24 RL1(LL*N+LL)=-DM1

C CALCULATE THE RIGHT HAND SIDE CONSTANT FOR THOMAS ALGORITM
     DO 36 LL=1,N
     DO 36 K=1,N
  36 RR2((LL-1)*N+K)=0.D0
     DO 37 LL=1,N
  37 RR2((LL-1)*N+LL)=2.D0*(1.D0-DM2)
     DO 34 LL=1,NX
     RR2((LL-1)*N+LL+1)=DM2
  34 RR2(LL*N+LL)=DM2
C CALCULATE THE MATRIX FOR THE LEFT HAND SIDE
     DO 46 LL=1,N
```

```
      DO 46 K=1,N
   46 RL2((LL-1)*N+K)=0.D0
      DO 47 LL=1,N
   47 RL2((LL-1)*N+LL)=2.D0*(1.D0+DM2)
      DO 44 LL=1,NX
      RL2((LL-1)*N+LL+1)=-DM2
   44 RL2(LL*N+LL)=-DM2
      DO 20 I=1,LT2
      DO 18 LL=1,N
      RKO1(LL)=0.D0
      RKR1(LL)=0.D0
      RKO2(LL)=0.D0
      RKR2(LL)=0.D0
   18 CONTINUE
      DO 19 K=1,N
      DO 19 LL=1,N
      RKO1(K)=RR1((LL-1)*N+K)*FOOL1(LL)+RKO1(K)
      RKR1(K)=RR1((LL-1)*N+K)*FROL1(LL)+RKR1(K)
      RKO2(K)=RR2((LL-1)*N+K)*FOOL2(LL)+RKO2(K)
   19 RKR2(K)=RR2((LL-1)*N+K)*FROL2(LL)+RKR2(K)
      RATIO=DEXP(EMOD)
      DOEDGE=FOOL2(1)
      DREDGE=(BETA*FROL2(1)+FROL1(N))/(1.D0+BETA)
      DRSURF=(FOOL1(1)+FROL1(1))/(1.D0+RATIO)
      DOSURF=RATIO*DRSURF
C     RKR2(N)=RKR2(N)
C     RKO2(N)=RKR2(N) 20 dec 2012
      CUR=ABS(601788.D0*DSQRT(DIFF1*SCAN)*PCHI(I-1))
C     WRITE(6,83)PCHI(I-1),CUR
C   83 FORMAT('   PCHI = ',F12.8,'   CUR = ',F12.8)
      EMOD=EMOD+DELTAE+CUR*RES/0.02569D0
      RATIO=DEXP(EMOD)
      FOEDGE=FOOL1(N)
      FREDGE=(BETA*FROL2(1)+FROL1(N))/(1.D0+BETA)
      FRSURF=(FOOL1(1)+FROL1(1))/(1.D0+RATIO)
      FOSURF=RATIO*FRSURF
      FONW1(1)=FOOL1(1)+DM1*(FOSURF-2.D0*FROL1(1)+FOOL1(2))
      FRNW1(1)=FROL1(1)+DM1*(FRSURF-2.D0*FROL1(1)+FROL1(2))
      FONW2(1)=FOOL2(1)+DM2*(FOEDGE-2.D0*FOOL2(1)+FOOL2(2))
      FRNW2(1)=FROL2(1)+DM2*(FREDGE-2.D0*FROL2(1)+FROL2(2))
C     INCLUDE KINETIC EFFECTS
      FRNW1(N)=FROL1(N)+DM1*(FROL1(N-1)-2.D0*FROL1(N))
```

```
      FONW1(N)=FOOL1(N)+DM1*(FOOL1(N-1)-2.D0*FOOL1(N)+1.D0)
      FONW2(N)=FOOL2(N)+DM2*(FOOL2(N-1)-2.D0*FOOL2(N))
      FRNW2(N)=FROL2(N)+DM2*(FROL2(N-1)-2.D0*FROL2(N))
      RKO1(1)=RKO1(1)+DM1*(DOSURF+FOSURF)
      RKR1(1)=RKR1(1)+DM1*(DRSURF+FRSURF)
      RKO1(N)=RKO1(N)+DM1*(DOEDGE+FOEDGE)
C   RKFTW IS THE FILM TO WATER TRANSFER RATE CONSTANT THAT APPLIED
C    ONLY TO THE EDGE
      RKR1(N)=RKR1(N)+DM1*(DREDGE+FREDGE)-RKFTW1*FREDGE
      RKO2(1)=RKO2(1)+DM2*(DOEDGE+FOEDGE)
      RKR2(1)=RKR2(1)+DM2*(DREDGE+FREDGE)
C      RKR2(N)=RKR2(N)
C      the following line is in error?...
C      RKO2(N)=RKR2(N)
C ADJUSTING THE RIGHT HAND SIDE.
      CALL THOMAS (FRNW1,RKR1,RL1,N)
      CALL THOMAS (FONW1,RKO1,RL1,N)
      CALL THOMAS (FRNW2,RKR2,RL2,N)
      CALL THOMAS (FONW2,RKO2,RL2,N)
C CALCULATE CURRENT
      FACT=SQRT(DM1*FLOAT(L))/(1.D0+RATIO)
      WZ(I)=FACT*(FONW1(1)-RATIO*FRNW1(1))
      PCHI(I)=WZ(I)/DSQRT(EI-EF)
C RESET CONCENTRATIONS....
      DO 40 J=1,N
      FOOL1(J)=FONW1(J)
      FROL1(J)=FRNW1(J)
      FROL2(J)=FRNW2(J)
      FOOL2(J)=FONW2(J)
   40 CONTINUE
C TEST FOR SWEEP DIRECTION
      IF(I.EQ.L)DELTAE=(-DELTAE)
      IF(I.EQ.L)EMOD=-0.3/0.02569
      IF(I.EQ.L)RES=-RES
   20 CONTINUE
C OUTPUT DATA
      DELTAE=-DELTAE
      EMOD=EI
C      WRITE(N,*)I
C      WRITE(L,*)I
C      WRITE(PCHI(I),*)D
C      PRINT *,PCHI(I)
```

```
      WRITE(6,88)N,L
C     WRITE(*,88)N,L
      DO 50 I=1,LT2
      EMOD=EMOD+DELTAE
      V=-EMOD*0.02569D0
   88 FORMAT( 'NUMBER OF POINTS =',I6,I12)
      WRITE (6,100)V,PCHI(I)
      IF (I.EQ.L)DELTAE=-DELTAE
   50 CONTINUE
  100 FORMAT(2(E11.4,3X))
      CLOSE(UNIT=5)
      CLOSE(UNIT=6)
      STOP
      END
      SUBROUTINE THOMAS(RNEW,RK,RMAT,N)
      IMPLICIT REAL*8(A-H,O-Z)
      DIMENSION W(500),RMAT(500000),G(500)
      DIMENSION RNEW(500),RK(500)
      W(1)=RMAT(N+1)/RMAT(1)
      G(1)=RK(1)/RMAT(1)
      DO 10 I=2,N
      W(I)=RMAT(I*N+I)/(RMAT((I-1)*N+I)-RMAT((I-2)*N+I)*W(I-1))
   10 G(I)=(RK(I)-RMAT((I-2)*N+I)*G(I-1))/(RMAT((I-1)*N+I)-
     1RMAT((I-2)*N+I)*W(I-1))
      RNEW(N)=G(N)
      N11=N-1
      DO 20 I=1,N11
      J=N-I
   20 RNEW(J)=G(J)-W(J)*RNEW(J+1)
      RETURN
      END
```

Electrochimica Acta 74 (2012) 117–122

Contents lists available at SciVerse ScienceDirect

Electrochimica Acta

journal homepage: www.elsevier.com/locate/electacta

Characterization and electrochromic properties of poly(2,3,5,6-tetrafluoroaniline): Progress towards a transparent conducting polymer

Lavinia Astratine[a], Edmond Magner[a,*], John Cassidy[b,*], Anthony Betts[c,*]

[a] Materials Surface and Science Institute & Department of Chemical and Environmental Sciences, University of Limerick, Limerick, Ireland
[b] School of Chemical and Pharmaceutical Sciences, Dublin Institute of Technology, Kevin St, Dublin 8, Ireland
[c] Applied Electrochemistry Group, Dublin Institute of Technology, Focas Institute, Camden Row, Dublin 8, Ireland

ARTICLE INFO

Article history:
Received 26 October 2011
Received in revised form 5 April 2012
Accepted 6 April 2012
Available online 12 April 2012

Keywords:
Poly(2,3,5,6-tetrafluoroaniline)
Transparent conducting polymer
Cyclic voltammetry
Spectroelectrochemistry

ABSTRACT

Electrochromic films of poly(2,3,5,6-tetrafluoroaniline) (PTFA) were formed on ITO substrates from aqueous solutions utilising perchloric acid ($HClO_4$) as dopant. Electrochemical and spectroscopic characterization of PTFA films was performed in background electrolyte and in solutions with the addition of tetrahydrofuran. When the PTFA film was removed from its growth medium, a significant decrease in the faradaic current was observed. The faradaic response increased on addition of tetrahydrofuran which facilitates ion movement through the polymer matrix. PTFA films deposited on ITO substrate were orange and light orange in the oxidized and reduced forms, respectively. The films were ca. 25 nm in thickness. In aqueous solution the films showed a porous structure with a non-uniform distribution of pore diameters. In the presence of tetrahydrofuran a less porous structure was observed.

1. Introduction

Since their discovery, conducting polymers (CPs) [1] which are also known as electroactive polymers have been extensively investigated for electrochromic applications [2,3]. The energy gap between the valence and conduction bands of the polymer provides a first estimation of the electronic excitation energy which can be measured spectroscopically. The spectroscopic signal depends not only on the energy of the electronic transition but also on the efficiency of the transition [4]. The colour change between doped and undoped forms of the polymer depends on the magnitude of the band gap of the undoped polymer. For example oxidative p-doping shifts the optical absorption band towards the lower energy part of the spectrum [4].

Polypyrrole (PPy), polythiophene (PTh) and polyaniline (PANI) [5] are formed during anodic oxidation and are amongst the most extensively studied electroactive polymers [6]. Polyaniline (PANI) and its derivatives are of particular interest due to their stability [7]. Polyaniline films can be formed during electrochemical deposition using potentiostatic, potentiodynamic and galvanostatic methods [8]. The polymer possesses three oxidation states: leucoemeraldine (neutral), emeraldine (polaron) and pernigraniline (bipolaron). The leucoemeraldine form represents the fully reduced form, emeraldine is half-oxidized and pernigraniline is the fully oxidized state of polyaniline. The electrical conductivity of polyaniline based materials can be closely controlled over a wide range. The most common, protonated emeraldine, has a high conductivity of 100 S cm^{-1}, similar to that of a semiconductor [7].

Polymerization of aniline monomers containing fluorine has been performed both chemically and electrochemically; however the properties of these polymers have not been fully characterised. Monofluoro-substituted anilines [9] have been synthesised from acidic solutions using a chemical oxidation process and characterised by a range of spectroscopic methods. Chemically synthesised poly(2-fluoroaniline) and poly(3-fluoroaniline) showed similar absorption spectra to that of the 2-fluoroaniline monomer. With the 4-fluoroaniline monomer, dehalogenation occurred during polymerization, with fluorine being displaced to yield a more favourable head-to-tail polymer with the resultant UV–Vis spectrum being identical to that of polyaniline [9]. The solubilities of polyfluoroanilines in organic solvents were improved in comparison to polyaniline [9]. Poly(tetrafluroaniline) was used as a substrate for a bacterial fuel cell [8], but was not examined as an electrochromic material. Electrochemical polymerization of 2,3,5,6-tetrafluoroaniline was carried out in aqueous-acidic solutions under potentiostatic control. Poly(2,3,5,6-tetrafluoroaniline) modified platinum electrodes showed improved stability compared to poly(2-fluoroaniline) when they were exposed to microbially aggressive conditions such as sewage or sewage sludge

* Corresponding authors. Tel.: +353 061 234168; fax: +353 061 203529.
E-mail addresses: lavinia.astratine@ul.ie (L. Astratine), edmond.magner@ul.ie (E. Magner), john.cassidy@dit.ie (J. Cassidy), anthony.betts@dit.ie (A. Betts).

0013-4686/$ – see front matter © 2012 Elsevier Ltd. All rights reserved.
http://dx.doi.org/10.1016/j.electacta.2012.04.032

for long time periods [8]. Poly(2,3,5,6-tetrafluoroaniline) was the most resistive material towards microbial degradation and prevented poisoning of platinum by metabolic by-products [8].

The electrochemical behaviour of 2-fluoroaniline, 3-fluoroaniline and 4-fluoroaniline electrodeposited on platinum electrode were examined in aqueous acidic and organic media using $NaClO_4$ as electrolyte [10]. During electrochemical oxidation, poly (2-, 3- and 4-) fluoroanilines were successfully deposited on the surface of the electrode but the transition from the emeraldine to the pernigraniline form was not observed, due to the fluorine electron withdrawing group [10].

A significant number of reports have described the development of transparent conducting polymers and in particular the use of chemically synthesised poly(3,4-ethylenedioxythiophene) (PEDOT) with polystyrenesulphonate (PSS) as counter ion to form conductive films. For example, dispersions of films of PEDOT: PSS in DMSO with single walled carbon nanotubes have been sprayed on polyethyleneterephthalate (PET) [11]. The resultant films had a resistance of 118 Ω/sq and 90% transmittance over the wavelength range 400–800 nm. In situ polymerization of EDOT with 2,3-dichloro-5,6-dicyanobenzoquinone (DDQ) (molar ratio of 1:1.33) yielded films with 80% transmittance over the range 300–700 nm [12]. Similar films were formed with a sulfonated derivative of polythiophene [13]. No electrochromic studies have been described for these transparent polymers. However a polypyrrole/polythiophene co-polymer had a uniform absorbance between 400 nm and 800 nm while reduced [14] only upon oxidation a strong absorbance at 600 nm resulted. Another system of aniline/thiophene co-polymer displayed a relatively constant change in absorbance with potential, but had a slight absorbance maximum at 800 nm [15].

To our knowledge, there have been no electrochromic studies of PTFA. This paper describes the formation of PTFA thin films on a conducting ITO substrate by successive potential cycling in acidic solutions. The films obtained were characterised by electrochemical and spectroscopic techniques. PTFA polymer showed an improved electrochemical response when tetrahydrofuran was added to the solution. The UV–Vis spectra displayed a single broad absorbance peak over the visible spectrum which can be attributed to a neutral to polaron electronic transition. The effects of different electrolytes on the properties of the polymer are described.

2. Experimental

2,3,5,6-Tetrafluoroaniline and tetrahydrofuran were purchased from Sigma–Aldrich and perchloric acid (60%) from BDH Laboratory Supplies, UK. In order to avoid degradation, 2,3,5,6-tetrafluoroaniline was stored under dry conditions in the dark. Cyclic voltammetry was employed to electropolymerize PTFA films onto conducting indium tin oxide glass (ITO). A three electrode cell was used with an ITO glass slide (Solaronix, Switzerland), platinum coil (0.5 mm, Alfa-Aesar, UK) and Ag/AgCl (3 M KCl) (CH Instruments Inc., UK) as working, counter and reference electrodes, respectively. All potentials are reported vs Ag/AgCl (3 M KCl). The dimensions of the ITO electrodes were 0.5 cm × 2.5 cm. The ITO sheet resistance was 18 Ω/sq. The electrodes were carefully cleaned by successive ultrasonication in deionized water, followed by acetone and then deionized water to ensure removal of all traces of acetone and finally dried in air prior to use. Water with a resistivity of 18 MΩ cm (Elgastat Maxima) was used for all studies. Solutions (10 ml volume) containing 50 mM monomer (2,3,5,6-tetrafluoroaniline) and 2 M $HClO_4$ were prepared in deionized water. Monomer solutions were deoxygenated with nitrogen for 5 min prior to use. All solutions were freshly prepared for each experiment. Electrochemical experiments were performed using a CHI 620 model potentiostat. UV–Vis absorption spectra were recorded on a Shimadzu 1800 UV-Vis spectrophotometer. The colouration efficiency was measured by chronoamperometry, by switching the potential between 0 V and 1.2 V. SEM images were obtained using a Hitachi SU-70 scanning electron microscope.

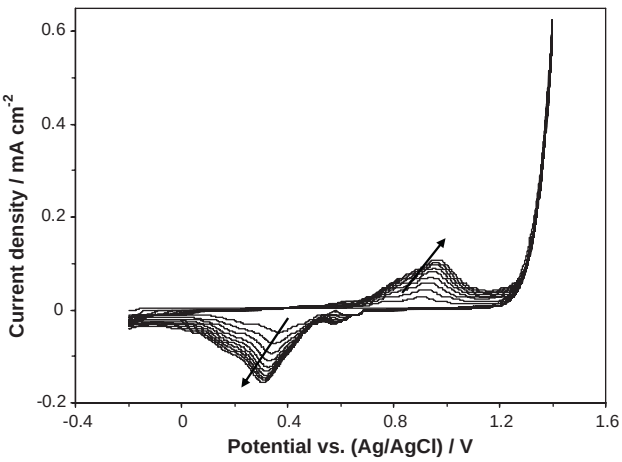

Fig. 1. Cyclic voltammograms of PTFA film deposited on ITO glass from an aqueous solution containing 50 mM TFA and 2 M $HClO_4$. Scan rate of 40 mV s^{-1}. Number of cycles: 15.

3. Results and discussion

3.1. Cyclic voltammetry of PTFA films

PTFA films were deposited onto ITO electrodes under potentiodynamic conditions from aqueous media with the addition of perchloric acid ($HClO_4$) as dopant. Cyclic voltammograms of TFA in aqueous solution (Fig. 1) indicated that the optimal conditions for electropolymerization were obtained over the potential range −0.2 V to +1.4 V at a constant scan rate of 40 mV s^{-1}. Monomer oxidation commences at a potential of ca. 1.2 V. Thin films were formed since thicker films possess an increased resistance which compromises the conductivity of the polymers. On successive scans, the peak currents at ca. 0.9 V increased slightly, indicating that a conductive polymeric film was formed on the electrode. As the number of cycles increased, the potential for oxidation of the polymer increased to more positive values and the potential for reduction to more negative values. Also on the reduction scan, two peaks were observed at 0.6 V and 0.3 V. The appearance of the small peak at ca. 0.3 V depends on the upper potential limit used. On increasing the upper potential to 1.6 V, the reduction peak potential at 0.3 V increased to 0.4 V.

Electropolymerization of tetrafluoroaniline on ITO is proposed to occur via the same mechanism (Scheme 1) described for the polymerization of aniline. As evident from the first anodic scan, it is the electron-withdrawing effect of fluorine which gives rise to the increase in potential required for monomer oxidation. On continuous sweeping the peak potential separation increases indicating that the polymer oxidation/reduction process is becoming more difficult, which is likely due to the increased hydrophobicity of the film. Note that PTFA films were also deposited on fluorine doped SnO_2, however a very poor electrochemical response was obtained and all studies were thus performed with ITO electrodes.

3.2. Electrochemical characterization of the PTFA films

PTFA polymer characterization was performed in different solutions: with background electrolyte alone, with the addition of monomer, or with the addition of tetrahydrofuran. The nature of the supporting electrolyte used during electrochemical cycling of

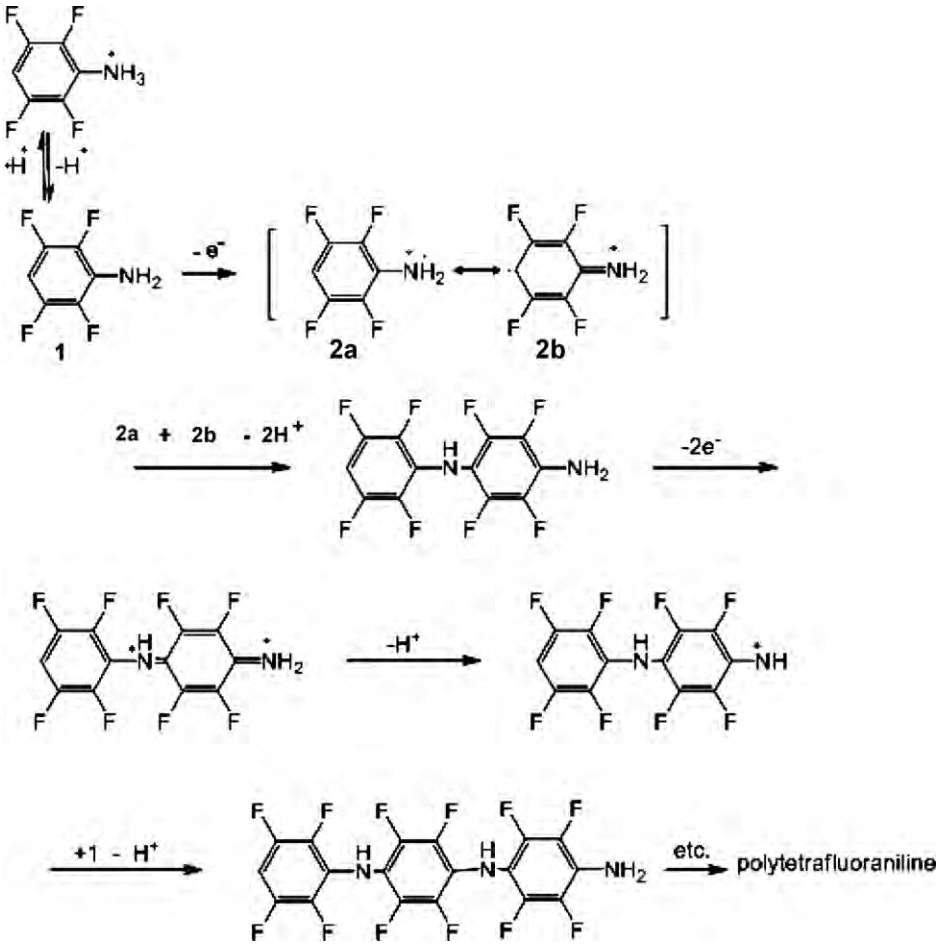

Scheme 1. Proposed mechanism for polymerization of 2,3,5,6-tetrafluoroaniline.

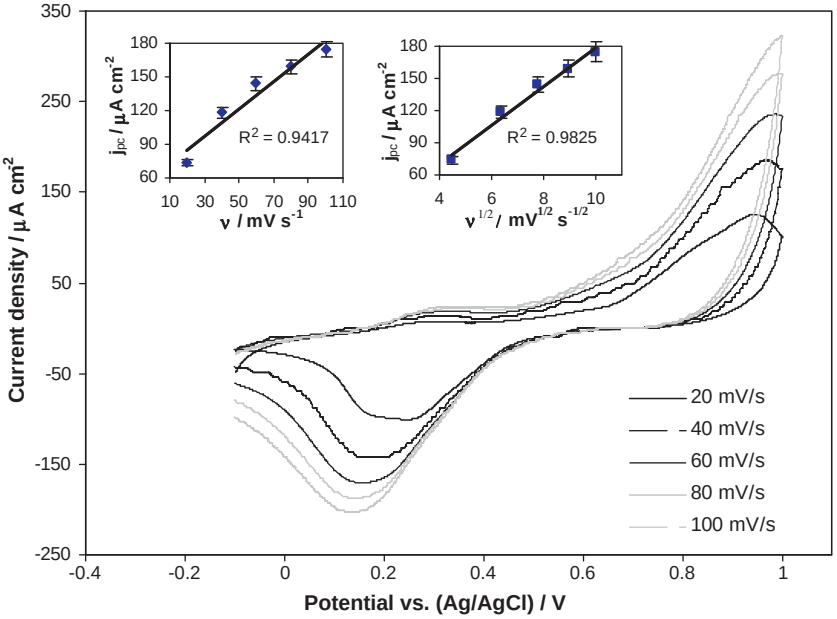

Fig. 2. Cyclic voltammograms of PTFA film as a function of scan rate in a solution containing 50 mM TFA and 2 M $HClO_4$. Insert graphs show plots of cathodic peak current versus ν and $\nu^{1/2}$.

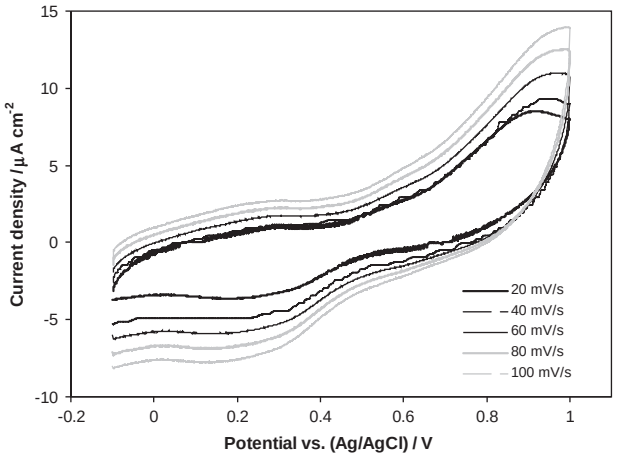

Fig. 3. Cyclic voltammograms of PTFA film deposited on ITO as a function of scan rate in 2 M $HClO_4$ aqueous solution.

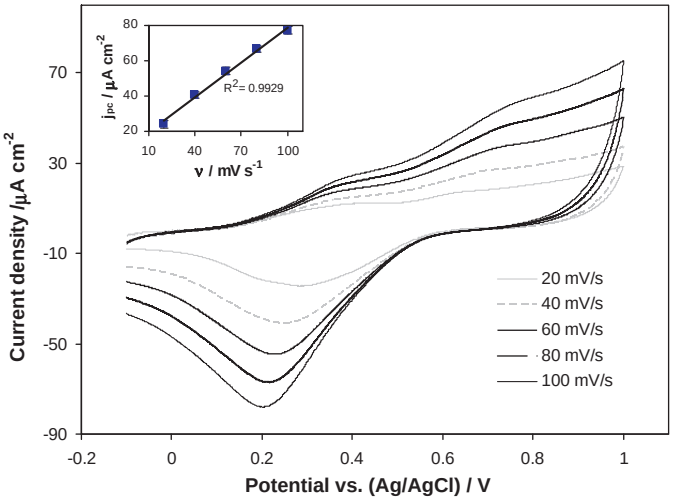

Fig. 4. Cyclic voltammograms of a PTFA film on ITO in 2 M $HClO_4$ aqueous solution with 16.66% THF.

PTFA has considerable influence on the properties of the polymer [16]. Voltammetric characterization of the PTFA films deposited on ITO glass was performed in the same solution used for film formation, over the potential range −0.2 V and 1.0 V to avoid further monomer oxidation. The polymer was characterised in the presence of the monomer as the voltammetric response deteriorated in solutions containing only background electrolyte. The resultant cyclic voltammograms (Fig. 2) exhibited a similar response to that obtained during polymer deposition (Fig. 1). On the cathodic sweep, the peak currents were well defined, while upon oxidation the peak potentials shifted towards more positive values with increasing scan rate. The ratio of j_{pa} to j_{pc} should be close to one for an ideal thin layer system, but the rate of the oxidation process was slow and j_{pa} could not be measured (Fig. 2). Cyclic voltammograms of films in the presence of monomer displayed an increase in the oxidation peak potential with increasing scan rate and also a slight shift in the peak potentials with increased scan rate. The inset in Fig. 2 shows that the polymer does not display thin layer behaviour, instead displaying behaviour corresponding to bulk diffusion. The linear plot of j_p vs $\nu^{1/2}$ can be ascribed to slow ion movement arising from the hydrophobic nature of the film [17].

On transferring the electrode to monomer-free solution containing 2 M $HClO_4$ a dramatic change in response was observed (Fig. 3). The anodic peak currents were significantly reduced and the peaks broadened, possibly indicating that ion incorporation during the polymer oxidation/reduction process was slow. It is obvious that the absence of the monomer caused a decrease in the peak currents which are three times lower in 2 M $HClO_4$ compared to those in the monomer solution. The electrochemical response of PTFA in background electrolyte alone is in contrast with other conducting polymers such as polypyrrole and polythiophene which have large capacitive currents [18,19]. In general, for conducting polymers the conductivity correlates with the capacitance of the film [20]. In aqueous 2 M $HClO_4$ the decrease in current densities is due to a loss in conductivity of the film.

The addition of tetrahydrofuran to the aqueous 2 M $HClO_4$ solution changes the electrochemical behaviour of the polymer (Fig. 4). Tetrahydrofuran (THF) is a polar aprotic solvent characterised by a low dielectric constant of 7.5 [21]. In the presence of THF, the peak currents increase, possibly indicating that the hydrophobic polymeric layer is more open and allows counter ions to move in and out more readily during the redox cycle. In contrast to the data in Fig. 2, the reduction peak current increases linearly with scan rate, indicative of thin layer behaviour [22] (Fig. 4). Increasing the amount of THF resulted in increases in the peak current which are associated with increased ion mobility into and out of the film during the redox cycle [23] (Fig. 5).

3.3. Spectroelectrochemistry of the PTFA polymer

Spectroelectrochemical analysis was performed in the presence and absence of THF to investigate the optical properties of the polymer. There is a uniform increase in absorbance as a function of potential over the wavelength range 420 nm to 730 nm (Fig. 6). In addition the spectral band is particularly broad, covering this entire wavelength range. This is reflected in the change from a delicate orange to a much deeper orange colour as the potential is increased [12].

The changes in absorbance (Fig. 6) due to the electronic transition corresponding to a neutral to a polaron state, similar to that seen for monofluorinated anilines [10]. The isosbestic point related to a simple two stage system is not present as the neutral polymer electronic transition is at lower wavelengths below 420 nm. The band-gap (π–π^*) transition for aniline is generally observed around and sometimes below 300 nm which represents a limitation for electro-optical applications [24]. Compared to spectra of polyaniline, the range of wavelengths associated with the transition in PTFA is very wide, which is due to the presence of fluorine electron withdrawing group. The PTFA films did not exhibit large

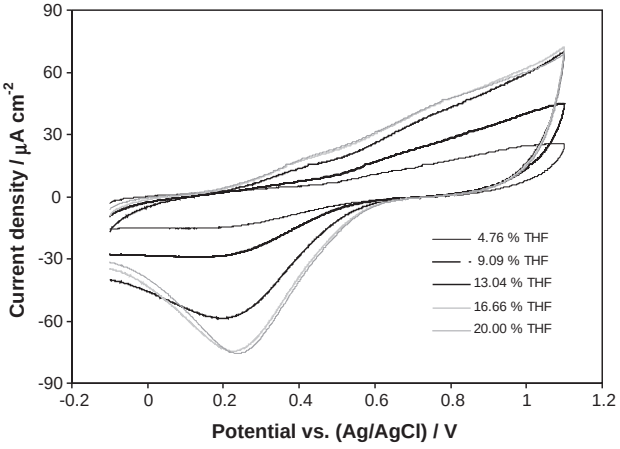

Fig. 5. Cyclic voltammograms of a PTFA film cycled at 100 mV s^{-1} in 2 M $HClO_4$ aqueous electrolyte while increasing the tetrahydrofuran concentration.

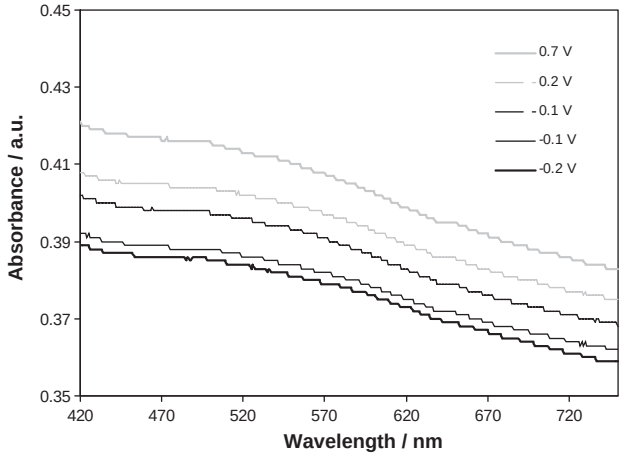

Fig. 6. UV–Vis spectra of PTFA film in 2 M $HClO_4$ aqueous solution as a function of applied potential.

absorbance changes on oxidation/reduction, even on addition of THF.

3.4. Electrochromic switch

The response time measured upon switching the polymer film between its neutral and oxidized states was monitored at 450 nm (Fig. 7). The polymer thickness was controlled by adjusting the number of potential cycles. The film used for this study was a thin film as the charge passed through during deposition was 13.6×10^{-4} C cm^{-2}. The colouration efficiency (CE) is an important characteristic for electrochromic materials and corresponds to the amount of charge injected in the polymer as a function of the change in optical density. The coulombic efficiency (η) is related to the performance of the electrochromic device and is defined as the ratio between the change in optical density (ΔOD) and the injected/ejected charge per unit area of the electrode at a specific wavelength (λ_{max}) [23]. Absorbance variations with time under a step potential oscillating between the oxidized and reduced states of the polymer at λ_{max} in the visible range are essential for an electrochromic material. The absorbance change as the polymer is cycled between oxidized and reduced state provides details of the optical contrast and electro-optical stability [25].

The polymer film on ITO does not display dramatic colour variations, changing from orange in the oxidized form to a more bleached orange colour in the reduced form. Consequently, the colouration efficiency had a value of 36.6 cm^2 C^{-1} at 450 nm, which is low when compared to other electrochromic materials. A dual electrochromic system containing poly(3,4-ethylenedioxythiophene) and poly(3-methylthiophene) had a high colouration efficiency of 460 cm^2 C^{-1} at 665 nm [26] where the colours ranged between deep red and deep blue.

The colour changes recorded at 450 nm wavelength require longer times, due to the increasing difficulty of inserting ions into the polymer matrix. The hydrophobic nature of PTFA polymer makes the injection of ions on oxidation more difficult in aqueous media, while upon reduction they are more easily released. As stated in the literature the polymer colour depends on the polymer

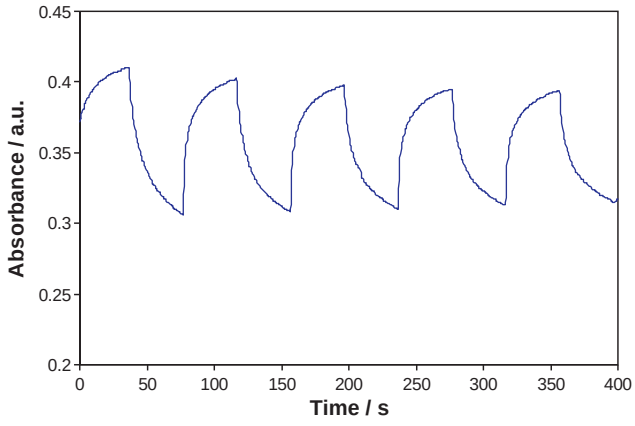

Fig. 7. Plot of absorbance (λ = 450 nm) vs time of a PTFA film as the potential was switched between 0 V and 1.2 V. The solution contained 2 M $HClO_4$ and 50 mM monomer. Switching interval of 40 s.

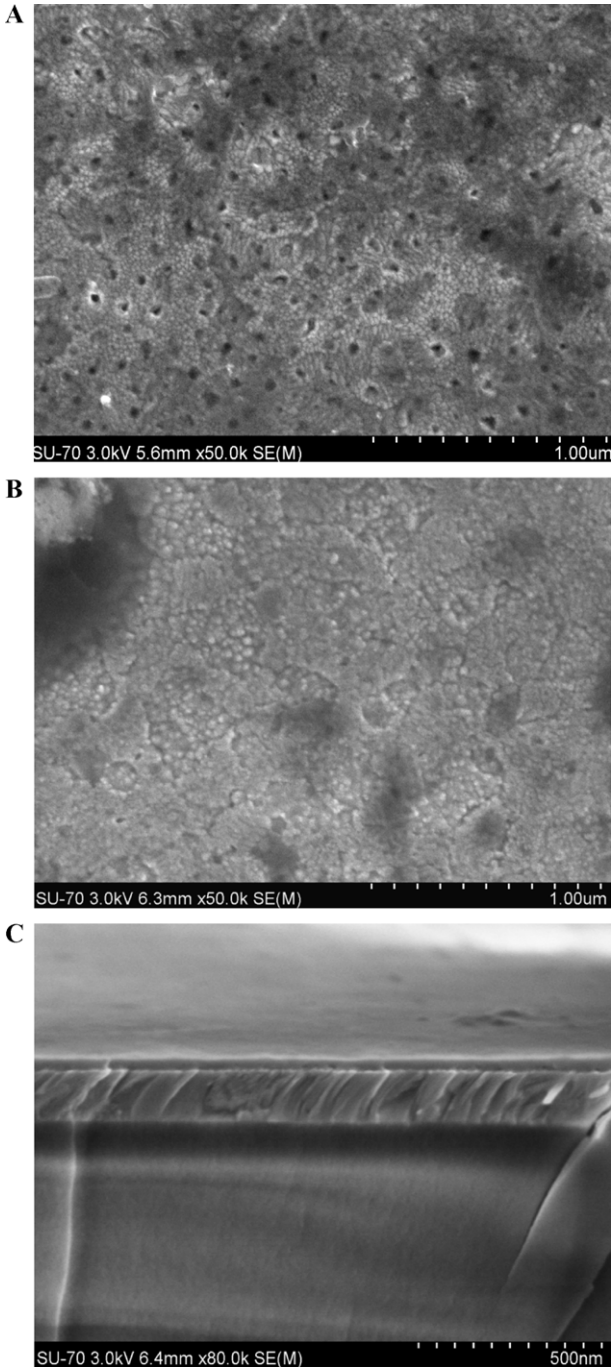

Fig. 8. (A) SEM image of PTFA polymer from aqueous solutions; (B) SEM image of PTFA polymer from solutions with tetrahydrofuran (20%); (C) SEM cross-section image of PTFA film run in aqueous solution.

chain-length. An increase in resistivity was observed from cyclic voltammetry (Fig. 1) and UV–Vis spectra (Fig. 7). The changes in absorbance spectra seen at 450 nm are very small and the rate of the oxidation–reduction process is very slow as the system required over 40 s to switch between different oxidation states. Ideally a fast switching time of less than a few seconds is required for most electrochromic device applications [27].

Slow transients have been reported elsewhere in the literature for a polypyrrole/polythiophene system (>20 s) [14] and for Tempo/viologen electrochromic devices (>50 s) [28,29].

3.5. Morphology investigation

SEM was used to study the detailed surface morphology of two polymer films in 2 M $HClO_4$ aqueous solution with and without THF deposited ITO substrate. Both films were removed from solution and allowed to dry without any post treatment. Fig. 8A shows the morphology of PTFA films obtained in aqueous solution containing 2 M $HClO_4$ without THF deposited on ITO substrate. PTFA films had an uneven highly porous structure (Fig. 8A) with pore diameters of ca. 50 nm. On addition of THF (Fig. 8B) the film morphology is less porous than for the PTFA in aqueous solutions. It is interesting to notice the changes of polymer structure in the presence of 20% THF which shows less numerous pores. In general a less porous structure (Fig. 8B) may affect the diffusion of ions into and out of the entire bulk film decreasing the electroactivity [23]. This contradicts the electrochemical study of PTFA/20% THF (Fig. 4) which indicates the presence of a more electroactive layer compared to PTFA/aqueous solution (Fig. 3). However, SEM images were obtained after the films were removed from solution and completely dried and may not reflect the structure of the films in solution. The presence of 20%THF created films with reduced numbers of pore but with increased pore size which facilitates the insertion/expulsion of ClO_4^- into the polymer [23,30]. The thickness of the polymeric film was 25 nm (Fig. 8C), in reasonable agreement with the value of 15.2 nm calculated from the charge passed during polymer oxidation ($Q = 13.6 \times 10^{-4}$ C cm^{-2}).

4. Conclusions

PTFA films were successfully deposited on a ITO substrate and characterised by electrochemical and spectroscopic methods. Spectroelectrochemical measurements showed a broad absorbance peak over the visible region of the spectrum with an increase in absorbance across the spectrum as the potential was increased. The addition of THF improved the electrochemical response of PTFA films in aqueous solutions. In 2 M $HClO_4$ aqueous solution the films showed a significant decrease in the faradaic response. An increase in the peak currents was observed on addition of THF. The presence of fluorine substituents to form PTFA did not introduce extra stability, as ion movement was hindered and the voltammetric response was more sluggish than that of polyaniline in aqueous solution due to the hydrophobic nature of the films. However with PTFA films the neutral to polaron transition was observed from 420 to 730 nm, while the neutral transition was moved to lower wavelengths. A low colouration efficiency of 36.6 cm^2 C^{-1} was observed while PTFA polymer exhibited a contrast change of orange to a more transparent orange.

Acknowledgements

This work was performed with the support of the joint University of Limerick and Dublin Institute of Technology Common Interest Group and the Programme for Research in Third Level Institutions (INSPIRE). The assistance of Dr. C. Dickinson and A. Singh in SEM analysis is acknowledged. We would like to thank the reviewers for their helpful comments.

References

[1] J. Heinze, in: H. Lund, O. Hammerich (Eds.), Electrochemistry of Conducting Polymers in Organic Electrochemistry, Marcel Dekker, New York, Basel, 1991.
[2] T.A. Skotheim, R.L. Elsenbaumer, J.R. Reynolds (Eds.), Handbook of Conducting Polymers, 2nd edition, Marcel Dekker, New York, 1998.
[3] P.M.S. Monk, D.R. Rosseinsky, Electrochromism: Fundamentals and Applications, Cambridge University Press, New York, 1995.
[4] R.J. Mortimer, A.L. Dyer, J.R. Reynolds, Displays 27 (2006) 2.
[5] K. Aydemir, S. Tarkuc, A. Durmus, G.E. Gunbas, L. Toppare, Polymer 49 (2008) 2029.
[6] R.J. Mortimer, Chemical Society Reviews 26 (1997) 147.
[7] M. Freund, B. Deore, Self-doped Conducting Polymers, John Wiley & Sons Ltd., Chichester, UK, 2007.
[8] J. Niessen, U. Schroder, M. Rosenbaum, F. Scholz, Electrochemistry Communications 6 (2004) 571.
[9] A.H. Kwon, J.A. Conklin, M. Makhinson, R.B. Kaner, Synthetic Metals 84 (1997) 95.
[10] A. Cihaner, A.M. Onal, Polymer International 51 (2002) 680.
[11] J. Zhang, L. Gao, J. Sun, Y. Liu, Y. Wang, J. Wang, Diamond and Related Materials 22 (2012) 82.
[12] M.L. Machala, L. Muller-Meskamp, S. Gang, S. Olthof, K. Leo, Organic Electronics 12 (2011) 1518.
[13] S.A. Mauger, A.J. Moule, Organic Electronics 12 (2011) 1948.
[14] A.J.C. da Silva, F.A. Ribeiro Nogueira, J. Tonholo, A.S. Ribeiro, Solar Energy Materials and Solar Cells 95 (2011) 2255.
[15] S. Vogel, R. Holze, Electrochimica Acta 50 (2005) 1587.
[16] S. Little, S.F. Ralph, C.O. Too, G.G. Wallace, Synthetic Metals 159 (2009) 1950.
[17] N. Sato, T. Nonaka, Nippon Kagaku Kaishi (1997) 451.
[18] M. Grzeszczuk, A. Kepas, G. Zabinska-Olszak, Electrochimica Acta 49 (2004) 2405.
[19] A. Lima, P. Schottland, S. Sadki, C. Chevrot, Synthetic Metals 93 (1998) 33.
[20] B. Garcia, D. Bélanger, Synthetic Metals 98 (1998) 135.
[21] V. Eric, D.A. Anslyn, Dougherty, Modern Physical Organic Chemistry, 2006.
[22] A.J. Bard, L.R. Faulkner, Electrochemical Methods: Fundamentals and Applications, 2nd edition, Wiley, New York, 2001.
[23] M. Gao, Y. Yang, M. Diao, S.G. Wang, X.-h. Wang, G. Zhang, G. Zhang, Electrochimica Acta 56 (2011) 7644.
[24] J. Arjomandi, R. Holze, Central European Journal of Chemistry 6 (2008) 199.
[25] A.V. Rosario, E.D. Rios, A.F. Nogueira, L. Micaroni, Solar Energy Materials and Solar Cells 94 (2010) 1338.
[26] D.M. Welsh, A. Kumar, E.W. Meijer, J.R. Reynolds, Advanced Materials 11 (1999) 1379.
[27] L. Ma, Y. Li, X. Yu, Q. Yang, C.-H. Noh, Solar Energy Materials and Solar Cells 93 (2009) 564.
[28] J.S. Zhao, B. Wang, C.S. Cui, R.M. Liu, J.F. Liu, H.S. Wang, H.T. Liu, Electrochimica Acta 56 (2011) 4819.
[29] C.-W. Hu, K.-M. Lee, K.-C. Chen, L.-C. Chang, K.-Y. Shen, S.-C. Lai, T.-H. Kuo, C.-Y. Hsu, L.-M. Huang, R. Vittal, K.-C. Ho, Solar Energy Materials and Solar Cells 99 (2012) 135.
[30] B. Sarı, M. Talu, Synthetic Metals 94 (1998) 221.

List of Publications

1. **Lavinia Astratine**, Edmond Magner, John Cassidy, Anthony Betts, *Characterization and electrochromic properties of poly(2,3,5,6- tetrafluoroaniline): Progress towards a transparent conducting polymer*, *Electrochimica Acta, Volume 74, 15 July 2012, Pages 117-122.*

2. **Lavinia Astratine**, Edmond Magner, John Cassidy, Anthony Betts, *Copolymerization and Characterization of Polypyrrole-Poly(3,4-ethylenedioxythiophene) Copolymer In a Air and Water Stable Ionic Liquid* – in preparation

3. **Lavinia Astratine,** Edmond Magner, John Cassidy, Anthony Betts, *Model for Thin Layer of Ionic Liquid Coating on an Electrode* **–** in preparation

List of Conferences

1. **L. Astratine,** J. Cassidy, E. Magner, A. Betts, *Copolymerization of Polypyrrole-Poly(3,4-ethylenedioxythiophene) In a Air and water Stable Ionic Liquid*, Electrochem 2012: Electrochemical Horizons, Trinity College Dublin, 2-4 September 2012

2. **L. Astratine**, E. Magner, J. Cassidy, A. Betts, *Copolymerization and Characterization of Polypyrrole-Poly(3,4-ethylenedioxythiophene) Copolymer In a Air and Water Stable Ionic Liquid*, 63rd Annual ISE Meeting, 19-24 August, 2012, Prague, Czech Republic - Poster Presentation.

3. **L. Astratine,** *Electrochemical Deposition of Poly(2,3,5,6-tetrafluoroaniline) From Aqueous Solutions*, International Workshop: Polymers at Electrodes. A Quarter of Century Later. 6 – 9 November 2011, Bad Schandau, Germany – Oral Presentation.

4. **L. Astratine**, Formation and Characterization of Poly(2,3,5,6- tetrfluoroaniline) From Aqueous Solution, Electrochemical Horizons 2011, 4-6 September 2011, University Of Bath, UK - Oral Presentation.

5. **L. Astratine**, E. Magner, J. Cassidy, A. Betts, *Forming conducting polymers utilising room temperature ionic liquids,* 61st Annual Meeting of the International Society of lectrochemistry, September 26th – October 1st, 2010, Nice, France - Poster Presentation.